The Role of the Serine/Threonine Phosphatase PstP in Regulating the Mycobacterial Cell Wall

BY

FARAH SHAMMA

Presented to the Faculty of the Graduate School of

The University of Texas at Arlington

in Partial Fulfillment of the Requirements for the Degree of

DOCTOR OF PHILOSOPHY

Department of Biology

December 2021

Supervising committee

Cara Boutte
Supervising Professor

Clay Clark

Jeffery Demuth

Woo-Suk Chang

Joseph Boll

Table of Contents

List of Figures:

List of Tables:

Dedication

My parents

- The two most wonderful, kind and loving people in this world I am lucky to be born to

My husband

- The talented, wise and patient man I have been lucky to share this journey with

Acknowledgments

I thank the Almighty God, the most Merciful, without Whose help it would have never been possible for me to accomplish any work ever.

It would have been next to impossible to achieve my doctoral degree without my parents' constant support and inspiration. I am forever grateful to my parents for being there for me in every way possible throughout my studies, my career and my life. I cannot thank my husband enough for insisting me to pursue my doctoral studies in the United States and for being there with me in this journey. Being literally the only person physically present with me at all times during my time spent here in the United States as an international student, he witnessed the highs and lows I have been through and has been by my side all through.

It is a pleasure to thank all the people who contributed to the successful completion of my dissertation.

I owe my deepest gratitude, indebtedness and appreciation to my revered supervisor **Dr. Cara Boutte**, Assistant Professor, Department of Biology, University of Texas at Arlington. She has taught me everything I know as a young scientist today. I deeply appreciate her patience and sincere enthusiasm to mentor me, her passion for science and for being a strong woman who has established herself in the world of academia. Being an excellent teacher and a wonderful scientist, she constructively guided and trained me using her fine expertise to be able ask the right questions in a project, develop my scientific thinking abilities, design experiments, write well, review journal articles critically, and helped me achieve my experimental skills. She has been an understanding and a supportive, transparent and great mentor to work with.

I thank my committee members Dr. A. Clay Clark, Dr. Jeffery Demuth, Dr. Woo-Suk Chang and Dr. Joseph Boll for their valuable opinions regarding my work, asking the right questions that guided me to think about the next step and being quick in complementing me on my success and good work. I really appreciate their time and effort that helped me grow up as a scientist. I will forever be grateful to Dr. Clark for giving me a chance by allowing me

to start my research work in his lab when the Boutte lab was still not set up.

I thank Dr. Laura Mydlarz for her generous support and I thank Dr. Christensen for introducing me to my supervisor Dr. Cara Boutte when I was looking for a supervisor to work with.

Life for an international graduate student may not be always easy in a foreign country but a wonderful group of people around can certainly make abroad seem like home. Fortunately, there were always people around me who provided the much needed help and support.

My awesome lab mates are some of those people. Thanks to Augusto Cesar Hunt Serracin for being my 'twin from the other world'. Having him in the lab definitely made my days extremely fun filled and easier all these years. Angela Freeman has been a great lab mate to discuss science with. I appreciate how she is independent and figures out issues herself without relying on anyone's help. Thanks to Neda Habibi Arejan for being a 'protein purification buddy' in the lab. Thanks to Karen Samaga-de-Tembiwa for being very helpful and a fun person to be with in the lab. Thanks to the undergraduate researcher Samantha Quintanilla for being such a great lab partner. She has such a courteous and kind personality that makes working with her very pleasant. Thanks to the other undergraduate researcher Parthvi Patel for all her help that we could not do without. Thanks to all the undergraduate lab mates who left- Deven, Heather, Madeline, Dominic, Fernanda, Rita, Oshione and particularly Susana Pimentel, for being the most amazing undergraduate research partner one can ever have.

I heartily thank my friends from all the other labs. Thanks to Misha Kazi for all the great food and fun, Katie Kang for being such a wonderful and kind person and for understanding my weird jokes, Nowrosh Islam for being a little sister in the lab who took care of me so much and for all the great science brainstorming discussions we had. I thank Liqi Yao and Suman Shrestha for their cooperation when I worked with them in the Clark lab for a little while, especially Liqi- who is an honest and a hard-working person with a strong hold of scientific knowledge and skills. Her help has played an integral role in building and honing my protein purification skills. Thanks to Douja Chamseddine for being the fun, awesome, and self-less herself. Surely, all the food (that she is very keen to feed everyone in the vicinity) and

goofing around with her made me feel alive in the lab.

There are some names that cannot just go unmentioned, because these are very nice people who I learnt something from or helped make my day better in some way or are great friends. So I thank all the awesome friends I made from Pellegrino lab, Chang lab, Clark lab, Ghose lab; Balan Ramesh, Lindsay Davis, Anisha Mahajan, Anna Williford and Kimberly Bowles. Thanks to Joydeep Chatterjee for being my 'radioactivity buddy' at UTA. I cordially thank Soroush Ghaffari and Manoj Sabnani for all their help all through especially with getting the liquid nitrogen and for being so welcoming. I have been fortunate enough to learn a lot about US classrooms and effective communication by shadowing A. Wadud Khan in the Microbiology lab classes in my very first semester. I thank him for being our go-to person in the US when we came here, for all his help and guidance and for introducing us to his lovely wife Rumman. I thank Rumman for being so kind and a generous host to us.

Some people become like a family in a foreign land for an international student. I cannot thank Feroz Ahmed enough for being the little brother that I never had and for introducing us to Shamsad Nuri Mouri, his wife. Thanks to Mouri to whom I should have been a better elder sister but she has a great heart to reverse the role and feed and take care of me instead. Thanks to Feroz and Mouri for bringing little Reehan in our lives, who I realize is the only person that can brighten my days lately. Thanks to Fatema Begum Ruma for being an important part of my life and for being there in my most critical times.

I can never thank enough my childhood friends in Bangladesh who definitely helped me keep sane in the US during my time here as a graduate student, especially Taiyeeba Samia.

The list of names can go on but people who know me well and have really been friends all through know already that how grateful I am to them, regardless of whether their names are included here or not.

——————

Abstract

Mycobacterium tuberculosis (*Mtb*) is the causative agent of the deadly infection Tuberculosis (TB). The current standard antibiotic regimen for TB treatment combines fours drugs to be taken for at least six months. *Mtb* shows intrinsic phenotypic tolerance to antibiotics contributing to the long treatment regimen. In addition, *Mtb* cells can achieve a non-replicating state exhibiting antibiotic tolerance, reduced metabolism and altered cell wall staining. The changes in the cell wall and reduced permeability to antibiotics in stressed cells suggest that the regulation of the cell wall is a major contributor to antibiotic tolerance. The mycobacterial cell wall consists of covalently cross-linked peptidoglycan, arabinogalactan and mycolic acid layers. While this complex architecture is well studied, not much is known about how cell wall is regulated in stress. Mycobacteria use reversible Serine/Threonine phosphorylation as an important mechanism to regulate their cell wall. In contrast to the eleven Serine/Threonine protein kinases (STPKs), which regulate a number of known cell wall regulatory factors, there is only one essential Serine/Threonine phosphatase- PstP in Mycobacteria, which is also itself phosphorylated by the STPKs. In this study we investigate the role of PstP in regulating the cell wall using the non-pathogenic model *Mycobacterium smegmatis*. We report some novel substrates of PstP *in vitro*, describe the significance of PstP's phospho-sites in regulating its activity and specificity and the effects of phospho-misregulation of PstP in cell wall metabolism and antibiotic tolerance. Our findings provide substantial insights for future studies on cell wall regulation and assessing PstP as a drug target.

Chapter 1

Introduction

Preface: This dissertation and the pre-Robert Koch days

Centuries ago, when people became infected with Tuberculosis, all they could get as 'treatment' was the advice to rest and eat healthy (Fogel, 2015). The term 'Tuberculosis' was coined much later, and the disease was known as 'consumption' back in the days (Fogel, 2015). In 1882, the revolutionary discovery by the German physician Robert Koch identifying Mycobacterium tuberculosis as the etiological agent of this deadly disease led to vaccines and anti-tuberculosis drugs in the later period (Nguyen *et al.*, 2007; Keshavjee and Farmer, 2012)*. What found success as the initial treatment was the very first anti-tubercular drug Streptomycin (Nguyen, 2016). The emerging resistance of this pathogen to this single drug not long after created the need to find new antibiotics. Over time, the current treatment regimen of multiple antibiotics for at least half a year was established (Nguyen, 2016). To date, this pathogen has remained a most successful one to adopt to survive within its host, which is human, continuing to pose challenges to the increasing burden of TB* (Chai *et al.*, 2018)*. The complex yet somewhat fascinating cell wall architecture of this pathogen, which is distinct from that of the Gram-positive or a Gram-negative bacteria, acts like an armor to drugs, contributing to its inherent drug tolerance (Jarlier and Nikaido, 1990). Its cell wall is regulated in conditions that create stresses on the pathogen, leading to antibiotic tolerance* (Cunningham and Spreadbury, 1998; Betts *et al.*, 2002; Xie *et al.*, 2005; Bhamidi *et al.*, 2012; Sarathy *et al.*, 2013; Liu *et al.*, 2016; Sarathy *et al.*, 2017)*. This dissertation is part of an effort to find promising drug targets in Mycobacteria. The dissertation unveils the importance of the phosphorylation-mediated role of PstP- the only essential Serine/Threonine Phosphatase in Mycobacteria- in cell wall modulation and antibiotic tolerance. It is hoped that this work will offer useful information for future studies aimed to target the cell wall in order to fight the age-old peril better.*

1.1 Tuberculosis and its causative agent *Mycobacterium tuberculosis*

Tuberculosis (TB), caused by *Mycobacterium tuberculosis (Mtb),* is among the top ten fatal diseases worldwide. It is an airborne pulmonary disease characterized by severe coughing, chest pain and fever (Fogel, 2015). *Mtb* causes about 10 million of active infections and over a million of deaths every year (World Health Organization, 2021). Vaccines, antibiotics and improved diagnostic approaches are currently available (Nguyen, 2016); nevertheless, the TB disease burden continues to remain high.

TB can have a latent phase of infection, where people are infected without being ill, but may develop the disease at some point of their life (Getahun *et al.*, 2015) . It is thought that about a quarter of the people in the world has latent TB (Fogel, 2015). So it is likely that in addition to the current active illnesses, there will be more TB illnesses with time.

1.2 TB Treatment

TB treatment remains complicated for various reasons. One of the reasons is TB's latent stage, where people remain infected without any manifestation of illness, and therefore do not get treated. The other major reason is that TB treatment is arduous and lengthy- two months with four drugs (rifampicin (RIF), isoniazid (INH), pyrazinamide and ethambutol (EMB) and two drugs (RIF and INH) for the following four months (Botella *et al.*, 2017).

Moreover, spontaneous mutations in the *Mtb* genome may favor survival of *Mtb* in presence of a specific antibiotic. Continuous exposure to antibiotics along with patient's poor-compliance to the lengthy treatment regimen act as a selective pressure to cause

the emergence of drug resistant *Mtb* mutants (Nguyen, 2016). Hence, the emergence of drug resistant TB continues to be a threat. In 2020, 0.13 million Multi-drug resistant (MDR)/RIF (the first-line treatment) resistant TB cases have been reported (World Health Organization, 2021). Therefore, shorter and simpler regimens to treat TB are urgently needed.

1.3 *Mtb*'s drug tolerance- a difficulty in TB treatment

In order to develop drugs that will treat TB faster, it is necessary to understand why it takes such a long time to kill *Mtb* with the current regimen. The fact that TB treatment requires at least six months is partly due the intrinsic phenotypic tolerance of *Mtb* to antibiotics. It has been reported that, *Mtb* can be drug tolerant in its stationary growth phase and under stresses, which poses a great problem for antibiotic treatment of TB (Wallis *et al.*, 1999). *Mtb* cells can achieve a dormant, non-replicating state in the host in which they are antibiotic tolerant, having reduced metabolism and altered cell wall staining (Seiler *et al.*, 2003). In the non-growing state, *Mtb*'s cell wall undergoes chemical alteration and thickening (Jarlier and Nikaido, 1994; Seiler *et al.*, 2003). It is thought that the conditions that *Mtb* encounter in the host like hypoxia, low pH, high carbon dioxide may act as stresses that could induce dormancy. This *in vivo* dormant phenotype is typically mimicked *in vitro* by applying stresses like hypoxia or nutrient starvation e.g. carbon and nitrogen starvation (Gomez and McKinney, 2004), which also cause antibiotic tolerance.

1.4 *Mtb*'s cell wall, drug tolerance and stress

The cell wall of *Mtb* itself acts as a permeability barrier to drugs (Jarlier and Nikaido, 1990). And, *Mtb* cells become antibiotic tolerant in nutrient deprivation conditions (Xie *et al.*, 2005). The cell wall is a key player in *Mtb's* antibiotic tolerance.

Understanding this regulation of cell wall biosynthesis in starvation is of thus immense importance. However, little is known about *Mtb* cell wall regulation in stress. Knowing more about cell wall regulation in stress could lead to the development of antibiotics that could shorten the treatment duration of TB.

1.5 The *Mtb* cell wall has multiple layers

The currently accepted cell wall architecture of *Mtb* can be termed as the mycolyl-arabinogalactan-peptidoglycan complex (Daffé and Draper, 1997) (Figure 1).

Peptidoglycan (PG) is the first layer surrounding the plasma membrane. Alternative repeats of disaccharide *N*-acetyl glucosamine (NAG) and *N*-acetyl muramic acid (NAM) compose this layer, and these sugar chains are cross-linked with short peptides. An arabinogalactan layer is covalently bound to this PG layer. A lipid layer composed of mycolic acids is covalently linked to the arabinogalactan layer. The mycolic acid layer is the inner leaflet of the outer membrane, and the outer leaflet contains mainly glycolipids as well as glycans and proteins (Marrakchi *et al.*, 2014). The mycolic acid layer is the thick lipid coat of mycobacteria and is the major contributor to impermeability of the cell wall (Hett and Rubin, 2008). This mycolic acid layer is the distinctive feature of the *Mtb* cell wall, which is 60% of the cell wall weight, mainly consisting of long chain (60-90 carbons) mycolic acids (Minnikin, 1991). A capsule layer composed of proteins and polysaccharides surrounds the mycolic acid layer. There are fewer porins in the cell wall

so the hydrophilic solutes permeate inefficiently and slowly and the low fluidity and thickness of the lipid bilayer slows down lipophilic drugs (Liu *et al.*, 1996).

While the architecture of the cell wall is well known, little is known about the regulation of this well-understood cell wall structure.

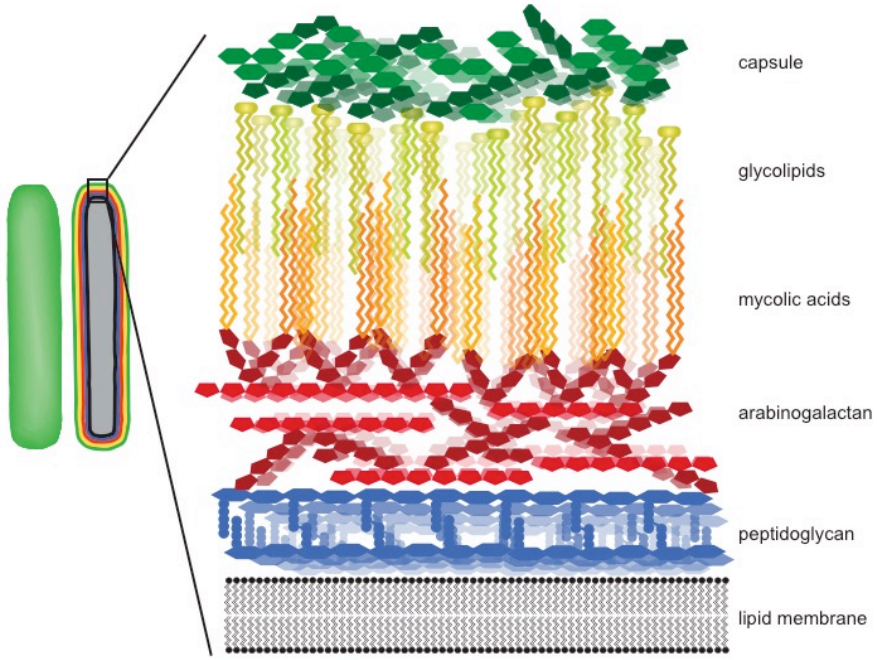

Figure 1.1 Schematic diagram of the Mycobacterial cell wall

1.6 *Mtb*'s cell wall is regulated in stress causing drug tolerance

Mtb cells lose acid-fastness in Ziehl-Nielsen staining due to altered mycolic acid biosynthesis, and undergo cell wall thickening in stress conditions *in vitro* (Cunningham and Spreadbury, 1998; Seiler *et al.*, 2003; Deb *et al.*, 2009; Sarathy *et al.*, 2013). These are the same features of non-replicating *Mtb* cells *in vivo*. So it is very likely that, stress conditions encountered in the host may induce *Mtb* to regulate its cell wall in response to environmental stimuli, leading to tolerance to antibiotics. It is very important to

understand the cell wall regulatory events that occur when the cells encounter stress and thus become drug tolerant.

1.7 Phosphorylation mediated cell wall regulation in *Mtb*

While much is known about the cell wall structure of *Mtb*, little is known about the regulation of the cell wall during stress or the mechanisms of antibiotic tolerance. The signaling pathways regulating *Mtb* cell wall might be an important clue to understand how *Mtb* adapts to stressful environments.

Reversible Serine/Threonine (S/T) protein phosphorylation is a crucial regulatory mechanism used by bacteria for environmental signal transduction to regulate cell growth (Galyov *et al.*, 1993; Wang *et al.*, 1998; Juris *et al.*, 2000; Echenique *et al.*, 2004). *Mtb* uses the process of reversible S/T phosphorylation to regulate cell growth (Kieser and Rubin, 2014). In this mechanism, an S/T protein kinase (STPK) will phosphorylate a substrate on serine (S) or threonine (T) residues, and an S/T protein phosphatase dephosphorylates the S/T residue(s) to revert the effect of phosphorylation (Sajid *et al.*, 2011).

Mtb has 11 STPKs (PnkA-B and PknD-L) and only one S/T protein phosphatase, PstP (Cole *et al.*, 1998; Bach *et al.*, 2009). Among the STPKs, PknA and PknB are essential for *Mtb* growth and regulate mycobacterial cell division and elongation via phosphorylation of substrates involved in these processes (Sassetti and Rubin, 2003; Kang *et al.*, 2005; Fernandez *et al.*, 2006; Kusebauch *et al.*, 2014).

1.8 Cell wall regulatory enzymes and proteins in *Mtb*

1.8.1 Phospho-regulated cell wall enzymes (InhA, KasA and KasB):

Some of the cell wall substrates of STPKs are cell wall enzymes whose activities are directly altered by phosphorylation, of which a few are mentioned below:

InhA:

InhA (NADH-dependent 2-*trans*-enoyl-ACP reductase) is an enzyme of the fatty acid-synthase (FAS)-II system in the mycolic acid biosynthesis pathway in *Mtb* and is mainly phosphorylated the STPK PknA and to a lesser degree by PknB *in vitro* (Molle and Kremer, 2010). Phosphorylation reduces the enzymatic activity of InhA (Molle and Kremer, 2010; Khan *et al.*, 2010), suggesting a phospho-inhibited regulatory role of this enzyme *in vivo* to regulate the mycolic acid content of the cell wall.

KasA and KasB:

The ketoacyl acyl-carrier-protein (AcpM) synthases KasA and KasB are also enzymes of the FAS-II system in the mycolic acid biosynthesis pathway and their activities are reduced when phosphorylated *in vitro* by different STPKs (Molle *et al.*, 2006). KasA and KasB are dephosphorylated by PstP (Molle *et al.*, 2006) suggesting that they might be activated by dephosphorylation to upregulate mycolic acid biosynthesis *in vivo*.

All the enzyme of the FAS-II system in *Mtb* are inhibited when phosphorylated (Molle *et al.*, 2006; Molle and Kremer, 2010; Veyron-Churlet *et al.*, 2010; Khan *et al.*, 2010). Although only KasA and KasB have been verified as substrates of PstP, it can be expected that dephosphorylation of these substrates may activate these enzyme for

active mycolic acid biosynthesis *in vivo*.

1.8.2 Phospho-regulated cell regulatory proteins (CwlM, Wag31 and FhaA)

There are also cell wall regulators that are not enzymes but whose essential presence and phosphorylation affect cell shape and growth. The ones we focus on in our study are introduced below:

CwlM: CwlM is an important regulator of the cell wall that is controlled by phosphorylation. CwlM helps regulate peptidoglycan (PG) biosynthesis. The enzyme MurA catalyzes the first step in PG precursor synthesis (Typas *et al.*, 2012). In mycobacteria, the MurA enzyme is inactive by default. CwlM is phosphorylated by the kinase PknB and, when phosphorylated, activates MurA, allowing PG biosynthesis and cell growth to proceed (Boutte *et al.*, 2016). In the transition to starvation, CwlM has been found to be rapidly dephosphorylated, implying that there is a phosphatase for CwlM (Boutte *et al.*, 2016). A mutation in *murA* disrupts proper downregulation in PG biosynthesis and the cells show more sensitivity to antibiotics in early starvation (Boutte *et al.*, 2016). So it seems probable that the dephosphorylation of CwlM to downregulate PG synthesis is crucial for the formation of antibiotic tolerant cells.

Wag31: Wag31, involved in regulating cell shape and polar cell wall synthesis, is an essential protein for both *Mtb* and *Mycobacterium smegmatis* (*Msmeg*) (Sassetti and Rubin, 2003; Kang *et al.*, 2008; Jani *et al.*, 2010). Depletion of Wag31 changes *Msmeg* cell shape from bacillus to coccus due to a defect in cell wall synthesis at the poles (Kang *et al.*, 2008). Wag31 is phosphorylated by the STPKs PknA and PknB *in vivo* and PknA *in vitro* (Kang *et al.*, 2005). Wag31 is highly phosphorylated when expressions of

the kinases *pknA/B* are the highest in the exponential phase (Kang *et al.*, 2005; Kang *et al.*, 2008). The phosphorylation of Wag31 affects its localization to the poles and possibly also its homo-oligomerization (Jani *et al.*, 2010). Wag31 and PknB are localized at the cell poles, which are the sites of PG turnover (Kang *et al.*, 2008; Mir *et al.*, 2011; Prisic and Husson, 2014). Interestingly enough, the mycobacterial enzymes of Fatty Acid Synthase-II (FAS-II) complex, which regulate membrane lipid biosynthesis, have been found to be co-localized at the poles and septum with Wag31 (Carel *et al.*, 2014). Also, Wag31 interacts with enzymes involved in synthesis of precursors for the mycolic acid layer of cell wall (Meniche *et al.*, 2014). It seems probable Wag31 is involved in regulating the coordination of PG and mycolic acid layer synthesis in growing cells.

Based on the data that Wag31 is highly phosphorylated in log phase when PG is required for polar elongation, we think that Wag31 may activate cell wall enzymes when it is phosphorylated and it is likely to be dephosphorylated when cell wall growth is downregulated. There has to be a phosphatase that acts on dephosphorylating Wag31 in transition to downregulation of cell wall synthesis machinery.

FhaA:

FhaA is a Forkhead Associated (FHA) domain-containing protein in Mycobacteria. The FHA domains in proteins can bind to phosphorylated Threonine residues to regulate protein function (Pallen *et al.*, 2002). In *Msmeg*, FhaA likely regulates PG metabolism and also cell elongation via its interactions with the PG precursor Lipid-II flippase MurJ (Gee *et al.*, 2012), the phosphoform of the PG regulator CwlM and the class B penicillin

binding protein PBPA (Viswanathan *et al.*, 2017), though the exact nature of this regulation is yet unclear. It is important in regulating integrity of the cell envelope and antibiotic tolerance (Viswanathan *et al.*, 2015). Moreover, *fhaA* (Rv0020c) is located downstream of the gene cluster that includes *pstP* (Rv0018c)*, pbpA (Rv0016c), pknA Rv0015c* and *pknB* (Rv0014c) and FhaA is localized at the poles and septum (Gee *et al.*, 2012). The role of phosphorylation of FhaA is yet unclear but its interactions with the PG regulators indicate a possible phosphorylation-mediated regulation and role of FhaA in the PG synthetic network.

1.9 The phosphatase for cell wall regulatory proteins

The phosphatase for CwlM had not been studied, although the findings (Boutte *et al.*, 2016) strongly point to its significant role in downregulating cell wall synthesis, leading to antibiotic tolerance. The phosphatase for Wag31 and FhaA had also not been identified. Identifying and understanding the regulation of the phosphatase involved in downregulation of cell wall synthesis could help in developing a more complete molecular model for antibiotic tolerance of *Mtb* during infection.

1.10 PstP- the possible S/T phosphatase of the cell wall regulators

A recent study suggests that PstP serves as a global negative regulator of phosphorylation (Iswahyudi *et al.*, 2019). Since PstP is the only cognate S/T phosphatase of the 11 STPKS (Cole *et al.*, 1998; Bach *et al.*, 2009), it can be expected to dephosphorylate a lot of substrates.

PstP is essential in *Mtb* and *Msmeg* (Sharma *et al.*, 2016; DeJesus *et al.*, 2017). It is a member of the Protein phosphatase 2C (PP2C) subfamily of PPM (metal-dependent

protein phosphatase) Serine/Threonine phosphatases (Chopra *et al.*, 2003) which strictly require divalent metal ions for activity (Shi, 2009). In addition to the two characteristic metal binding sites of PP2C phosphatases, the $PstP_{Mtb}$ catalytic domain has a third Mn^{2+} binding site close to the flap subdomain adjacent to the active site (Pullen *et al.*, 2004) (Figure 1. 2).

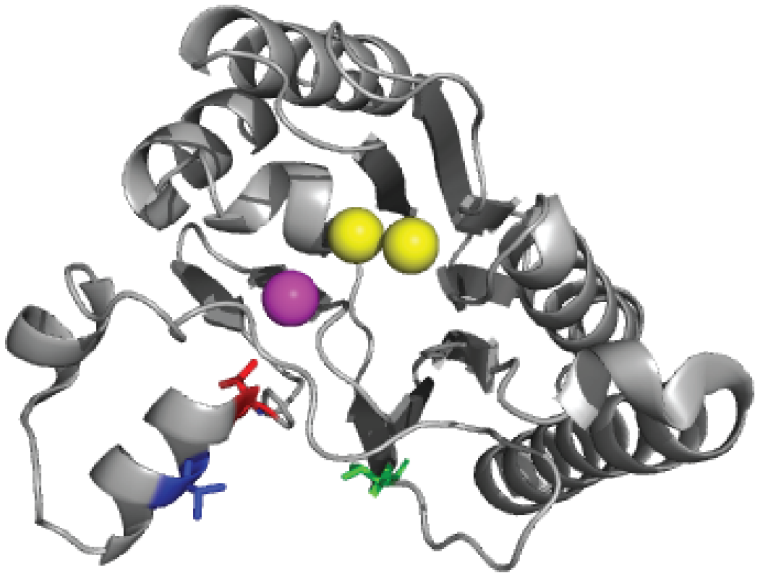

Figure 1.2 Schematic diagram of the crystal structure of $PstP_{Mtb}$

Crystal structure of PstP from *M. tuberculosis (*$PstP_{Mtb}$) (Pullen *et al.*, 2004) (PDB ID: 1TXO). The threonine (T) sites on $PstP_{Mtb}$ phosphorylated by the kinases PknA and PknB (Sajid *et al.*, 2011) are highlighted on the structure: red- $PstP_{Mtb}$ T137 (the corresponding threonine in $PstP_{Msmeg}$ is T134), blue- $PstP_{Mtb}$ T141 (the corresponding threonine in $PstP_{Msmeg}$ is T138) and green- $PstP_{Mtb}$ T174 (the corresponding threonine in $PstP_{Msmeg}$ is T171). T134 and T141 maps on the flap subdomain. The two Manganese (Mn) ions in the catalytic core typical of the PP2C group of phosphatases are highlighted in yellow. The third Mn ion close to the flap subdomain is highlighted in pink.

$PstP_{Mtb}$ shares structural folds and conserved residues with the human PP2Cα, which serves as the representative of the PP2C family (Chopra *et al.*, 2003). $PstP_{Mtb}$ has an N-

terminal cytoplasmic enzymatic domain of 237 residues (shown in Figure 1.2) which is joined by a 63 amino acids long segment to a transmembrane pass of 18 residues connecting the C-terminal extracellular domain of 191 residues (not shown) (Chopra *et al.*, 2003).

PP2C phosphatases are involved in responding to environmental signals, regulating metabolic processes, sporulation, cell growth, division and stress response in a diverse range of prokaryotes and eukaryotes (Vijay *et al.*, 2000; Irmler and Forchhammer, 2001; Mougous *et al.*, 2007; Lu and Wang, 2008; Vijay *et al.*, 2014; Bradshaw *et al.*, 2017).

In *Mtb*, PstP can dephosphorylate PknA, PknB, PknH other STPKs (Boitel *et al.*, 2003; Durán *et al.*, 2005; Sharma *et al.*, 2006; Sajid *et al.*, 2011), KasA, KasB (Molle *et al.*, 2006) and EmbR (Sharma *et al.*, 2006). Dephosphorylation of PknB significantly reduces protein kinase activity (Boitel *et al.*, 2003), which likely results in downregulation of growth (Betts *et al.*, 2002; Ortega *et al.*, 2014). Many of the other proteins dephosphorylated by PstP are involved in cell wall metabolism; however, the effects of this activity differ. Dephosphorylation of CwlM should decrease peptidoglycan metabolism (Boutte *et al.*, 2016). But dephosphorylation of KasA (Molle *et al.*, 2006) and the other FAS-II enzymes (Molle and Kremer, 2010; Veyron-Churlet *et al.*, 2010; Khan *et al.*, 2010; Slama *et al.*, 2011) should upregulate lipid metabolism. These phospho-signaling events are likely involved in the transitions between growth and stasis during infection. However, peptidoglycan and lipid metabolism should be largely correlated (Dulberger *et al.*, 2020), so PstP must be able to minutely toggle its substrate specificity between growth and stasis. For example, we expect that PstP should dephosphorylate

KasA but not CwlM during growth, and should switch this specificity in stasis. How does PstP control its activity and substrate specificity?

1.11 PstP is itself phosphorylated

We think that the phospho-threonine sites of PstP might be involved in somehow toggling activity and substrate specificity of PstP to help regulate growth and cell wall metabolism in changing environments.

$PstP_{Mtb}$ is itself phosphorylated in the catalytic domain on Threonine (T) residues 137, 141, 174 and 290 (Figure 1.2) and phosphorylated PstP shows increased activity against small molecules *in vitro* (Sajid *et al.*, 2011) (Figure 1.2). The corresponding phospho-threonine residues in $PstP_{Msmeg}$ are 134, 138 and 171. We hypothesize that phosphorylation of the threonine residues of PstP might help determine substrate specificity, either directly or indirectly. Addition of a phosphate group to a protein will change surface charge, which could affect protein confirmation, activity (Bibb and Nestler, 2005) or binding to substrates (Ardito *et al.*, 2017) or regulators (Johnson and Barford, 1993). Mutating T138 to alanine on the PP2C S/T phosphatase PphA of *Thermosynechococcus elongatus* changes its substrate specificity (Su and Forchhammer, 2013). Thus, changing the surface polarity in this class of enzymes can change substrate specificity. Interestingly, T138 in *T. elongatus* corresponds to T137 In $PstP_{Mtb}$, which is phosphorylated (Sajid *et al.*, 2011).

1.12 Questions asked in this dissertation

Mtb is an obligate human pathogen without an environmental niche (Gengenbacher *et al.*, 2010). The non-pathogenic soil mycobacterium species *Msmeg* has been used as

the model organism for the *in vivo* experiments in this dissertation. *Mtb* has a 24 hour doubling time and takes 21 days to form colonies on solid media (Sakamoto, 2012). In addition, it is a BSL3-rated pathogen and cannot be studied on the UTA campus. On the other hand, *Msmeg* has a doubling time of 3 hours and takes 3 days to grow on solid media. The proteins focused on in this dissertation are all conserved between *Msmeg* and *Mtb*. Using *Msmeg* will allow to determine how these cell wall regulatory proteins function in the signaling circuitry of mycobacteria.

1.12.1 Identify substrates of PstP involved in cell wall regulation

The STPKs phosphorylate many important cell wall regulatory enzymes and substrates that regulate the PG, the arabinogalactan and the mycolic acid layer of the cell wall (Grundner *et al.*, 2005; Kang *et al.*, 2005; Sharma *et al.*, 2006; Molle *et al.*, 2006; Molle and Kremer, 2010; Veyron-Churlet *et al.*, 2010; Khan *et al.*, 2010; Slama *et al.*, 2011; Roumestand *et al.*, 2011; Boutte *et al.*, 2016; Vilchèze and Kremer, 2017). Among these, only some STPKs (Boitel *et al.*, 2003; Chopra *et al.*, 2003; Durán *et al.*, 2005; Sharma *et al.*, 2006; Sajid *et al.*, 2011), the mycolic acid biosynthesis regulatory enzymes KasA and KasB (Molle *et al.*, 2006) and the transcription factor EmbR involved in the arabinogalactan regulation (Sharma *et al.*, 2006) are biochemically verified substrates of PstP. I aimed to identify some novel cell wall regulatory substrates of PstP in my project that could significantly help to understand the regulatory circuitry of STPK-PstP mediated cell wall regulation better. In this project, I chose to study some cell wall regulatory proteins mainly phosphorylated by PknB and to some extent by PknA among other STPKs. The genes encoding PstP and the kinases PknA and PknB are all located the same operon. So the substrates phosphorylated by PknA and PknB may be

substrates of PstP too.

The PknB-phosphorylated protein CwlM acts as a regulatory activator of PG biosynthesis and is quickly dephosphorylated when switching to stasis in *Msmeg* (Boutte *et al.*, 2016), strongly indicating the presence of a phosphatase in cell, most likely to revert the effect of phosphorylation in order to downregulate PG synthesis in stasis.

Phosphorylated CwlM's interaction partner is another PG regulatory protein FhaA (Turapov *et al.*, 2018) which also is subjected to STPK phosphorylation (Roumestand *et al.*, 2011; Gee *et al.*, 2012), interacts with the phosphorylated PG precursor Lipid-II flippase MurJ (Gee *et al.*, 2012) and maps close to the operon that encodes PknA, PknB and PstP, suggesting FhaA to be an important regulatory part of the phospho-mediated PG regulatory network.

Wag31, which like FhaA, is also a part of a gene cluster that encodes some PG biosynthetic enzymes (Nguyen *et al.*, 2007), is phosphorylated (Kang *et al.*, 2005), mostly in growth upregulating polar PG synthesis and to a lesser degree in stasis (Kang *et al.*, 2008; Jani *et al.*, 2010), suggesting a reversal in polar PG metabolism in stasis due to dephosphorylation of Wag31 most likely mediated by a phosphatase.

PstP being the only known essential S/T phosphatase in *Mtb* (Chopra *et al.*, 2003), I hypothesize that PstP is the phosphatase for dephosphorylating CwlM, FhaA and Wag31. PstP's overexpression perturbs cell shape and its depletion affects cell division (Sharma *et al.*, 2016) and overall phosphorylation of substrates in the cell (Iswahyudi *et*

al., 2019), suggesting PstP's cell wall regulatory role via dephosphorylation of a number of substrates. So, the cell wall regulators like CwlM, FhaA and Wag31 are likely targets of PstP.

Approach: *In vitro* phosphatase assays with purified *Mtb* proteins (full-length substrate proteins) and PstP (cytosolic domain) were performed in this study to directly identify whether PstP can dephosphorylate CwlM (Figure 1.3A), FhaA (Figure 1.3B) and Wag31 (Figure 1.3C), where these proteins were first phosphorylated with their respective purified kinases (cytosolic domains) in presence of ATP as the source of the phosphate group to be transferred.

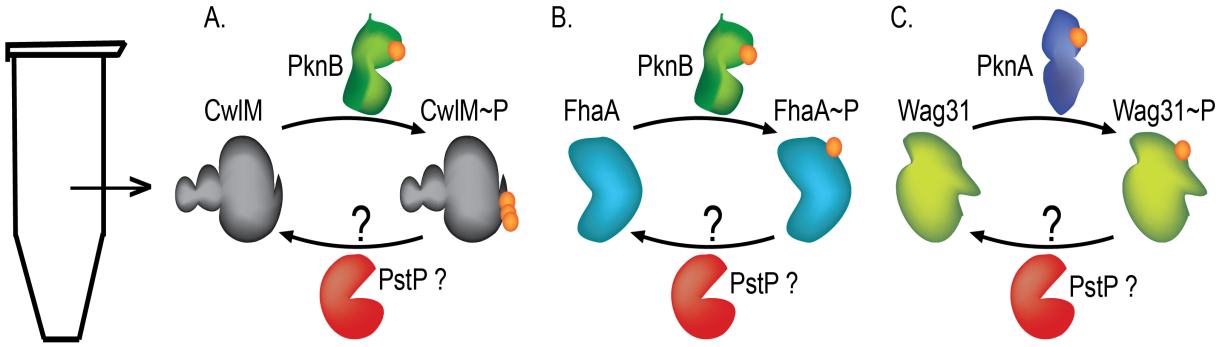

Figure 1.3 Schematic diagram of the *in vitro* phosphatase assay with purified *Mtb* proteins and enzymes

1.12.2 Examine the role of phosphorylation on PstP in regulating different cell wall regulatory pathways

$PstP_{Mtb}$ is itself phosphorylated by PknB at T137, T141 and T174 sites on its cytosolic domain (Sajid *et al.*, 2011). The equivalent sites in *Msmeg* are T134, T138 and T171 respectively. Phosphorylation may affect an enzyme's catalytic activities or specificities

(Johnson and Barford, 1993; Bibb and Nestler, 2005; Ardito *et al.*, 2017). So, it seems probable that the phosphorylations on these sites are important for regulation of PstP's activity and thus might contribute to cell wall regulatory pathways and overall growth of the cell.

***In vitro* approach:**

To understand how each phosphorylation site on PstP might affect its activity or specificity against different substrates directly, I performed *in vitro* phosphatase assays with the purified *Mtb* substrates and individually phospho-mutated PstP cytosolic domains. To understand the effect of phosphorylation, each phospho-site was changed from threonine to a negatively charged amino acid Glutamic acid (E) (Cottin *et al.*, 1999) that mimics a phospho-threonine. These phospho-mimetic $PstP_{Mtb}$ were individually used in assays to see how it affected dephosphorylation of CwlM~P (Figure 1.4A), FhaA~P (Figure 1.4B) and Wag31~P (Figure 1.4C).

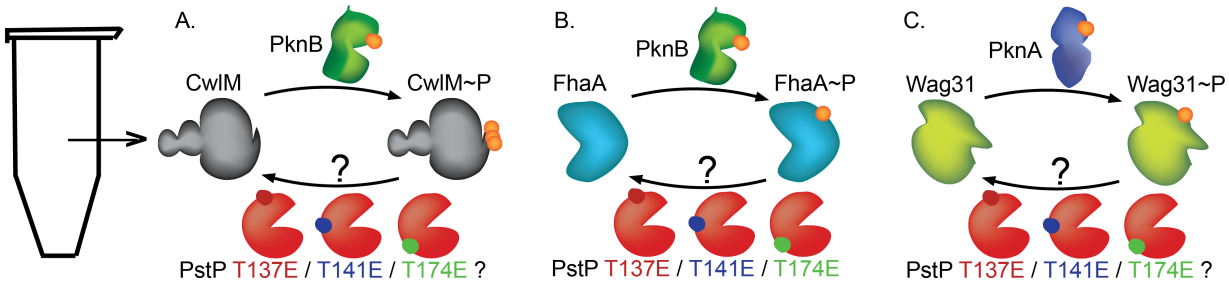

Figure 1.4 Schematic diagram of *in vitro* phosphatase assay with purified *Mtb* proteins and PstP T137E, T141E and T174E

***In vivo* approach:**

Both PknB and PstP have extracellular domains and similar expression profiles (Betts *et al.*, 2002; Kang *et al.*, 2005). The kinase PknB modulates cell wall synthesis by phosphorylating cell wall substrates in response to extracellular signals perceived by its extracellular PG-binding domains. PstP may also dephosphorylate the same substrates upon sensing environmental signals via its extracellular domain. I hypothesize that the phosphorylation of PstP is important to dephosphorylate cell wall regulatory substrates and that misregulating PstP phosphorylation would affect cell growth.

To understand the effect of phospho-misregulated PstP on cell wall metabolism, I used individual *Msmeg* strains with individual phosphomimetic mutations in *pstP* and observed cell growth, length and cell wall metabolism of these strains. The model below (Figure 1.5A) shows an *in vivo* scenario where PstP is supposed to upregulate mycolic acid metabolism in growth by dephosphorylating FAS-II enzymes (KasA in the model) (Molle *et al.*, 2006) but should upregulate PG metabolism if it dephosphorylates CwlM (Boutte *et al.*, 2016). So in growth, to continue both mycolic acid and PG biosynthesis in order to build up the cell wall, PstP should choose CwlM to dephosphorylate but not KasA hypothetically. If PstP's activity or specificity were regulated by its phosphorylation, then misregulating these phosphosites would impair the balance of overall cell wall metabolism via misregulation of PstP's activity against different cell wall regulatory substrates (Figure 1.5B).

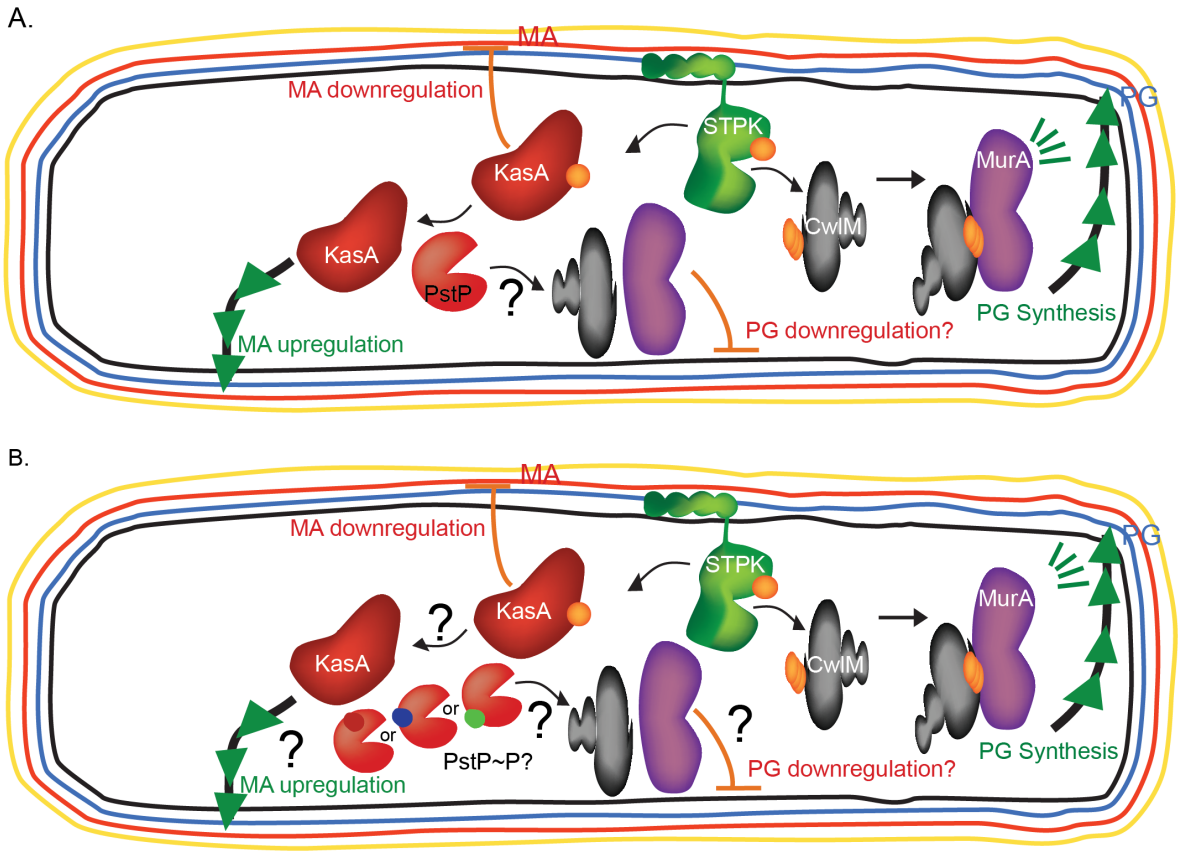

Figure 1.5 An *in vivo* model of the effect of phospho-misregulated PstP on cell wall metabolic pathways

A. Phosphorylated CwlM can interact with and stimulate MurA's (the first enzyme in PG precursor biosynthesis) activity, which should upregulate (represented by green arrowheads) PG synthesis. Phosphorylation inhibits the mycolic acid biosynthesis enzyme KasA's activity which should be in when mycolic acid biosynthesis is downregulated. PstP dephosphorylates KasA and is expected to dephosphorylate CwlM (represented by question mark) in our study. Dephosphorylation of these substrates *in vivo* should revert the effects of phosphorylation (represented by question marks) but both should not be dephosphorylated at the same time to coordinate upregulation of the mycolic acid (MA) and the PG layer.

B. Misregulation of the individual phospho-sites on PstP (represented by red, blue and green circles on PstP) may give an idea of whether PstP's phospho-sites play a role in regulating the cell wall metabolism to coordinate up- or downregulation of different layers of the cell-wall (e.g. MA and PG here) probably by affecting PstP's specificity against different substrates.

1.12.3 Identify the effect of misregulating PstP on antibiotic tolerance

To date, there is no data on antibiotic susceptibility of PstP-misregulated cells. I hypothesize that PstP can be a potential drug target because cell wall regulators are likely to be involved in antibiotic tolerance. The substrates mentioned in this study are all involved in cell wall regulation and phosphorylated by PknA/B. If PstP is the crucial phosphatase, then misregulation of PstP will lead to uncoordinated cell wall regulation, which is supposed to increase antibiotic susceptibility.

***In vivo* approach:**

I used the phospho-site misregulated *pstP*$_{Msmeg}$ strains to find out the role of PstP's phospho-sites in antibiotic tolerance. If cell wall metabolism is imbalanced due to PstP's impaired activity on its cell wall regulatory substrates on account of its misregulated phospho-sites, then an overall disruption in cell wall integrity may increase antibiotic susceptibility (Figure 1.6).

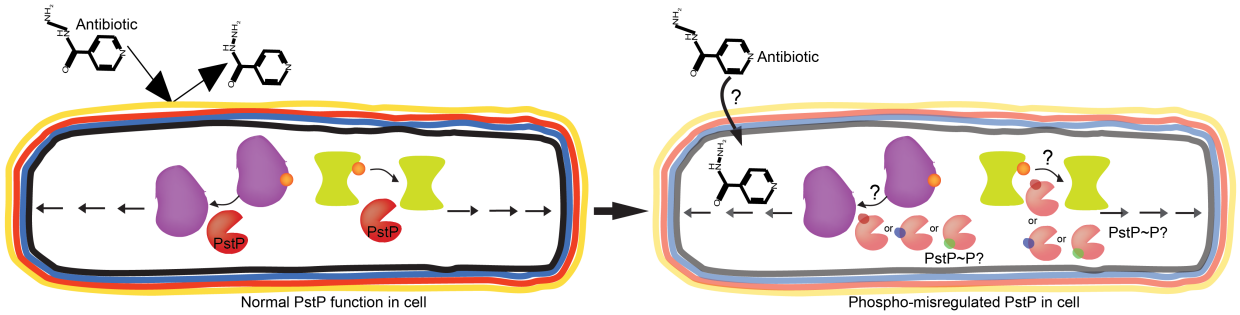

Figure 1.6 An *in vivo* model of effect of PstP's phospho-misregulation on antibiotic tolerance of *Msmeg*.

(Left) An antibiotic tolerant mycobacterial cell is shown where we think that PstP might be contributing to the tolerance by regulating the cell wall metabolism (represented by black arrows) via dephosphorylating different substrates (shown in purple and lime green).

(Right) Misregulating PstP's function via misregulation of its phospho-sites (represented by red, green and blue circles on PstP) may affect its regulatory activity against substrates (represented by question marks) resulting in misregulation of overall cell-wall metabolism (represented by the dimmed out cell wall layers and arrows), which could affect the antibiotic tolerance as well.

Chapter 2

Phosphorylation on PstP regulates cell wall metabolism and antibiotic tolerance in *Mycobacterium smegmatis*

Farah Shamma[1], Kadamba Papavinasasundaram[2], Samantha Y. Quintanilla[1], Aditya Bandekar[2], Christopher Sassetti[2], and Cara C. Boutte[1]*

[1]Department of Biology, University of Texas Arlington, Arlington, Texas

[2]Department of Microbiology and Physiological Systems, University of Massachusetts Medical School, Worcester, Massachusetts

Journal of Bacteriology, Vol. 203, No. 4, 2021, https://doi.org/10.1128/JB.00563-20

Preface

The contents of this chapter were published as: Farah Shamma, Kadamba Papavinasasundaram, Samantha Y. Quintanilla, Aditya Bandekar, Christopher Sassetti, and Cara C. Boutte in the Journal of Bacteriology, Vol. 203, No. 4, (2021). This manuscript describes the effect of a phospho-mimetic mutation on the phospho-site T171 of the essential Serine Threonine Phosphatase PstP on the cell growth, length, peptidoglycan and mycolic acid metabolisms and antibiotic tolerance in *Mycobacterium smegmatis (Msmeg)* and reports the discovery of a novel substrate of PstP *in vitro*.

For the *in vivo* studies, an *Msmeg* strain was used where the native $pstP_{Msmeg}$ was deleted and the $pstP_{Msmeg}$ phospho-mutant alleles were inserted at a phage integration site in the genome. Kadamba Papavinasasundaram from the Sassetti lab constructed the native $pstP_{Msmeg}$ deleted *Msmeg* strain with $pstP_{Mtb}$ cloned at the L5 phage integration site, Aditya Bandekar from the same lab helped with obtaining the strain, I constructed all the $pstP_{Msmeg}$ phospho-mutant and WT strains by swapping these alleles at the L5 site of that strain, performed all the *in vivo* assays, purified all the proteins and performed the *in vitro* assays and my undergraduate researcher Samantha Y. Quintanilla helped with taking some samples in antibiotic susceptibility assays. Some supplementary figures of this published paper have not been included in this chapter so the manuscript is a bit modified accordingly.

2.1 Abstract

Mycobacterium tuberculosis and its relatives, like many bacteria, have dynamic cell walls that respond to environmental stresses. Modulation of cell wall metabolism in

stress is thought to be responsible for decreased permeability and increased tolerance to antibiotics. The signaling systems that control cell wall metabolism under stress, however, are poorly understood. Here, we examine the cell wall regulatory function of a key cell wall regulator, the Serine Threonine Phosphatase PstP, in the model organism *Mycobacterium smegmatis.* We show that the peptidoglycan regulator CwlM is a substrate of PstP. We find that a phospho-mimetic mutation, *pstP* T171E, slows growth, mis-regulates both mycolic acid and peptidoglycan metabolism in different conditions, and interferes with antibiotic tolerance. These data suggest that phosphorylation on PstP affects its activity against various substrates and is important in the transition between growth and stasis.

2.2 Introduction

Tuberculosis (TB), an infectious disease caused by the bacterium *Mycobacterium tuberculosis* (*Mtb*) is one of the leading causes of death from infectious diseases (World Health Organization, 2019). The fact that TB treatment requires at least a six month regimen with four antibiotics is partly due to the intrinsic antibiotic tolerance of *Mtb (Jarlier and Nikaido, 1994; Nguyen, 2016)*. Stressed *Mtb* cells can achieve a dormant or slow-growing state (Seiler *et al.*, 2003; Muñoz-Elías and McKinney, 2006) which exhibits antibiotic tolerance (Wallis *et al.*, 1999), cell wall thickening (Cunningham and Spreadbury, 1998) and altered cell-wall staining (Seiler *et al.*, 2003).

The currently accepted cell wall structure of *Mtb* is composed of three covalently linked layers (Minnikin, 1991): surrounding the plasma membrane, a peptidoglycan (PG) layer

is covalently bound to an arabinogalactan layer. A lipid layer composed of mycolic acids surrounds the arabinogalactan layer, and the inner leaflet of this layer is covalently linked to the arabinogalactan (Kieser and Rubin, 2014). The outer leaflet of the mycolic acid layer contains free mycolic acids, trehalose mycolates and other lipids, glycolipids, glycans and proteins (Marrakchi *et al.*, 2014). The mycolic acid layer, or mycomembrane, is the outer membrane of mycobacteria and is the major contributor to impermeability of the cell wall (Jarlier and Nikaido, 1990; Hett and Rubin, 2008; Hoffmann *et al.*, 2008).

In addition to serving as a permeability barrier, regulation of the cell wall likely contributes to antibiotic tolerance, either through further changes in permeability (Sarathy *et al.*, 2013), or by changing the activity of antibiotic targets (Batt *et al.*, 2020). Several studies have observed changes in the cell wall under stress (Cunningham and Spreadbury, 1998; Betts *et al.*, 2002; Bhamidi *et al.*, 2012; Sarathy *et al.*, 2013). These cell wall changes have been shown to correlate with increased antibiotic tolerance (Xie *et al.*, 2005; Liu *et al.*, 2016; Sarathy *et al.*, 2017). This has led the prevalent model that stress-induced regulation of the cell wall contributes to antibiotic tolerance (Dulberger *et al.*, 2020). While most of the extant data to support this model is correlative, we recently identified a mutant in *Msmeg* which specifically upregulates peptidoglycan metabolism in starvation and also causes decreased antibiotic tolerance in that condition (Boutte *et al.*, 2016). This shows that there is a causal relationship between cell wall regulation and antibiotic tolerance, at least in limited conditions in *Msmeg*.

Reversible protein phosphorylation is a key regulatory tool used by bacteria for

environmental signal transduction to regulate cell growth (Galyov *et al.*, 1993; Wang *et al.*, 1998; Juris *et al.*, 2000; Echenique *et al.*, 2004). In *Mtb*, Serine/Threonine phosphorylation is important in cell wall regulation (Gee *et al.*, 2012). *Mtb* has 11 Serine/Threonine Protein Kinases (STPKs) (PknA, PknB and PknD-L) and only one Serine/Threonine protein phosphatase (PstP) (Cole *et al.*, 1998; Av-Gay and Everett, 2000).

Among the STPKs, PknA and PknB are essential for growth, and phosphorylate substrates many involved in cell growth and division (Sassetti and Rubin, 2003; Kang *et al.*, 2005; Fernandez *et al.*, 2006; Kusebauch *et al.*, 2014; Boutte *et al.*, 2016). Some of these substrates are enzymes whose activity is directly altered by phosphorylation. For example, all the enzymes in the FAS-II system of mycolic acid biosynthesis are inhibited by threonine phosphorylation (Molle *et al.*, 2006; Molle and Kremer, 2010; Veyron-Churlet *et al.*, 2010; Khan *et al.*, 2010; Slama *et al.*, 2011; Vilchèze *et al.*, 2014). There are also cell wall regulators that are not enzymes, but whose phosphorylation by STPKs affects cell shape and growth. For example, the regulator CwlM, once it is phosphorylated by PknB, activates MurA (Boutte *et al.*, 2016), the first enzyme in PG precursor biosynthesis (Marquardt *et al.*, 1992). In the transition to starvation, CwlM is rapidly dephosphorylated in *Msmeg* (Boutte *et al.*, 2016). Mis-regulation of MurA activity increases sensitivity to antibiotics in early starvation (Boutte *et al.*, 2016), implying that phospho-regulation of CwlM promotes antibiotic tolerance. CwlM may also regulate other steps of PG synthesis (Turapov *et al.*, 2018). A recent phospho-proteomic study showed that transcriptional repression of the operon that contains both *pstP* and *pknB* leads to increased phosphorylation of CwlM (Iswahyudi *et al.*, 2019). While the effects

of the individual genes were not separated (Iswahyudi *et al.*, 2019), this suggests that PstP could dephosphorylate CwlM.

PstP is essential in *Mtb* and *Msmeg* (Sharma *et al.*, 2016; DeJesus *et al.*, 2017). It is a member of the Protein phosphatase 2C (PP2C) subfamily of metal-dependent protein Serine/Threonine phosphatases (Chopra *et al.*, 2003) which strictly require divalent metal ions for activity (Cohen, 1989; Barford, 1996). PP2C phosphatases are involved in responding to environmental signals, regulating metabolic processes, sporulation, cell growth, division and stress response in a diverse range of prokaryotes and eukaryotes (Vijay *et al.*, 2000; Irmler and Forchhammer, 2001; Mougous *et al.*, 2007; Lu and Wang, 2008; Bradshaw and Losick, 2015; Bradshaw *et al.*, 2017)(Mougous et al. 2007; Irmler and Forchhammer 2001; Bradshaw and Losick 2015; Bradshaw et al. 2017; Lu and Wang 2008; Vijay et al. 2000). $PstP_{Mtb}$ shares structural folds and conserved residues with the human PP2Cα (Pullen *et al.*, 2004), which serves as the representative of the PP2C family. $PstP_{Mtb}$ has an N-terminal cytoplasmic enzymatic domain, a transmembrane pass and a C-terminal extracellular domain (Chopra *et al.*, 2003).

Many of the proteins known to be dephosphorylated by PstP (Boitel *et al.*, 2003; Chopra *et al.*, 2003; Durán *et al.*, 2005; Sharma *et al.*, 2006; Molle *et al.*, 2006; Sajid *et al.*, 2011) are involved in cell wall metabolism; however, the effects of this activity seem to differ. For example, dephosphorylation of CwlM should decrease PG metabolism in stasis (Boutte *et al.*, 2016). But, dephosphorylation of the FAS-II enzymes (Molle *et al.*, 2006; Molle and Kremer, 2010; Veyron-Churlet *et al.*, 2010; Khan *et al.*, 2010; Slama *et al.*, 2011; Vilchèze *et al.*, 2014) should upregulate lipid metabolism in growth. However,

PG and lipid metabolism are expected to be coordinated (Dulberger *et al.*, 2020). Therefore, PstP must be able to alter substrate specificity in growth and stasis.

$PstP_{Mtb}$ is itself phosphorylated on Threonine residues 137, 141, 174 and 290 (Sajid *et al.*, 2011). We hypothesized that phosphorylation of the threonine residues of PstP might help coordinate activity against different substrates through changes in access to substrates, or through toggling catalytic activity against substrates.

We report here that phospho-ablative and phospho-mimetic mutations at the phospho-site T171 of $PstP_{Msmeg}$ (T174 in $PstP_{Mtb}$) alter growth rate, cell length, cell wall metabolism and antibiotic tolerance in *Msmeg*. Strains of *Msmeg* with *pstP* T171E alleles grow slowly, are unable to properly downregulate PG metabolism and upregulate antibiotic tolerance in the transition to starvation. We observed that the same mutation has nearly opposite effects on mycolic acid layer metabolism. We also report that $PstP_{Mtb}$ dephosphorylates $CwlM_{Mtb.}$

2.3 Materials and Methods

2.3.1 Bacterial strains and culture conditions

All *Mycobacterium smegmatis* mc^2155 ATCC 700084 cultures were started in 7H9 (Becton, Dickinson, Franklin Lakes, NJ) medium containing 5 g/liter bovine serum albumin (BSA), 2 g/liter dextrose, 0.003 g/liter catalase, 0.85 g/liter NaCl, 0.2% glycerol, and 0.05% Tween 80 and incubated at 37°C until log. phase. Hartmans-de Bont (HdB) minimal medium made as described previously (Hartmans *et al.*, 2006) without glycerol was used for starvation assays. Serial dilutions of all CFU counts were plated on LB

Lennox agar (Fisher BP1427-2).

E. coli Top10, XL1Blue and Dh5α were used for cloning and *E. coli* BL21 Codon Plus was used for protein expression. Antibiotic concentrations for *M. smegmatis* were 25 µg/ml kanamycin, 50 µg/ml hygromycin and 20 µg/ml zeocin. Antibiotic concentrations for *E. coli* were 50 µg/ml kanamycin, 25 µg/ml zeocin, 20 µg/ml chloramphenicol and 140 µg/ml ampicillin.

2.3.2 Strain construction

The $PstP_{Msmeg}$-knockdown strain was made first by creating a merodiploid strain and then by deleting the native $pstP_{Msmeg}$ gene from its chromosomal location. The merodiploid strain was generated by introducing a constitutively expressing $pstP_{Mtb}$ gene cloned on an StrR plasmid at the L5 attB integration site. The $pstP_{Msmeg}$ gene (MSMEG_0033) at the native locus was then deleted by RecET-mediated double stranded recombineering approach using a 1.53 kb loxP-hyg-loxP fragment carrying a 125 bp regions flanking the $pstP_{Msmeg}$ gene, as described (Murphy, Papavinasasundaram, and Sassetti 2015). The recombineering substrate was generated by two sequential overlapping PCR of the loxP-hyg-loxP substrate present in the plasmid pKM342. The downstream flanking primer used in the first PCR also carried an optimized mycobacterial ribosome binding site in front of the start codon of MSMEG_0032 to facilitate the expression of the genes present downstream of $pstP_{Msmeg}$ *in* the *Msmeg pstP-pknB* operon.

Deletion of the $pstP_{Msmeg}$ gene was confirmed by PCR amplification and sequencing of

the 5' and 3' recombinant junctions, and the absence of an internal wild-type $pstP_{Msmeg}$ PCR product. The $pstP_{Mtb}$ allele present at the L5 site was then swapped, as described (Schnappinger *et al.*, 2015), with a tet-regulatable $pstP_{Mtb}$ allele (RevTetR-P750-$pstP_{Mtb}$-DAS tag-L5-Zeo plasmid). The loxP-flanked *hyg* marker present in the chromosomal locus was then removed by expressing Cre from pCre-sacB-Kan, and the Cre plasmid was subsequently cured from this strain by plating on sucrose. We named this strain CB1175.

Different alleles of *pstP* were attained by swapping the wild-type (WT) allele at L5 site of CB1175 as described (Pashley and Parish, 2003). In order to do so, WT and the phosphoablative alleles of $pstP_{Msmeg}$ alleles were at first cloned individually into a kanamycin resistant-marked L5 vector pCT94 under a TetO promoter to generate vectors pCB1206-1208 and pCB1210, which would swap out the zeocin-resistance marked vector at the L5 site in CB1175. The strong TetO promoter in the vectors pCB1206-1208 and pCB1210 was swapped with an intermediate strength promoter p766TetON6 (cloned from the vector pCB1030 (pGMCgS-TetON-6 sspB) to generate the L5 vectors pCB1282-85. pCB1285 was used as the parent vector later on to clone in the phosphomimetic $pstP_{Msmeg}$ alleles under p766TetON6.

These kanamycin resistance-marked vector constructs were then used to swap out the zeocin resistance-marked vector at the L5 site of CB1175 to attain different allelic strains of $pstP_{Msmeg}$ as described (Pashley and Parish, 2003).

2.3.3 Growth Curve assay

At least three biological replicates of different *pstP*$_{Msmeg}$ allele variants (T171A, T171E and WT) were grown in 7H9 media up to log. phase. The growth curves were performed in non-treated 96 well plate using plate reader (BioTek Synergy neo2 multi mode reader) in 200µl 7H9 media starting at OD_{600}=0.1. Exponential growth equation was used to calculate the doubling times of each strain using the least squared ordinary fit method in GraphPad Prism (Version 7.0d). P values were calculated using two-tailed, unpaired t-tests.

2.3.4 Cell staining

Three biological replicate strains of each *pstP* allelic variant (T171A, T171E and WT) were used for this assay. For staining cells in log. phase, 100µl culture in 7H9 was incubated at 37°C with 1µl of 10mM DMN-Tre for 30 minutes and 1µl of 10mM HADA for 15 minutes. Cells were then pelleted and resuspended in 1x phosphate buffered saline (PBS) supplemented with 0.05% Tween 80 and fixed with 10µl of 16% paraformaldehyde (PFA) for 10 minutes at room temperature. Cells were then washed and resuspended in PBS + Tween 80.

For starvation microscopy, cultures were shaken for 4 hours in HdB media without glycerol at 37°C. 500µl of each culture were pelleted and concentrated to 100µl, then incubated at 37°C with 1µl of 10mM DMN-Tre for 1 hour and 3µl of 10mM HADA for 30 minutes. Cells were then washed and fixed as above. The total time of starvation before fixation was 5.5 hours.

2.3.5 Microscopy and Image Analysis

Cells were imaged with a Nikon Ti-2 widefield epifluorescence microscope with a Photometrics Prime 95B camera and a Plan Apo 100x, 1.45 NA objective lens. The green fluorescence images for DMN-Tre staining were taken with a 470/40nm excitation filter and a 525/50nm emission filter. Blue fluorescence images for HADA staining were taken using 350/50nm excitation filter and 460/50nm emission filter. All images were captured using NIS Elements software and analyzed using FIJI and MicrobeJ (Ducret *et al.*, 2016). For cell detection in MicrobeJ, appropriate parameters for length, width and area were set. The V-snapping cells were split at the septum so that each daughter cell could be considered as a single cell. Any overlapping cells were excluded from analysis.

Length and mean-intensities of HADA and DMN-Tre signals of 300 cells from each of $pstP_{Msmeg}$ T171A, $pstP_{Msmeg}$ T171E and $pstP_{Msmeg}$ WT (100 cells from each of three biological replicate strain of each genotype) were quantified using MicrobeJ. The values of the mean intensities of 300 cells of each *pstP* allelic mutant and WT are represented in the graph as percentages of the highest mean intensity from all the cells in that experiment. GraphPad Prism (v7.0d) was used to generate the graphs and perform t-tests. To compare two groups ($pstP_{Msmeg}$ T171A vs. $pstP_{Msmeg}$ WT and $pstP_{Msmeg}$ T171E vs. $pstP_{Msmeg}$ WT), the lengths and the percentage-intensity values of 300 cells per *pstP* allelic variant genotype (100 per biological replicate strain per genotype) were used as data array inputs to perform unpaired, two-tailed t-tests in GraphPad Prism.

Medial intensity profiles of DMN-Tre and HADA signals in cells from different *pstP* allelic strains in log. phase and starvation analyzed with MicrobeJ were plotted on Y-axis over relative positions of cells using the "XStatProfile" plotting feature in MicrobeJ to show subcellular localization of fluorescent intensities.

Demographs of DMN-Tre and HADA signal intensity across cell lengths in log. phase and starvation were built using the "Demograph" feature of MicrobeJ by plotting the medial intensity profiles of DMN-Tre and HADA signals.

2.3.6 Western Blots

Cultures were grown in 7H9 to OD_{600}=0.8 in 10ml 7H9 media, pelleted and resuspended in 500µL PBS with 1mM PMSF and lysed (MiniBeadBeater-16, Model 607, Biospec). Supernatants from the cell lysate were run on 12% resolving Tris-Glycine gels and then transferred onto PVDF membrane (GE Healthcare). Rabbit a-strep antibody (1:1000, Abcam, ab76949) in TBST buffer with 0.5% milk and goat a-rabbit IgG (H+L) HRP conjugated secondary antibody (1:10,000, ThermoFisher Scientific 31460) in TBST were used to detect PstP-strep. For starvation experiments, cultures were first grown to log. phase, then starved in HdB no glycerol media starting at OD=0.5 for 1.5 hour.

For Western blots of *in vitro* assays, samples were run on 12% SDS gel (Mini-Protean TGX, Biorad, 4561046) and then transferred onto PVDF membrane (GE Healthcare). Mouse a-His antibody (1:1000, Genscript A00186) in TBST buffer with 0.5% BSA and goat a-mouse IgG (H+L) HRP conjugated secondary antibody (1:10,000, Invitrogen A28177) were used to detect His-tagged proteins on the blot. The blots were stripped (Thermo Scientific, 21059) and re-probed with Rabbit a-Phospho-Threonine antibody

(1:1000, Cell Signaling #9381) and goat a-rabbit IgG (H+L) HRP conjugated secondary antibody (1:10,000, ThermoFisher Scientific 31460) to detect phosphorylation on the blots.

2.3.7 Antibiotic assays

Biological triplicates of each *pstP* allelic variant were used for all antibiotic assays. For antibiotic assays in log. phase, log. phase cultures were diluted in 7H9 media to OD600= 0.05 before treatment. For starvation assays, cells were grown to OD_{600}=0.5, pelleted, washed and resuspended in HdB starvation (with no glycerol and 0.05% Tween) media at OD_{600}=0.3 and incubated at 37°C for a total of 5.5 hours. The cultures were then diluted to OD_{600}=0.05 before antibiotic treatment. 8 µg/ml and 45 µg/ml meropenem was used for log. phase and starved cultures, respectively. 10 µg/ml and 90 µg/ml isoniazid was added to log. phase and starved cultures, respectively. 100 µg/ml and 900 µg/ml D-cycloserine was used for log. phase and starved cultures, respectively. 50 µg/ml and 360 µg/ml trimethoprim was added to log. phase and starved cultures, respectively. Samples from the culture were serially diluted and plated on LB agar before and after treatment, and colony forming units were calculated.

2.3.8 Protein Purification

All the proteins were expressed using *E. coli* BL21 Codon Plus cells.

N-terminally his-MBP tagged $PknB_{Mtb}$ was expressed and purified as described (Kieser *et al.*, 2015). His-$PstP_cWT_{Mtb}$ (1-300 amino acids of the cytosolic domain (Gupta *et al.*, 2009) and His-SUMO-$CwlM_{Mtb}$ were both expressed overnight by IPTG induction (1mM

and 1.3mM, respectively), purified on Ni-NTA resin (G-Biosciences, #786-940 in 5 ml Bio-Scale™ Mini Cartridges, BioRad #7324661), then dialyzed, concentrated and run over size exclusion resin (GE Biosciences Sephacryl S-200 in HiPrep 26/70 column) to obtain soluble proteins. The buffer for His-SUMO-CwlM$_{Mtb}$ was 50mM Tris pH 8, 350mM NaCl, 1mM DTT and 10% glycerol. The buffer for His-PstP$_c$WT$_{Mtb}$ was 50mM Tris pH 7.5, 350mM NaCl, 1mM DTT and 10% glycerol. 20mM imidazole was added to each buffer for lysis and application to the Ni-NTA column, and 250mM imidazole was added for elution. His-PstP$_c$T174E$_{Mtb}$ was expressed and purified using the same conditions and buffers used for His-PstP$_c$WT$_{Mtb}$.

2.3.9 *In vitro* Dephosphorylation assay

Purified His-SUMO-CwlM$_{Mtb}$ was phosphorylated with the purified kinase His-MBP-PknB$_{Mtb}$ for 1 hour at room temperature in presence of 0.5mM ATP, 1mM $MnCl_2$ and buffer (50mM Tris pH 7.5, 250mM NaCl, and 1mM DTT). The amount of kinase was one-tenth of the amount of substrate in the phosphorylation reaction. To stop the kinase reaction by depleting ATP, 0.434 units of calf intestinal alkaline phosphatase (Quick CIP, NEB, MO525S) per µg of His-SUMO-CwlM$_{Mtb}$ was added to the reaction mixture and incubated for 1 hour at 37°C. The reaction mixture was then divided into five parts for the different phosphatase samples and a control with buffer.

Two individually expressed and purified batches of both His-PstP$_c$WT$_{Mtb}$ and His-PstP$_c$T1714E$_{Mtb}$ were used as biological replicates to perform the dephosphorylation assay. The reaction was carried out at room temperature for up to 90 minutes in presence of phosphatase buffer (50mM Tris pH 7.5, 10mM $MnCl_2$, and 1mM DTT). The

amount of phosphatase used was half the amount of His-SUMO-CwlM$_{Mtb}$.

The intensities of the a-His and the a-Phospho-Threonine signals on the blots were quantified with FIJI. The intensities of the a-His and the a-Phospho-Threonine signals at each time-point were normalized against the respective antibody-signal intensity at 0m. These relative intensities were used to calculate a-Phospho-Threonine/a-His for each time-point and the values were plotted over time using GraphPad Prism (version 7.0d).

2.4 Results

2.4.1 Phospho-site T171 of PstP$_{Msmeg}$ impacts growth rate

PstP is necessary for cell growth in *Msmeg* (Sharma *et al.*, 2016; Iswahyudi *et al.*, 2019) and phosphorylation increases PstP$_{Mtb}$'s activity against small molecule substrates *in vitro* (Sajid *et al.*, 2011). To see if the phosphorylations on PstP regulate cell growth, we made *Msmeg* strains with either phospho-ablative (T>A) or phospho-mimetic (T>E) alleles (Cottin *et al.*, 1999) at each of the three conserved phosphorylation sites of PstP$_{Mtb}$ (Pullen *et al.*, 2004; Sajid *et al.*, 2011) (Figure 2.1A) and performed growth curves. We found that biological replicates of the T134A, T134E, T138A and T138E mutant strains had bi-modal distributions of doubling times (Figure 2.1B). Phospho-sites T134 and T138 in PstP$_{Mtb}$ map to the flap subdomain (Pullen *et al.*, 2004) (Figure 2.1A). This subdomain varies greatly in sequence and structure across different PP2C family members and has been shown to be important in regulating substrate binding, specificity and catalytic activity (Pullen *et al.*, 2004; Greenstein *et al.*, 2007; Schlicker *et al.*, 2008; Su and Forchhammer, 2013). Particularly, T138A and T138E variants of the serine threonine phosphatase tPphA from *Thermosynechococcus elongatus* showed

differences in substrate reactivity (Su and Forchhammer, 2013). This suggests that phosphorylation at T134 and T138 could be very important in regulating the normal activity of $PstP_{Msmeg}$ in the cell. We think that the inconsistent doubling times of those strains result may result from the formation of suppressor mutants, which we will study in future work.

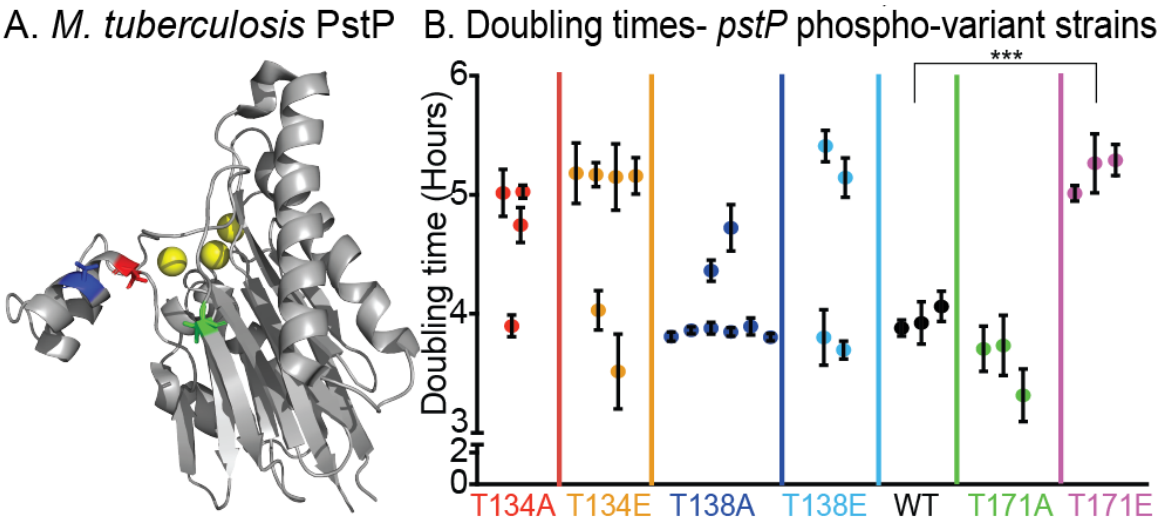

Figure 2.1 Phospho-site on PstP affects growth

(A) Crystal structure of PstP from *M. tuberculosis* ($PstP_{Mtb}$) (Pullen et al. 2004). The threonine (T) sites on $PstP_{Mtb}$ phosphorylated by the kinases PknA and PknB (Sajid et al. 2011) are highlighted on the structure: red- $PstP_{Mtb}$ T137 (T134 in $PstP_{Msmeg}$), blue- $PstP_{Mtb}$ T141 (T138 in $PstP_{Msmeg}$) and green- $PstP_{Mtb}$ T174 (T171 in $PstP_{Msmeg}$).

B) Doubling times of strains containing $pstP_{Msmeg}$WT, phospho-ablative mutant alleles $pstP_{Msmeg}$ T134A, T138A and T171A and phospho-mimetic mutant alleles $pstP_{Msmeg}$ T134E, T138E and T171E. Each dot is the mean of doubling times from two to three different experiments on different dates of a single isolated clone. The error bars represent the standard deviation. P value= 0.0009.

The *Msmeg* strains with *pstP* T171A and T171E mutations showed consistent and reproducible growth rates (Figure 2.1B). The T171A mutants showed no significant difference in doubling time compared to the wild-type, but the T171E grew more slowly than the wild-type. Since T171E mimics constitutive phosphorylation, this result suggests that the continuous presence of a phosphate on T171 downregulates or interferes with cell growth.

2.4.2 $PstP_{Mtb}$ WT and $PstP_{Mtb}$ T174E dephosphorylate $CwlM_{Mtb}$ *in vitro.*

Only a few substrates of PstP have been biochemically verified: some STPKs including PknA and PknB (Boitel *et al.*, 2003; Chopra *et al.*, 2003; Durán *et al.*, 2005; Sajid *et al.*, 2011), KasA and KasB (Molle *et al.*, 2006), and EmbR (Sharma *et al.*, 2006). The STPK PknB phosphorylates CwlM, which is an activator of PG biosynthesis (Boutte *et al.*, 2016). CwlM is rapidly dephosphorylated in the transition to starvation in *Msmeg* (Boutte *et al.*, 2016), and becomes hyper-phosphorylated when PstP is depleted in *Msmeg* (Iswahyudi *et al.*, 2019) which suggests PstP dephosphorylates CwlM.

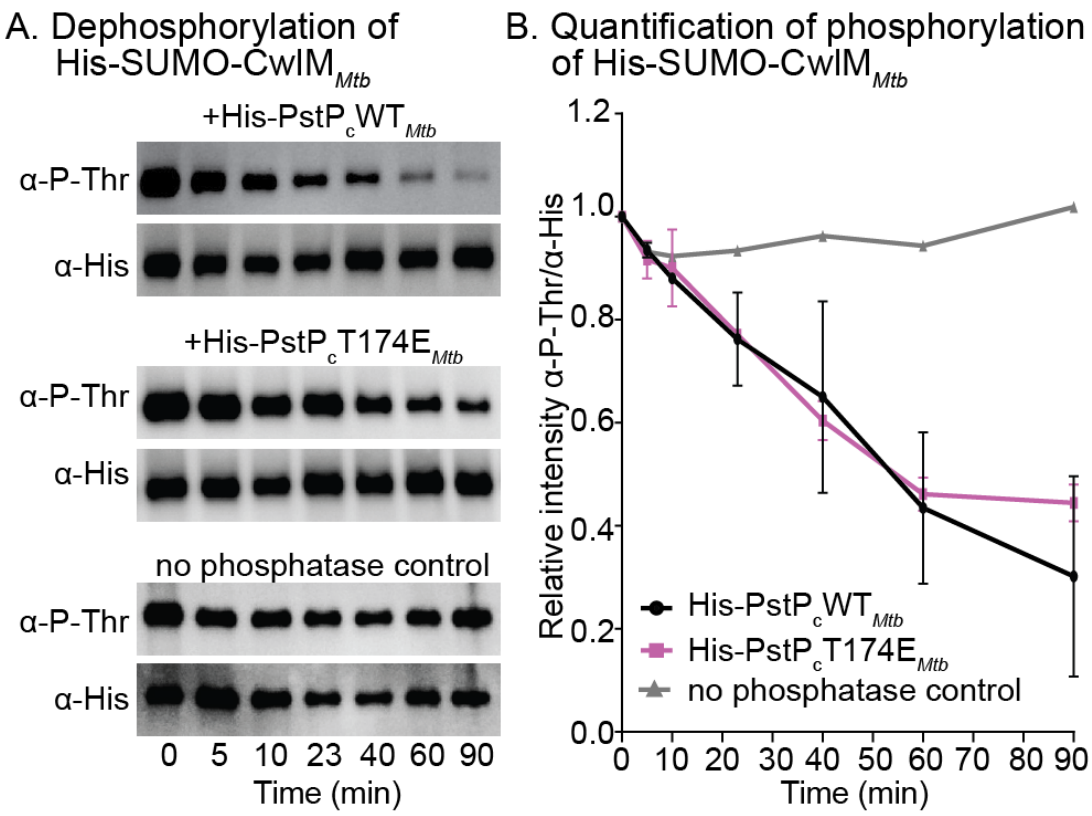

Figure 2.2 PstP$_{Mtb}$ dephosphorylates CwlM$_{Mtb}$

(A) α-P-Thr and α-His Western blots of *in vitro* phosphatase reactions with His-PstP$_c$WT$_{Mtb}$ (top panel) and His-PstP$_c$T174E$_{Mtb}$ (middle panel), and no phosphatase control (bottom panel) and phosphorylated His-SUMO-CwlM$_{Mtb}$. Assay was performed at least twice with two individually purified batches of each phosphatase, one set of images is shown here.

(B) Quantification of relative intensities of α-P-Thr over α-His on Western blots. P values were calculated using two-tailed unpaired t-test. All the P values of WT vs. T171E at any given time were non-significant. P values of WT vs T171E at 5min = 0.683, 10min= 0.809, 23min= 0.934, 40min= 0.831, 60min= 0.876 and 90min= 0.545. The error bars represent standard error of means.

To test whether PstP and its T174 (T171 in *Msmeg)* phospho-mimetic variant directly dephosphorylate CwlM, we performed an in *vitro* biochemical assay with purified *Mtb* proteins. We purified His-MBP-PknB$_{Mtb}$, His-SUMO-CwlM$_{Mtb}$ and the cytoplasmic region

of $PstP_{Mtb}$ that has the catalytic domain (His-$PstP_cWT_{Mtb}$ or $PstP_cT174E_{Mtb}$). PstP dephosphorylates itself rapidly (Sajid *et al.*, 2011), so the purified form is unphosphorylated. We phosphorylated His-SUMO-$CwlM_{Mtb}$ by His-MBP-$PknB_{Mtb}$, stopped the phosphorylation reaction with Calf Intestinal Phosphatase, and then added His-$PstP_cWT_{Mtb}$ or $PstP_cT174E_{Mtb}$ to His-SUMO-$CwlM_{Mtb}$~P. Our control assay with His-SUMO-CwlM~P without $PstP_cWT_{Mtb}$ or $PstP_cT174E_{Mtb}$ showed that the phosphorylation on the substrate is stable (Figure 2.2A, bottom panel). The phosphorylation signal on His-SUMO-$CwlM_{Mtb}$ started decreasing within 5 minutes after addition of His-$PstP_cWT_{Mtb}$ and kept decreasing over a period of 90 minutes (Figure 2.2A, top panel). This is direct biochemical evidence that the PG-regulator $CwlM_{Mtb}$ is a substrate of $PstP_{Mtb.}$ We observed that the WT and T174 phospho-mimetic forms of $PstP_{Mtb}$ have no significant differences in activity against His-SUMO-$CwlM_{Mtb}$~P *in vitro* (Figure 2.2B).

These data show that, *in vitro,* the activity of the catalytic domain of PstP against a single substrate is not affected by a negative charge on $T171_{Msmeg}$/$T174_{Mtb}$. The phenotypes of the full-length *pstP* T171 phospho-alleles (Figure 2.1B, 2.3, 2.4 and 2.5) indicate that this *in vitro* data do not reflect the full complexity of PstP's regulation *in vivo*.

2.4.3 Phospho-site T171 of $PstP_{Msmeg}$ regulates cell length

To assess how the phospho-site T171 affects growth, we examined the cell morphology of *pstP* T171 mutants and wild-type (Figure 2.3A and B). The quantification of cell length revealed that the *pstP* T171A cells were shorter (mean=4.26 ± 0.076) in log. phase than the wild-type cells (mean= 4.503 ± 0.07) (Figure 2.3A). The *pstP* T171E

strain has cell lengths similar to the wild-type (difference between means= 0.053 ± 0.116) (Figure 2.3A and B) despite the slower growth (difference between means= -1.37 ± 0.116) (Figure 2.1B) in log. phase.

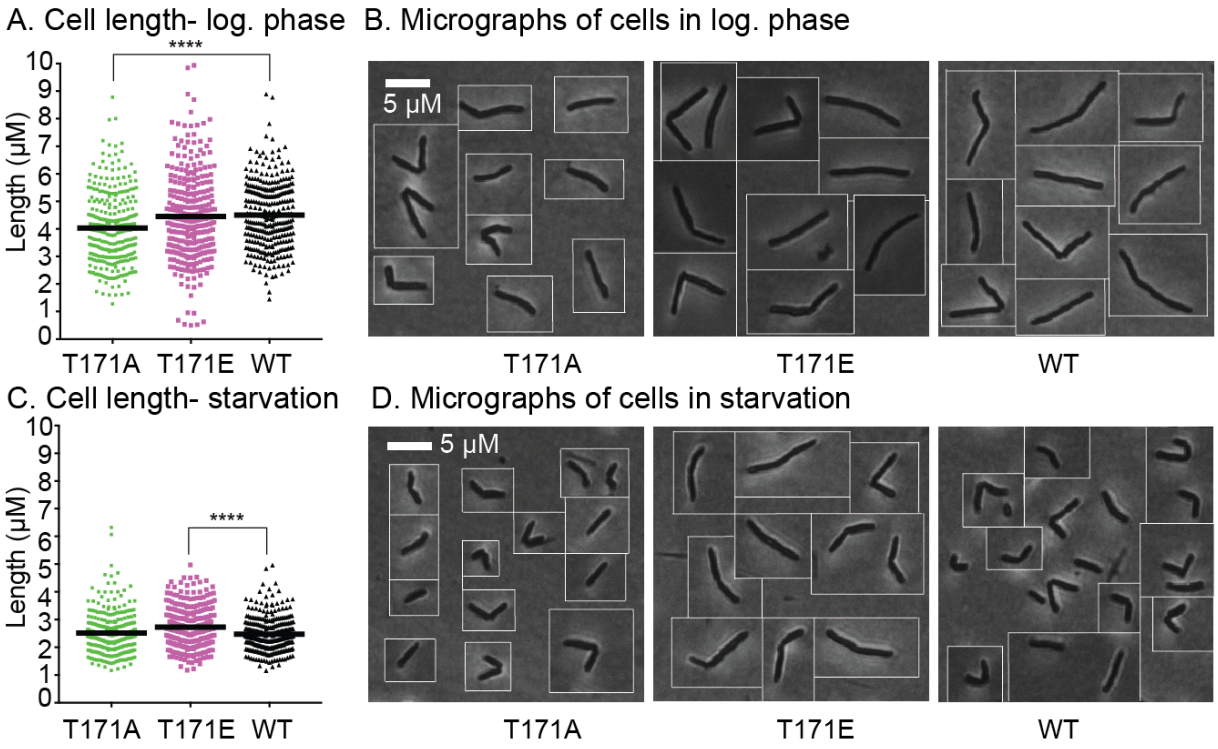

Figure 2.3 Phospho-site T171 on PstP$_{Msmeg}$ is important in regulating cell length

(A) Quantification of cell lengths of isogenic *pstP* allele strains (T17A, T171E and WT) grown in 7H9 in log. phase. 100 cells from each of three biological replicates of each *pstP* allelic variant were measured. P values were calculated by unpaired t-test. P value = 0.000005.

(B) Representative phase images of cells from (A).

(C) Quantification of cell lengths of isogenic *pstP* allele strains (T17A, T171E and WT) after starvation in HdB with no glycerol for five and a half hours. 100 cells from each of three biological replicates of each *pstP* allelic genotype were measured. P values were calculated by unpaired t-test. P value= 0.000003.

(D) Representative phase images of cells from (C).

PstP could promote the transition from growth to stasis by downregulating the activity of some growth regulatory substrates, such as CwlM, PknA or PknB, which all promote growth when phosphorylated (Boitel *et al.*, 2003). PstP likely has dozens of other substrates which may be regulated similarly (Boitel *et al.*, 2003; Chopra *et al.*, 2003; Sajid *et al.*, 2011; Boutte *et al.*, 2016; Iswahyudi *et al.*, 2019). To test if phospho-site T171 of $PstP_{Msmeg}$ affects the transition to stasis, we transferred the strains from log. phase to minimal HdB media with Tween 80 as the only source of carbon, which leads *Msmeg* cells to reductively divide (Wu *et al.*, 2016). We aerated the cultures for 5.5 hours before imaging (Figure 2.3C and D). The effects of phospho-mutations of $PstP_{Msmeg}$ on starved cells were the inverse of what we saw in the log. phase. $pstP_{Msmeg}$ T171E cells in starvation were longer than the wild-type and T171A, and looked like log. phase cells. These data imply that phosphorylation on T171 of $PstP_{Msmeg}$ is involved in cell size regulation upon carbon starvation.

2.4.4 Phospho-site T171 of $PstP_{Msmeg}$ regulates cell wall metabolism

Since $pstP_{Msmeg}$ T171 seems to play a role in regulating cell length in growth and stasis, we hypothesized that it affects cell wall metabolism in different phases. To test this, we used fluorescent dyes that preferentially stain metabolically active cell wall (Kuru *et al.*, 2012; Kamariza *et al.*, 2018). We stained T171 allele variant cells from log. phase and after 5.5 hours of carbon starvation with both the fluorescent D-amino acid HADA, which is incorporated into the PG (Kuru *et al.*, 2012; García-Heredia *et al.*, 2018; Baranowski *et al.*, 2019) (Figure 2.4A and C) and the fluorescent trehalose DMN-Tre, which stains the mycomembrane (Kamariza *et al.*, 2018) (Figure 2.4B and D).

The PG staining intensity between the strains was the same in log. phase (Figure 2.4A, Figure 2.5A and Figure 2.6A). In starvation, the *pstP*$_{Msmeg}$ T171E mutant stained much more brightly with HADA than the other strains (Figure 2.4C and E, Figure 2.6C). This suggests that phosphorylation on PstP$_{Msmeg}$ T171 may inhibit the downregulation of PG layer biosynthesis in the transition to stasis, but that this phospho-site is not important in modulating PG metabolism during rapid growth. The HADA staining is higher at the poles in starved T171E compared to T171A and wild-type cells (Figure 2.4E, Figure 2.6C).

Staining with DMN-Tre shows the inverse pattern of HADA staining. DMN-Tre stains the trehalose mycolates leaflet of the mycomembrane (Kamariza *et al.*, 2018). The mean intensities of the *pstP*$_{Msmeg}$ allelic variants are similar in starvation (Figure 2.4D). The intensity profiles of DMN-Tre signal (Figure 2.4F, Figure 2.6D) shows that the T171E cells have higher DMN-Tre signal at the poles and lower signal at the septal region compared to T171A and wild-type. Our HADA and DMN-Tre signal intensity profile analysis in starvation (Figure 2.4E and F, Figure 2.6C and D) suggest that the T171E cells prioritize elongation, which may account for their greater length in starvation (Figure 2.3C and D).

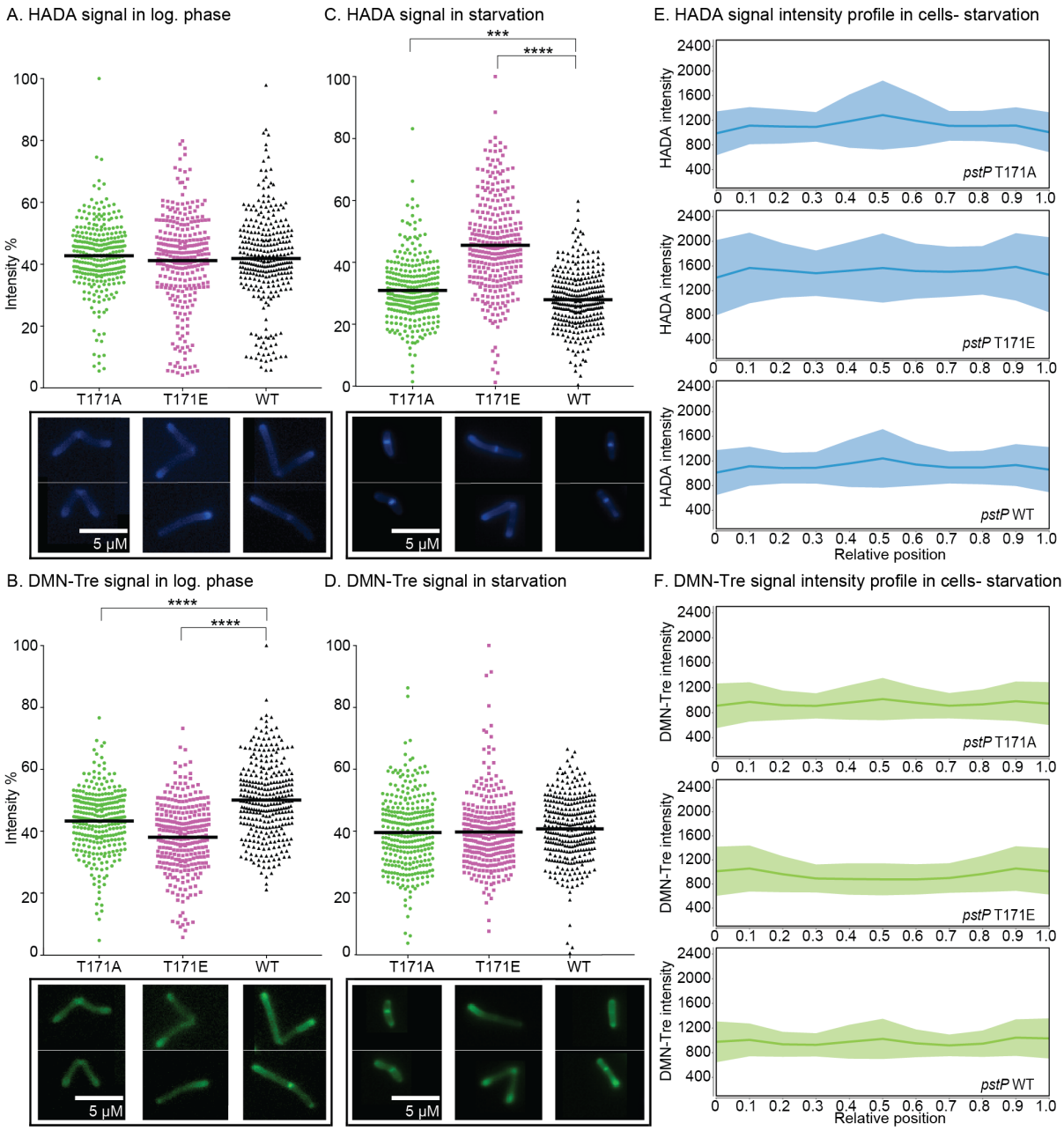

Figure 2.4 Phospho-site T171 on PstP$_{Msmeg}$ alters cell wall staining.

(A) and (B) Quantification of mean intensities of HADA (A) and DMN-Tre (B) signals of *pstP* allele strains (WT, T17A and T171E) in log. phase cells, with representative cells below. In B, P values of both WT vs. T171A and WT vs. T171E= 0.000001.

(C) and (D) Quantification of mean intensities of HADA (C) and DMN-Tre (D) signals of starved *pstP* allele strains (WT, T17A and T171E) after 5.5 hours in HdB with no

glycerol, with representative cells below. In C, P value of WT vs. T171A= 0.0002 and WT vs. T171E = 0.000001.

(E) and (F) Intensity profiles of HADA (E) and DMN-Tre (F) signal in cells from *pstP* allele strains (WT, T17A and T171E) after starving for 5.5 hours in HdB with no glycerol. Shaded region denotes standard deviation and solid line represents the mean intensity values.

Signal intensities from at least 100 cells from each of three biological replicates of every *pstP* allelic variant genotype were analyzed in MicrobeJ. In A-D the values of the intensities are represented in percentages of the maximum value of all intensities for all strains either in log. phase or starvation. P values were calculated by a two-tailed, unpaired t-test on all 300 values of each *pstP* allelic variant genotype (WT, T17A and T171E) using GraphPad Prism (v7.0d) (A-D).

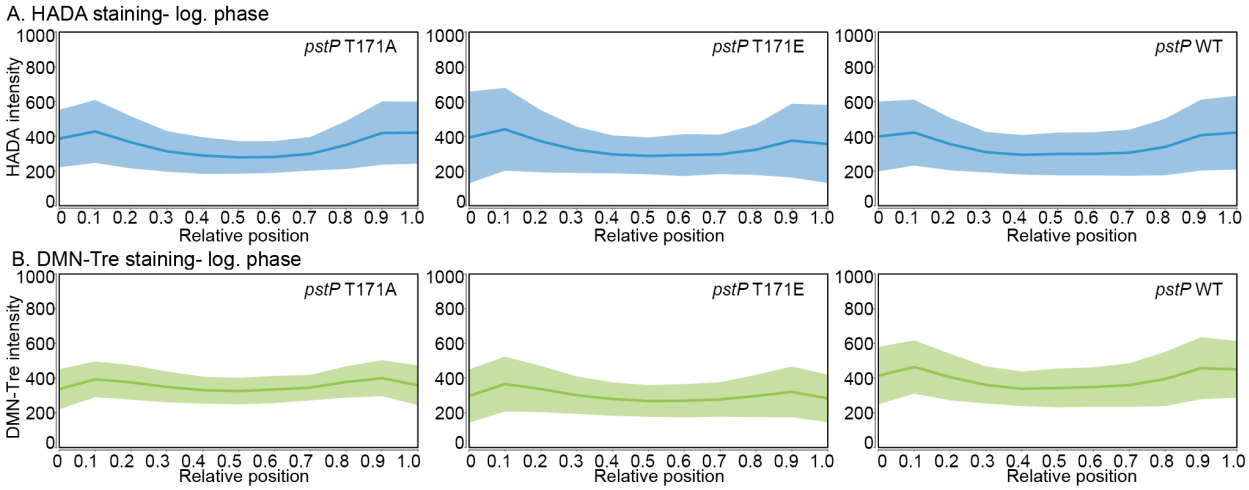

Figure 2.5 Intensity profiles of *pstP* allele strains

(A) and (B) Intensity profiles of HADA (A) and DMN-Tre (B) signal in cells (pole to pole) from *pstP* allele strains (WT, T17A and T171E) in log. phase. Shaded region represents standard deviation. Solid line represents mean of intensities. Biological triplicates of each *pstP* allelic variant were analyzed. At least 265 cells from each of the *pstP* allelic variant (at least 62 cells from each biological triplicate strain of each genotype) in log. phase were used to plot the signal intensities.

In log. phase, however, both mutants show a significant decrease in DMN-Tre signal compared to the wild-type (Figure 2.4B, Figure 2.5B and Figure 2.6B), although the *pstP*$_{Msmeg}$ T171E mutant has the weakest staining. DMN-Tre is incorporated via Ag85-mediated trehalose mycolate metabolism of the mycomembrane (Kamariza *et al.*, 2018). Inhibition of cytoplasmic mycolic acid synthesis through isoniazid treatment decreases DMN-Tre staining, and DMN-Tre fluorescence is sensitive to the hydrophobicity of the membrane (Kamariza *et al.*, 2018).

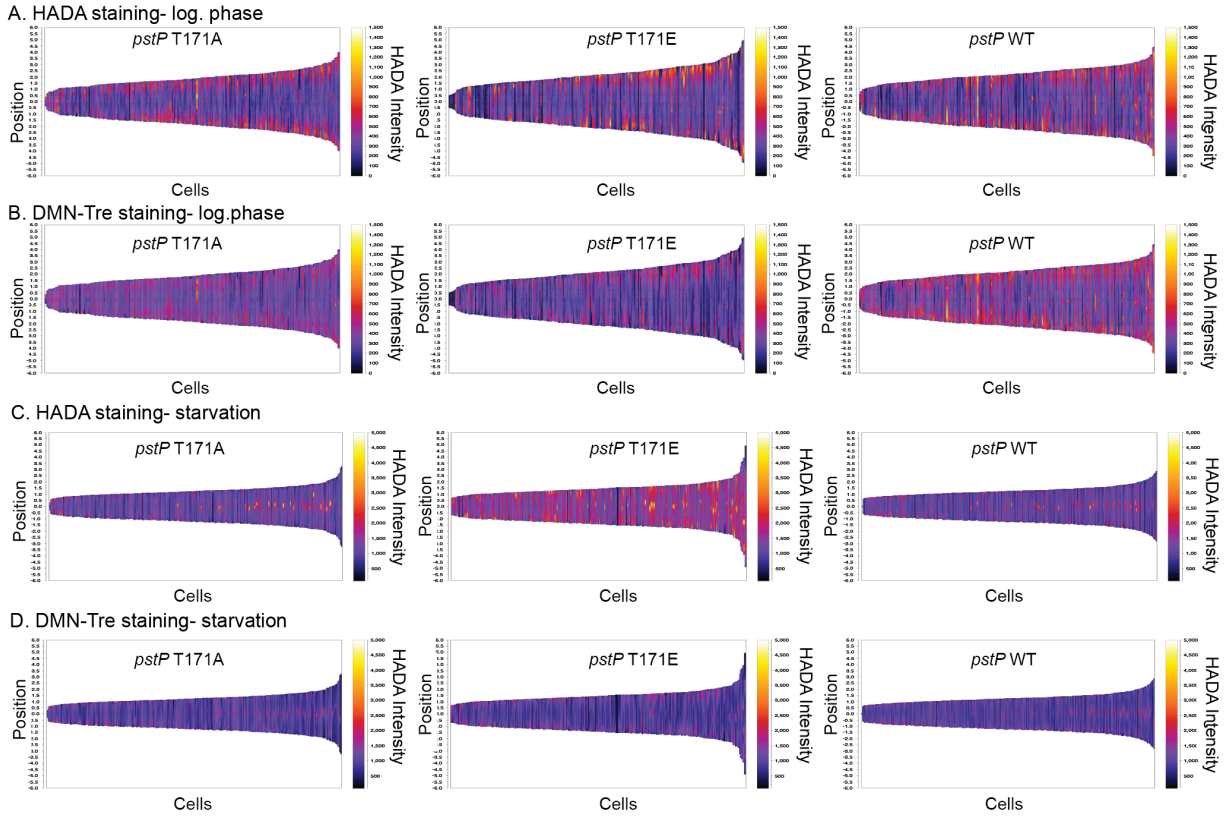

Figure 2.6 Demographic profiles of HADA and DMN-Tre intensity signals in *pstP*$_{Msmeg}$ allele strains in log. phase and starvation

(A) and (B) Demographs showing intensities of fluorescent dyes HADA (A) and DMN-Tre (B) signal in individual cells from *pstP* allele strains (WT, T17A and T171E) in log. phase. (C) and (D) Demographs showing intensities of HADA (C) and DMN-Tre (D) signal in individual cells starved in HdB with no glycerol for 5.5 hours from *pstP* allele strains (WT, T17A and T171E).

Biological triplicates of each *pstP* allelic variant were analyzed. Signal intensities from at least 265 cells from each *pstP* allelic variant (at least 62 cells from each biological triplicate of each genotype) in log. phase were plotted in the demograph (A) and (B). Signal intensities from at least 300 cells from each *pstP* allelic variant (at least 100 cells from each biological triplicate strain of each genotype) in starvation were plotted in the demograph (C) and (D).

Our data (Figure 2.4A, C and F, Figure 2.5A, Figure 2.6A and C) suggest that phosphorylation on $PstP_{Msmeg}$ T171 impacts PG layer metabolism in starvation, but not growth. But the same phosphorylation appears to regulate the trehalose mycolate metabolism in growth, but not starvation (Figure 2.4B, D and F, Figure 2.5B, Figure 2.6B and D).

2.4.5 Phospho-site T171 of $PstP_{Msmeg}$ affects antibiotic tolerance

Stresses that arrest cell growth in mycobacteria are associated with increased antibiotic tolerance (Wayne and Hayes, 1996; Betts *et al.*, 2002; Deb *et al.*, 2009; Sarathy *et al.*, 2013). We hypothesized that if *Msmeg* fails to downregulate PG synthesis in starvation, (Figure 2.4C and E, Figure 2.6C), then it might be more susceptible to a PG targeting drug. We treated $pstP_{Msmeg}$ WT, T171A and T171E strains in log. phase and starvation with meropenem, which targets the cross-linking in the PG cell wall (Cordillot *et al.*, 2013), and quantified survival by CFU. We saw that the $pstP_{Msmeg}$ T171E strain was more susceptible in starvation, compared to $pstP_{Msmeg}$ T171A and wild-type strains (Figure 2.7B), but survived similarly in log. phase (Figure 2.7A), except at very late time points when it was more tolerant.

We also treated *pstP*$_{Msmeg}$ wild-type, T171A and T171E strains in log. phase and starvation with D-cycloserine, which inhibits incorporation of D-alanine into PG pentapeptides in the cytoplasm (Neuhaus and Hammes, 1981; Feng and Barletta, 2003). The results were similar to those in meropenem: the strains survived similarly in log. phase (Figure 2.7C), but the *pstP*$_{Msmeg}$ T171E strain was more sensitive in starvation (Figure 2.7D). The apparent failure of the *pstP*$_{Msmeg}$ T171E strain to downregulate PG synthesis (Figure 2.4C and E, Figure 2.6C) likely makes it more sensitive to both the PG inhibitors in starvation (Figure 2.7B and D).

Next, we treated our wild-type and *pstP*$_{Msmeg}$ T171 mutant strains with isoniazid, which targets InhA in the FAS-II pathway of mycolic acid synthesis (Marrakchi *et al.*, 2014). We do not see significant differences in isoniazid sensitivity between the strains in starvation (Figure 2.7F). In log. phase, we see that the *pstP*$_{Msmeg}$ T171E strain is more susceptible to isoniazid than the *pstP*$_{Msmeg}$ T171A and the wild-type strains (Figure 2.7E). Our data (Figure 2.7E) suggest that phosphorylation on PstP$_{Msmeg}$ T171 mis-regulates the mycolic acid biosynthesis pathway of mycomembrane metabolism (Figure 2.4B, Figure 2.5B and Figure 2.6B), thus increasing isoniazid susceptibility.

To see if the PstP T171 phospho-site affects susceptibility to a drug that does not target the cell wall, we treated the strains with trimethoprim, which targets thymidine biosynthesis in the cytoplasm (Brogden *et al.*, 1982). We see that, in log. phase, *pstP* T171E is very susceptible to this drug (Figure 2.7G), while the wild-type and T171A strains are tolerant. All strains were tolerant to trimethoprim in starvation (Figure 2.7H).

This shows that mis-regulation of PstP may impact processes beyond cell wall metabolism.

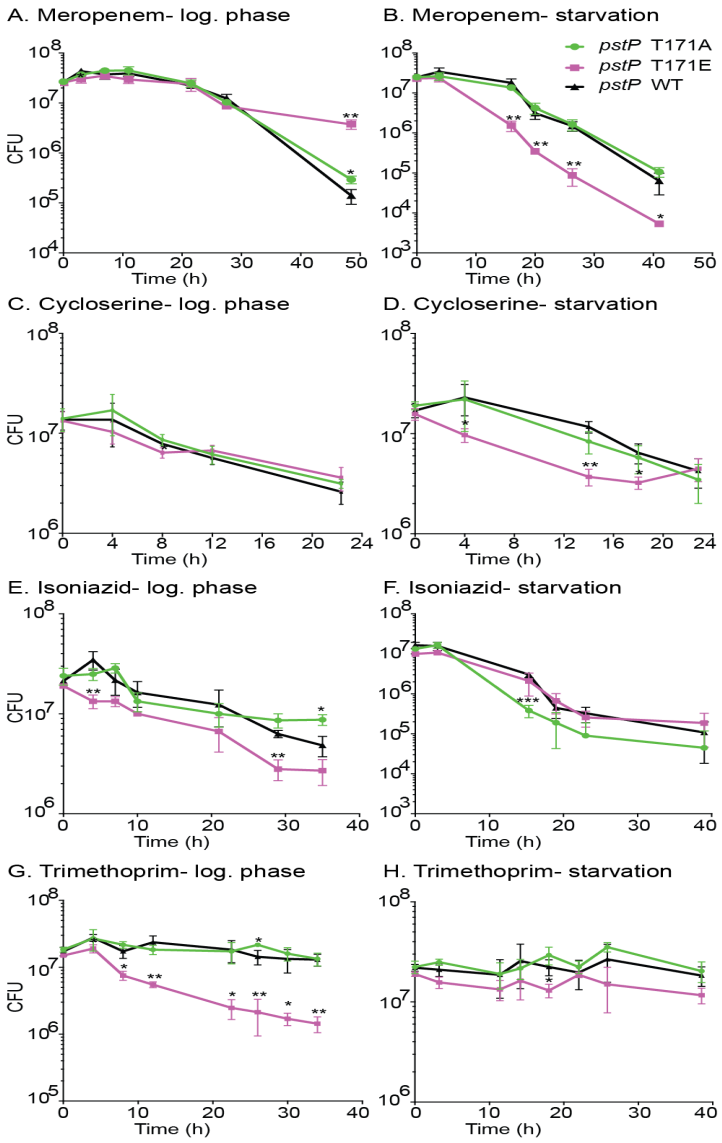

Figure 2.7 Phospho-site T171 of PstP$_{Msmeg}$ Plays a role in antibiotic sensitivity

Survival of *pstP* allele strains (WT, T17A and T171E) in different media and antibiotics. (A) In 7H9, treated with 8 µg/ml of meropenem. P values of WT vs. T171E at 3h= 0.043, WT vs. T171A at 48.5h= 0.001 and WT vs. T171E at 48.5h = 0.018.

(B) In HdB (no glycerol, 0.05% Tween) for 5.5 hours, then treated with 45 µg/ml of meropenem. P values of WT vs. T171E at 16h= 0.003, 23h=0.007, 26.3h= 0.004 and 41h= =0.046.

(C) In 7H9, treated with 100 µg/ml of D-cycloserine. P values of WT vs. T171E at 8h= 0.032.

(D) In HdB (no Glycerol, 0.05% Tween) for 5.5 hours, then treated with 900 µg/ml of D-cycloserine. P values of WT vs. T171E at 3.5h= 0.046, 14h= 0.001 and 18h= 0.022.

(E) In 7H9, treated with 10 µg/ml of isoniazid. P values of WT vs. T171E at 4h=0.008, WT vs. T171E at 29h= 0.002 and WT vs. T171A at 35h= 0.052.

(F) In HdB (no Glycerol, 0.05% Tween) for 5.5 hours, then treated with 90 µg/ml of isoniazid. P values of WT vs. T171A at 15.3h=0.009.

(G) In 7H9, treated with 50 µg/ml of trimethoprim. P values of WT vs. T171E at 4h= 0.023, 8h= 0.013, 12h= 0.005, 22.5h= 0.015, 26h= 0.005, 30h= 0.017 and 34h= 0.002.

(H) In HdB (no Glycerol, 0.05% Tween) for 5.5 hours, then treated with 360 µg/ml of trimethoprim. P values of WT vs. T171A at 18h= 0.023. All experiments were done with three biological replicate strains of each *pstP* allelic variant (T171A, T171E, and WT) at least twice. One representative trial (performed with three biological replicate strains of each *pstP* allelic variant genotype) is shown. All P values were calculated using two-tailed, unpaired t-test. All error bars represent standard deviation (SD).

Trimethoprim is a hydrophobic drug which is taken up via passive diffusion (Hancock and Bell, 1988). Therefore, permeability to trimethoprim is expected to be affected by changes in mycomembrane metabolism in log. phase (Figure 2.4B and 5E, Figure 2.5B and Figure 2.6B). It is notable that *pstP* phospho-allele strains in starvation do not exhibit differences in DMN-Tre staining (Figure 2.4D and F, Figure 2.6D) or isoniazid (Figure 2.7F) or trimethoprim sensitivity (Figure 2.7H), which suggests that susceptibility to trimethoprim, could be determined largely by permeability of the mycomembrane layer. D-cycloserine, on the other hand, is hydrophilic and therefore its uptake is likely dependent on porins (Neuhaus and Hammes, 1981; Stephan *et al.*, 2004), and therefore less sensitive to changes in the mycomembrane. So, sensitivity to D-

cycloserine (Figure 2.7C and D) appears to be largely dependent on regulation of PG metabolism (Figure 2.4A, C and F, Figure 2.5A, Figure 2.6A and B).

Our data show that phospho-site T171 of PstP regulates mycolic acid layer biosynthesis in growth, and PG layer metabolism in starvation. Mis-regulation of PstP can increase sensitivity to cell wall targeting drugs in both growth and stasis.

2.5 Discussion

Previous studies on mycobacterial phospho-regulation suggest that PstP could play a critical role in modulating cell wall metabolism in the transition between growth and stasis (Betts *et al.*, 2002; Boitel *et al.*, 2003; Molle *et al.*, 2006; Sajid *et al.*, 2011; Ortega *et al.*, 2014; Boutte *et al.*, 2016; Iswahyudi *et al.*, 2019; Dulberger *et al.*, 2020). In this work, we explored how the phosphorylation of PstP contributes to this regulation. We report here that the phospho-site T171 of $PstP_{Msmeg}$ impacts growth, cell wall metabolism and antibiotic tolerance. We found that the PG master regulator $CwlM_{Mtb}$ is a substrate of $PstP_{Mtb}$. Our findings indicate that the phosphorylation on PstP affects PG metabolism in stasis and the mycolic acid metabolism during growth.

PG is regulated by phosphorylation factors at several points along the biosynthesis pathway (Kieser *et al.*, 2015; Boutte *et al.*, 2016; Arora *et al.*, 2018; Turapov *et al.*, 2018), mostly by PknB. PknB's kinase activity is responsive to lipid II that it detects in the periplasm (Kaur *et al.*, 2019). PstP is a global negative regulator of STPK phosphorylation (Iswahyudi *et al.*, 2019) and has been proposed to be the cognate phosphatase of PknB in regulating cell growth (Boitel *et al.*, 2003; Iswahyudi *et al.*, 2019; Dulberger *et al.*, 2020; Le *et al.*, 2020). Our data suggest that mutations at T171

of PstP do not affect PG metabolism in growth (Figure 2.4A, Figure 2.5A and Figure 2.6A), but that the $PstP_{Msmeg}$ T171E strain fails to downregulate PG in starvation (Figure 2.4C and E, Figure 2.6C). We expect that PstP's activity against the PG regulator CwlM (Fig 2A, top panel) should be critical for this downregulation because it should de-activate MurA, the first enzyme in PG precursor synthesis (Marquardt *et al.*, 1992; Boutte *et al.*, 2016).

The *in vitro* biochemistry (Figure 2.2A and B) predicts the log. phase staining data (Figure 2.4A, Figure 2.5A and Figure 2.6A), where the *pstP* T171E variant has no difference in apparent PG activity. The proximity of a phospho-site to the substrate binding site of an enzyme may affect the catalytic activity directly (Veyron-Churlet *et al.*, 2009) but T174 maps to the β-sheet core (β8) in $PstP_{Mtb}$, which is distant from the active site (Figure 2.1A) (Pullen *et al.*, 2004). The PG staining in starvation (Figure 2.4C and E, Figure 2.6C) suggests that the $PstP_{Msmeg}$ T171E phospho-mimetic variant might dephosphorylate CwlM more slowly *in vivo* (Figure 2.7B and D), but this is not what we see *in vitro* (Figure 2.2A and B). Therefore, it is possible that, in starvation, phosphorylation at this site may affect PstP's interaction (Li *et al.*, 2020) with other regulatory proteins (Lin *et al.*, 1997; Roy and Cyert, 2009; Bollen *et al.*, 2010) that could modulate PstP's activity against PG substrates, or it could affect access to substrates via localization changes.

Synthesis of the various mycobacterial cell wall layers are likely synchronized (Kuru *et al.*, 2012; García-Heredia *et al.*, 2018; Baranowski *et al.*, 2019). PknB almost surely plays a crucial role in connecting PG and mycolic acid metabolism during growth. If PG

metabolism is slowed, PknB could sense the accumulation of periplasmic lipid II (Kaur *et al.*, 2019) and signal to halt mycolic acid biosynthesis by inactivating the FAS-II enzymes and the trehalose monomycolate transporter MmpL3 (Xu *et al.*, 2017) via phosphorylation (Molle *et al.*, 2006; Molle and Kremer, 2010; Veyron-Churlet *et al.*, 2010; Khan *et al.*, 2010; Slama *et al.*, 2011; Vilchèze *et al.*, 2014; Le *et al.*, 2020). Our data imply that PstP helps balance the effects of these inhibitory phosphorylations to allow coordinated synthesis of mycolic acids in log. phase (Figure 2.4B and 5E, Figure 2.5B and Figure 2.6B). Mis-phosphorylation of PstP likely disrupts this coordination and seems to decrease mycolic acid layer metabolism. This may partly explain the slow growth of the *pstP* T171E mutants (Figure 2.1B).

DMN-Tre incorporation into the mycomembrane is directly catalyzed by secreted (Harth *et al.*, 1996) Ag85 enzymes (Kamariza *et al.*, 2018). DMN-Tre fluorescence depends on mycomembrane hydrophobicity and is affected by inhibition of cytoplasmic mycolic acid synthesis (Kamariza *et al.*, 2018). Hydrophobicity can be affected by the glycolipid composition of the mycomembrane (Viljoen *et al.*, 2020). The differences in DMN-Tre fluorescence that we see (Fig 4B, Figure 2.5B and Figure 2.6B) could be due to changes in mycolic acid synthesis or due to changes in other glycolipids which affect hydrophobicity (Viljoen *et al.*, 2020). Our DMN-Tre data clearly indicates that the trehalose mycolate leaflet of the mycomembrane is affected due to phospho-misregulation of PstP although it does not yield detailed information about how it is affected.

We propose that PstP's regulation of mycolic acid layer biosynthesis occurs in the cytoplasm. PstP and all the STPKs work in the cytoplasm, and there are currently no known systems whereby secreted proteins like Ag85 can be regulated by phosphorylation. All the enzymes of the FAS-II complex, which elongates fatty acids into the long lipids used in mycolic acids (Marrakchi *et al.*, 2014), are downregulated by phosphorylation (Molle *et al.*, 2006; Molle and Kremer, 2010; Veyron-Churlet *et al.*, 2010; Khan *et al.*, 2010; Slama *et al.*, 2011; Vilchèze *et al.*, 2014), and two are biochemically verified substrates of PstP (Molle *et al.*, 2006). MmpL3, the mycolic acid flippase (Xu *et al.*, 2017), is also inhibited by phosphorylation (Le *et al.*, 2020). It is likely that PstP could affect the activity of the entire FAS-II complex, including the target of isoniazid, InhA, which is inactivated by threonine phosphorylation (Molle *et al.*, 2006; Khan *et al.*, 2010). Isoniazid is a small hydrophilic drug and undergoes active diffusion via the porins (Mailaender *et al.*, 2004; Stephan *et al.*, 2004); therefore, alterations in mycomembrane permeability are not likely to contribute substantially to differences in isoniazid sensitivity. Although our data (Figure 2.7E) does not reveal the exact mis-regulated spot in the mycolic acid synthesis and transport pathway, the higher susceptibility of the phosphomimetic strain (Figure 2.7E) to isoniazid suggests that this metabolic pathway is affected. Our DMN-tre staining also suggests that there should be a balance of non-phospho and phospho-form of $PstP_{Msmeg}$ T171 (Figure 2.4B) during growth to regulate mycomembrane biosynthesis.

PstP may dephosphorylate the cell wall substrates directly, and/ or by de-activating their kinases (Bhaskara, Wong, and Verslues 2019) in both the PG and mycolic acid

biosynthesis pathways. All these data combined suggest a complex cross-talk of the STPKs and PstP to regulate diverse cell wall substrates.

2.6 Acknowledgment

This work was supported by grants 1R15GM131317-01 and R01AI148917-01A1 to CCB from the National Institutes of Health, and by startup funds from the University of Texas at Arlington. We thank Kenan Murphy for the plasmids pDE54MCZD and pKM55 and Dirk Schnappinger for pDE43-MCS and RevTetR promoter plasmids used in this study.

Chapter 3

The essential Serine/Threonine phosphatase PstP dephosphorylates FhaA and Wag31 and is phospho-regulated to affect PG metabolism

Farah Shamma [1] **and Cara Boutte** [1]

[1]Department of Biology, University of Texas Arlington, Arlington, Texas

(Manuscript under preparation)

3.1 Preface

This chapter describes the *in vitro* identification of novel substrates of the essential Mycobacterial Serine/Threonine phosphatase PstP, the role of individual phosphorylation sites on PstP in regulating PstP's dephosphorylation activity and specificity against substrates and the importance of one phospho-site on PstP in regulation of peptidoglycan metabolism in *Mycobacterium smegmatis*. I purified all the proteins and enzymes, constructed the $pstP_{Msmeg}$ phospho-mutant allele swapped strains used this study, performed all the *in vitro* and *in vivo* assays and analyzed all data. The manuscript of this work soon to be submitted for publication is under preparation.

3.2 Abstract

The mycobacterial cell wall is profoundly regulated in response to environmental stresses, and this regulation contributes to antibiotic tolerance. The reversible phosphorylation of different cell wall regulatory proteins is a major mechanism of cell wall regulation. The integrated functions of The 11 Serine/Threonine protein kinases (STPKs) and only one cognate serine/threonine phosphatase, PstP, regulate the phosphorylation states of critical proteins and enzymes in Mycobacteria. Although a number of the cell wall regulatory substrates of the STPKs have been identified so far, few have been verified as PstP substrates. PstP is itself phosphorylated but the roles of its individual phospho-sites in regulating its activity is yet unclear. In this study we aim to discover novel substrates of PstP in *Mycobacterium tuberculosis* (*Mtb*). We show *in vitro* that PstP dephosphorylates two peptidoglycan (PG) regulators of *Mtb*, FhaA and Wag31. We also show phosphorylation regulates PstP's activity against CwlM, FhaA and Wag31. We find that a phopho-mimetic mutation of T137 on PstP negatively regulates its catalytic activity against the PG regulatory substrates FhaA, Wag31 and CwlM. Furthermore, phospho-mimetic mutations at phosphosites T141 and T174 affect PstP's specificity against these substrates. We examined whether the negative regulatory phosphosite T134 of PstP can affect PG metabolism *in vivo*. We found that a phosphomimetic mutation, *pstP*T137E, in *Mycobacterium smegmatis* (*Msmeg*) misregulates PG metabolism mildly in the exponentially growing cells and strongly in starved cells. Our findings on PstP's phospho-regulation and its new substrates in this study will help provide insight into understanding the phosphorylation-mediated cell wall regulatory network in Mycobacteria.

3.3 Introduction

Mycobacterium tuberculosis (*Mtb*), which causes Tuberculosis (TB), remains the age-old menace, infecting about 10 million and killing at least a million people worldwide each year (World Health Organization, 2021). The mycobacterial cell wall contributes to Mtb's inherent antibiotic tolerance (Jarlier and Nikaido, 1994; Sarathy *et al.*, 2013; Batt *et al.*, 2020) which is thought to partially account for TB's lengthy treatment time: 6 months for an antibiotic sensitive infection (Nguyen, 2016). The cell wall consists of a sequentially covalently cross-linked peptidoglycan-arabinogalactan-mycolic acid layer core surrounding the plasma membrane (Marrakchi *et al.*, 2014) and serves as permeability barrier (Jarlier and Nikaido, 1990; Hett and Rubin, 2008; Hoffmann *et al.*, 2008; Sarathy *et al.*, 2013). This complex cell wall architecture is strongly regulated in response to environmental stresses (Cunningham and Spreadbury, 1998; Betts *et al.*, 2002; Bhamidi *et al.*, 2012; Sarathy *et al.*, 2013) , including infection (Sharma *et al.*, 2006; Doerks *et al.*, 2012). The cell wall regulation is important for Mycobacteria since the cell wall changes in response to stresses correlate with increased antibiotic tolerance (Xie *et al.*, 2005; Liu *et al.*, 2016; Sarathy *et al.*, 2017) and also modulates the bacteria's interaction with the environment (Daffé and Draper, 1997).

The cell wall is also well regulated during mycobacterial growth to maintain proper elongation and division through the tight coordination of a number of protein machineries (Kieser and Rubin, 2014; Dulberger *et al.*, 2020). The mycolic acid layer, or mycomembrane, is mainly responsible for the antibiotic tolerance caused by lower permeability to drugs in mycobacteria. The peptidoglycan (PG) layer maintains cell shape and protects the cell from osmotic pressure (Ref). A number of regulators control

the activities of PG enzymes to modulate cell wall metabolism in growing cells (Typas *et al.*, 2012; Kieser and Rubin, 2014).

A crucial bacterial regulatory mechanism for transmission of environmental signals to control cell growth is Reversible Serine/Threonine (S/T) phosphorylation of a myriad of proteins and enzymes (Wang *et al.*, 1998; Juris *et al.*, 2000; Echenique *et al.*, 2004). *Mtb* uses this mechanism to regulate cell growth (Kang *et al.*, 2005; Gee *et al.*, 2012; Baer *et al.*, 2014; Boutte *et al.*, 2016) via its 11 Serine/Threonine kinases (STPKs) (PknA-B and PknD-L) and only one S/T protein phosphatase PstP (Cole *et al.*, 1998; Bach *et al.*, 2009). PstP is itself phosphorylated and its phosphorylation affects its activity *in vitro* (Sajid *et al.*, 2011) and cell wall metabolism *in vivo* (Shamma *et al.*, 2021).

Two essential STPKs PknA and PknB play important roles in cell wall regulation by phosphorylating enzymes or regulatory proteins involved in cell division and growth (Sassetti and Rubin, 2003; Kang *et al.*, 2005; Fernandez *et al.*, 2006; Kusebauch *et al.*, 2014; Boutte *et al.*, 2016). Phosphorylation of different cell wall regulatory substrates has different effects on their activities. For example, phosphorylation activates the PG regulatory protein CwlM (Boutte *et al.*, 2016) and inhibits the enzymatic activity of the enoyl-ACP reductase InhA- a key Mycolic acid (MA) biosynthesis enzyme in Mtb (Molle and Kremer, 2010; Khan *et al.*, 2010). PstP is suggested to be a global negative regulator of the STPK-mediated phosphorylation (Iswahyudi *et al.*, 2019) by reverting the effect of phosphorylation on substrates (Molle *et al.*, 2006; Shamma *et al.*, 2021).

Being the only S/T protein phosphatase, it can be expected to dephosphorylate many of the substrates phosphorylated by the 11 STPKs (Cole *et al.*, 1998).

Among the proteins and enzymes regulating the three layers of the Mycobacterial cell wall core, many are known to be substrates of the STPKs (Prisic and Husson, 2014) but only a few of them have been identified to be substrates of PstP. The biochemically-verified cell wall substrates of PstP include KasA and KasB, enzymes of the fatty acid synthase –II (FAS-II) system of the MA biosynthesis pathway, the arabinogalactan layer regulator EmbR, and CwlM, which regulates the peptidoglycan layer (Shamma *et al.*, 2021).

CwlM is a crucial PG synthesis regulator since its phosphorylated, active form interacts with and stimulates MurA to allow PG synthesis (Boutte *et al.*, 2016), the first enzyme of PG precursor synthesis (Marquardt *et al.*, 1992). So dephosphorylation of CwlM by PstP (Shamma *et al.*, 2021) should halt PG synthesis. Phosphorylated CwlM (CwlM~P) also interacts with another PG regulator FhaA and non-phosphorylated CwlM interacts with the PG precursor lipid-II flippase MurJ (Turapov *et al.*, 2018), suggesting that CwlM's activity and interaction with other PG regulatory substrates and enzymes is phospho-regulated and that both CwlM and FhaA are part of a phosphorylation controlled PG regulatory hub (Turapov *et al.*, 2018). Mycobacterial FhaA is a Forkhead-associated (FHA) domain containing protein which maintains cell envelope integrity, cell length and antibiotic tolerance (Viswanathan *et al.*, 2015; Viswanathan *et al.*, 2017) via regulation of PG biosynthesis (Gee *et al.*, 2012). FhaA interacts with the class B penicillin binding protein PbpA (Viswanathan *et al.*, 2017), phosphorylated MurJ and also the STPK PknB

(Grundner *et al.*, 2005) that phosphorylates it (Grundner *et al.*, 2005; Prisic *et al.*, 2010; Roumestand *et al.*, 2011). These findings, and the fact that *fhaA* is close to the gene cluster that encodes its phosphorylating STPK PknB, its interaction partner PbpA and the S/T phosphatase PstP, hint at a possible phospho-regulatory role of FhaA in PG synthesis where FhaA might need to be dephosphorylated when needed and that PstP might its dephosphorylating enzyme.

The PG regulator (Kang *et al.*, 2008; Jani *et al.*, 2010) Wag31, like FhaA, is also expressed from part of another gene cluster that includes the peptidoglycan biosynthetic enzymes (*murC-G and murX)* (Nguyen *et al.*, 2007; Kang *et al.*, 2008; Jani *et al.*, 2010). Wag31 regulates polar PG synthesis (Kang *et al.*, 2008; Jani *et al.*, 2010) and is phosphorylated by the STPK PknA (Kang *et al.*, 2005). Its phosphorylation seem to guide its polar localization and increase Wag31-mediated polar PG synthesis (Jani *et al.*, 2010) and it has been suggested that phosphorylated Wag31 is abundant in growing cells where the less or non-phosphorylated form is favored in stationary phase cells (Jani *et al.*, 2010). These results lead us to hypothesize that Wag31 is probably subjected to dephosphorylation *in vivo* to downregulate PG synthesis.

We wanted to see if PstP dephosphorylates PG regulators FhaA and Wag31. We show that $FhaA_{Mtb}$ and $Wag31_{Mtb}$ are substrates of $PstP_{Mtb}$ *in vitro*. PstP is itself phosphorylated on different Threonine (T) residues- 137, 141, 174 and 290 in *Mtb* (Sajid *et al.*, 2011) and we previously showed that phosphorylation of a particular conserved phospho-site (T174) on $PstP_{Mtb}$ did not affect its activity against CwlM *in vitro* (Shamma *et al.*, 2021). In this study we wanted to see whether the conserved phosphosites (T137,

T141 and T174) might individually regulate PstP's activity against these different PG regulators (FhaA$_{Mtb}$, Wag31$_{Mtb}$ and CwlM$_{Mtb}$) *in vitro*. We see that a phospho-mimetic mutation of PstPT137$_{Mtb}$ affected PstP$_{Mtb}$'s catalytic activity against all three PG regulators, and phospho-mimetic mutations of PstPT141$_{Mtb}$ and PstPT174$_{Mtb}$ affect PstP$_{Mtb}$'s substrate specificity *in vitro*.

In order for PG metabolism to match growth rate *in vivo*, balance must be maintained between phosphorylated and non-phosphorylated states of CwlM, FhaA and Wag31 through regulation of the STPKs and PstP. We showed previously that the phospho-regulation on T174 of PstP affects PG metabolism in starvation and mycolic acid metabolism in log. phase (Shamma *et al.*, 2021) in *Msmeg*. In this study we wanted to see if the phosphosite T134 on PstP$_{Msmeg}$ might affect PG metabolism since we see that PstP's activity is suppressed against the PG regulators FhaA, Wag31 and CwlM when this corresponding phosphosite T137 in *Mtb* is phosphorylated *in vitro*. In the *pstP*T134E$_{Msmeg}$ allelic strains, we see increased in PG metabolism in both exponentially growing and starved cells compared to that of the *pstP*WT$_{Msmeg}$ strains. We suggest a model where PstP's activity is phospho-regulated to regulate PG metabolism in changing conditions.

3.4 Methods and Materials

3.4.1 Bacterial strains and culture conditions

All *Mycobacterium smegmatis* mc^{2}155 ATCC 700084 cultures were grown in 7H9 (Becton, Dickinson, Franklin Lakes, NJ) medium containing 5 g/liter bovine serum albumin (BSA), 0.003 g/liter catalase, 2 g/liter dextrose, 0.85 g/liter NaCl, 0.2% glycerol,

and 0.05% Tween 80 and incubated at 37°C until log. phase. 1xPBS with 0.05% Tween 80 was used for starvation assays. Cultures were plated on LB lennox agar (Fisher BP1427-2).

E. coli Top10, XL1-Blue, and Dh5α strains were used for cloning and *E. coli* BL21 Codon Plus and BL21(DE3) strains were used for protein expression. Antibiotic concentrations for *M. smegmatis* were 25µg/ml kanamycin and 20 µg/ml zeocin. Antibiotic concentrations for *E. coli* were 50 µg/ml kanamycin, 25 µg/ml zeocin, 20 µg/ml chloramphenicol, and 140 µg/ml ampicillin.

3.4.2 Cloning and Strain construction

N-terminally Histidine (His) tagged cytosolic domains (1-300 amino acids (Gupta *et al.*, 2009)) of different *pstP*$_c$ alleles of *Mtb*- *pstP*$_c$T137E$_{Mtb}$ and *pstP*$_c$T141E$_{Mtb}$, and *fhaA*WT$_{Mtb}$ optimized in their codons for expression in *E. coli* were ordered from IDT, Inc. and cloned in to pET28a.

The *Msmeg* mc2155 strains Δ*pstP*::lox L5::pCT94-p766tetON6-*pstP*$_{Msmeg}$T134E and Δ*pstP*::lox L5::pCT94-p766tetON6-*pstP*$_{Msmeg}$WT were generated by swapping *pstP*$_{Msmeg}$T134E and WT alleles respectively under the promoter p766tetON6 in the integrative vector pCT94 at the L5 site of the *Msmeg* mc^{2}155 Δ*pstP*::lox strain as described previously (Pashley and Parish, 2003; Shamma *et al.*, 2021).

3.4.3 Growth Curve Assay

At least three biological replicates of *pstP*$_{Msmeg}$T134E and WT allelic variants were grown in 7H9 medium up to the mid-log. phase. The growth curve assays were

performed in non-treated non-tissue culture plates using a plate reader (BioTek Synergy neo2 multi mode reader) in 200µl of 7H9 medium at 37°C starting at an Optical Density at 600nm (OD_{600}) of 0.1.

The doubling times of each strain were calculated in the non-linear (curve fit) method using an exponential growth equation with the least squares (ordinary) fit in GraphPad Prism (version 7.0d). *P* values were calculated using two-tailed unpaired t-tests.

3.4.4 Protein purification

His-MBP-PknA$_{Mtb}$ was expressed in *E. coli* BL21(DE3) and all other proteins were expressed using *E. coli* BL21 Codon Plus cells. N-terminally His-tagged MBP-PknB$_{Mtb}$, SUMO-CwlM$_{Mtb}$, PstP$_c$WT$_{Mtb}$ and PstP$_c$T174E$_{Mtb}$ were expressed and purified as previously described (Kieser *et al.*, 2015; Shamma *et al.*, 2021)

His-PstP$_c$T137E$_{Mtb}$ and His-PstPcT141E$_{Mtb}$ were expressed and purified using the same conditions and buffers used to purify His-PstP$_c$WT$_{Mtb}$ and His-PstP$_c$T174E$_{Mtb}$ described previously in (Shamma *et al.*, 2021).

His-Wag31$_{Mtb}$ was induced with 0.5mM IPTG (isopropyl-*β*-D-thiogalactopyranoside) for 6h at 18°C, and purified on Ni-nitrilotriacetic acid (Ni-NTA) resin (G-Biosciences 786-940) then dialyzed and concentrated. The buffer for His-Wag31$_{Mtb}$ was 50mM Tris pH 8, 350mM NaCl, 1 mM dithiothreitol (DTT), and 10% glycerol. Imidazole (10mM and 20mM) was added to the buffers for lysis of the cell pellets and washing the Ni-NTA resin respectively, and 250mM imidazole was added for elution. The lysis buffer was supplemented with 1mM PMSF and 0.2% Triton X100.

His-MBP-PknA$_{Mtb}$ (1-279 amino acids containing the kinase domain (Baer *et al.*, 2014)) was induced with 0.5mM IPTG at 18°C overnight, purified with 5ml Ni-NTA resins (BIO-RAD EconoFit Nuvia IMAC, 12009287), then run over the size exclusion resin (Enrich SEC650, BIO-RAD 780-1650) after dialysis and concentration to get soluble protein. The buffer for purifying His-MBP-PknA$_{Mtb}$ was 50mM Tris pH 7.5, 150mM NaCl, 20% glycerol. PMSF (1mM) was added to the buffer while resuspending the cell pellets. Imidazole was used in buffer for application to (20mM) and for elution from Ni-NTA resin (200mM).

His-FhaA$_{Mtb}$ was induced with 1mM IPTG at 18°C overnight and purified on Ni-NTA resin (G-Biosciences, 786-940 in 5 ml Bio-Scale Mini Cartridges, BIO-RAD 7324661), then dialyzed, concentrated, and run over size exclusion resin (GE Healthcare Sephacryl S-200 in HiPrep 26/70 column). His-FhaA$_{Mtb}$ was purified using the buffers described in (Roumestand *et al.*, 2011).

3.4.5 *In vitro* dephosphorylation assays

His-SUMO-CwlM$_{Mtb}$ was phosphorylated *in vitro* with His-MBP-PknA$_{Mtb}$ for 30 minutes at room temperature with 0.15µCi/µl ATP [γ-^{32}P] (3000Ci/mmol, 10mCi/ml, PerkinElmer BLU002A250UC) and 2mM $MnCl_2$ in buffer (50mM Tris, pH 7.5, 250mM NaCl, and 1mM DTT). His-PstP$_c$WT$_{Mtb}$, His-PstP$_c$T137E$_{Mtb}$, His-PstPcT141E$_{Mtb}$ or His-PstPcT174E$_{Mtb}$ was added to the reaction mixture and incubated in presence of phosphatase buffer (50mM Tris pH 7.5, 10mM $MnCl_2$, and 1mM DTT) at room temperature up to 40 minutes.

His-FhaA$_{Mtb}$ was phosphorylated *in vitro* with His-MBP-PknA$_{Mtb}$ for 45 minutes at 37°C

at with 0.15µCi/µl ATP [γ-^{32}P] in presence of 5mM $MnCl_2$ in 25mM Tris pH 7.5 and 1mM DTT. This kinase reaction mixture was then incubated with either $PstP_cWT_{Mtb}$ or different phosphomimetic variants of it up to 80 minutes at room temperature in presence of the phosphatase buffer.

The amount of kinase and phosphatases used were each ten times the amount substrates in both the above-mentioned assays.

His-$Wag31_{Mtb}$ was phosphorylated with His-MBP-$PknA_{Mtb}$ for 2 hours at room temperature in presence of 0.2µCi/µl ATP [γ-^{32}P], 10mM $MnCl_2$ and buffer (50mM Tris pH 7.5, 20% glycerol and 150mM NaCl). $PstP_cWT_{Mtb}$ or its different phosphomimetic variants were added to the kinase-substrate reaction mixture and incubated at room temperature for up to 120 seconds in presence of the phosphatase buffer. Five and hundred folds His-$Wag31_{Mtb}$ was used compared to the amount of kinase and the phosphatases respectively.

A control assay with only the phosphatase buffer added to the kinase reaction mixture and with no phosphatase was performed in all the above-mentioned substrate dephosphorylation assays.

All *in vitro* dephosphorylation assays were carried out separately with two individually purified batches of WT and phospho-mimetic mutant of PstP to mimic biological replicates.

3.4.6 Quantification of γ-^{32}P signals

Samples from each *in vitro* biochemical reaction were collected before (0 minute) and after addition of each of the phosphatases at several different time points. The samples were run on 12% (Mini-Protean TGX, BIO-RAD, 4561046) gels and stained with Coomassie blue solution. After destaining, phospho-signals from the gels were transferred on phosphor screens (Molecular Dynamics) and imaged with a scanner (Storm 860, Amersham Biosciences) which were visualized with the ImageQuant software (Molecular Dynamics).

The protein bands on the gel and the phospho-signals on the autoradiogram were then quantified with FIJI. The intensities of the substrate on the gel and their corresponding phospho-signals at each time point were normalized against the respective protein band and phospho-signal at 0 minute before addition of the phosphatase. These relative intensities were used to calculate the intensity of phospho-signal/amount of substrate for each time point and the values were plotted in GraphPad Prism (version 7.0d)

3.4.7 Cell staining

At least three biological replicates of *pstP*$_{Msmeg}$ T134E and WT allelic variants were grown in 7H9 medium up to the mid-log. phase. Cultures were washed and then starved in 1xPBS with 0.05% Tween 80 fat an $OD_{600=}$ 0.3 or 15 minutes. 100µl of starved culture was then treated with 3µl of 10mM fluorescent D-amino acid HADA for 10 minutes. Cells were then pelleted and resuspended in 1xPBS with 0.05% Tween 80 and fixed with 10µl of 16% paraformaldehyde (PFA) for 10 minutes at room temperature. Cells were then pelleted and resuspended in PBS supplemented with Tween 80.

For staining cells in the log. phase, 1µl of 1mM HADA was added to 100µl culture grown up to the mid-log. phase and incubated at 37°C for 15 minutes. Stained cells were then pelleted, washed and fixed as described above.

3.4.8 Microscopy and Image analysis

A Nikon Ti-2 widefield epifluorescence microscope with a Photometrics Prime 95B camera and a Plan Apo 100x, 1.45 NA objective lens was used to image cells. The blue fluorescence images for HADA staining were taken using a 350/50nm excitation filter and a 460/50nm emission filter. All images were captured using NIS Elements software and analyzed using FIJI and MicrobeJ (Ducret *et al.*, 2016). Appropriate parameters for length, width and area were set in MicrobeJ for cell detection. The V-snapping (dividing) cells were split at the septum so that each daughter cell could be considered as a single cell. Any overlapping cells were excluded from analysis.

Length and mean-intensities of HADA signals of at least 330 cells from each of $pstP_{Msmeg}$T134E and $pstP_{Msmeg}$WT (at least 110 cells from each of three biological replicate strain of each genotype) were quantified using MicrobeJ. The values of the mean intensities of 330 cells of each *pstP* allelic mutant and WT are represented in the graphs generated using GraphPad Prism (v7.0d).

The medial intensity profiles of HADA signals in cells from different *pstP* allele strains in log. phase and starvation analyzed with MicrobeJ were plotted on the Y-axis over relative positions of cells using the “XStatProfile” plotting feature in MicrobeJ to show the subcellular localization of fluorescent intensities in cells. Demographs of HADA

signal intensity across cell lengths in log. phase and starvation were built using the "Demograph" feature of MicrobeJ by plotting the medial intensity profiles of HADA signals.

3.5 Results and Discussion

3.5.1 PstP$_{Mtb}$ dephosphorylates FhaA$_{Mtb}$ and Wag31$_{Mtb}$ *in vitro*

FhaA is a Forkhead Associated domain (FHA) containing protein that can bind to phospho-threonine residues via their FHA domain to regulate protein function (Pallen *et al.*, 2002). FhaA has been shown to be important for PG metabolism (Gee *et al.*, 2012), and to interact with MurJ, CwlM (Turapov *et al.*, 2018) and PbpA (Viswanathan *et al.*, 2017), though the exact regulatory function of these interactions has not been described. Wag31 is a homologue of the Gram- positive bacterial cell division protein DivIVA (Cole *et al.*, 1998; Flärdh, 2003) that is essential for polar cell wall synthesis (Kang *et al.*, 2008; Jani *et al.*, 2010).

FhaA$_{Mtb}$ is phosphorylated by PknB$_{Mtb}$ *in vivo* (Prisic *et al.*, 2010) and *in vitro* (Grundner *et al.*, 2005; Roumestand *et al.*, 2011) on T116 (Roumestand *et al.*, 2011) but not its FHA-domain although the FHA domain is required for phosphorylation by PknB$_{Mtb}$ (Grundner *et al.*, 2005). Wag31$_{Mtb}$ is phosphorylated at T73 by either PknA$_{Mtb}$ or PknA$_{Mtb}$ and PknB$_{Mtb}$ together *in vitro* but not by PknB$_{Mtb}$ alone (Kang *et al.*, 2005).

To see if FhaA$_{Mtb}$ and Wag31$_{Mtb}$ are substrates of PstP$_{Mtb}$, we performed *in vitro* dephosphorylation assays with purified full-length His-FhaA$_{Mtb}$, His-Wag31$_{Mtb}$, N-terminally His-MBP tagged cytosolic kinase domains of PknA$_{Mtb}$ and PknB$_{Mtb}$, and the cytosolic region of PstP$_{Mtb}$ containing the catalytic domain (His-PstP$_c$WT$_{Mtb}$).

We phosphorylated His-FhaA$_{Mtb}$ with His-MBP-PknB$_{Mtb}$ in presence of ATP [γ-^{32}P]. After addition of His-PstP$_c$WT$_{Mtb}$, we see the phosphorylation on his-FhaA$_{Mtb}$~P started to decrease within 5 minutes and kept decreasing over time to about 80% in 80 minutes (Figure 3.1A, first panel and B). Our control assay with no phosphatase shows that the phosphorylation on his-FhaA$_{Mtb}$~P is stable over time in presence of the phosphatase buffer (Figure 3.1A, bottom panel and B). This shows that the cell wall regulator FhaA$_{Mtb}$ is a substrate of PstPWT$_{Mtb}$ *in vitro*.

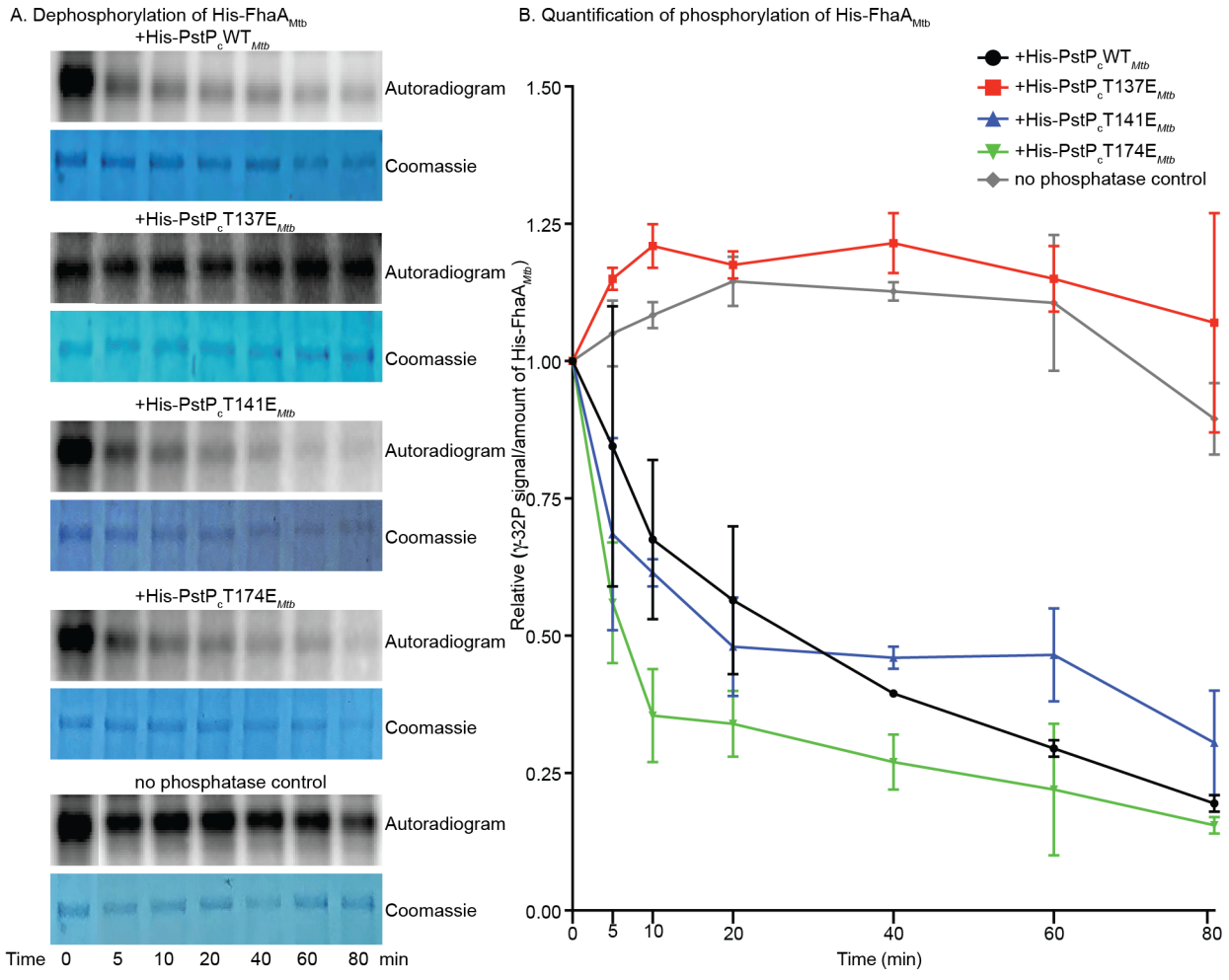

Figure 3.1 PstP$_{Mtb}$ dephosphorylates FhaA$_{Mtb}$.

A. Autoradiograms and their respective Coomassie stained SDS-gels of *in vitro* phosphatase assays performed with ATP-[γ-^{32}P]-phosphorylated His-FhaA$_{Mtb}$ and His-PstP$_c$WT$_{Mtb}$ (top panel), His-PstP$_c$WT$_{Mtb}$ (second panel), His-PstP$_c$T141E$_{Mtb}$ (third panel), His-PstP$_c$T174E$_{Mtb}$ (fourth panel) and no phosphatase control reaction (bottom panel). One set of representative images for each reaction is shown here from two individual assays performed with individually purified batches of phosphatases.

B. Quantification of relative intensities of [γ-^{32}P] on His-FhaA$_{Mtb}$ on autoradiogram over amount of His-FhaA$_{Mtb}$ on the SDS-gel. P values were calculated using two-tailed unpaired t-test.

P-values of T137E at 0 min *vs.* 80 min =0.7598, WT *vs.*T137E at 80 min= 0.0487, WT *vs.*T141E at 80 min =0.3712, WT *vs.* T174E at 80 min=0.2000. The error bars represent standard error of means.

To see if PstP$_c$WT$_{Mtb}$ can dephosphorylate Wag31$_{Mtb}$, we performed an *in vitro* dephosphorylation assay where we first phosphorylated his-Wag31$_{Mtb}$ with His-MBP-PknA$_{Mtb}$ in presence of ATP [γ-^{32}P]. After addition of His-PstP$_c$WT$_{Mtb}$, the phosphorylation on Wag31$_{Mtb}$ decreased by about 37% within 15 seconds and kept decreasing over time to about 93% in 2 minutes (Figure 3.2A, first panel and B). Our no phosphatase control assay showed that the phosphorylation on His-Wag31$_{Mtb}$~P is stable over time in presence of the phosphatase buffer (Figure 3.2A, bottom panel and B). This shows that the PG-regulator Wag31$_{Mtb}$ is a substrate of PstPWT$_{Mtb}$ *in vitro*, and also that Wag31 is dephosphorylated much more quickly than the other substrates we have studied.

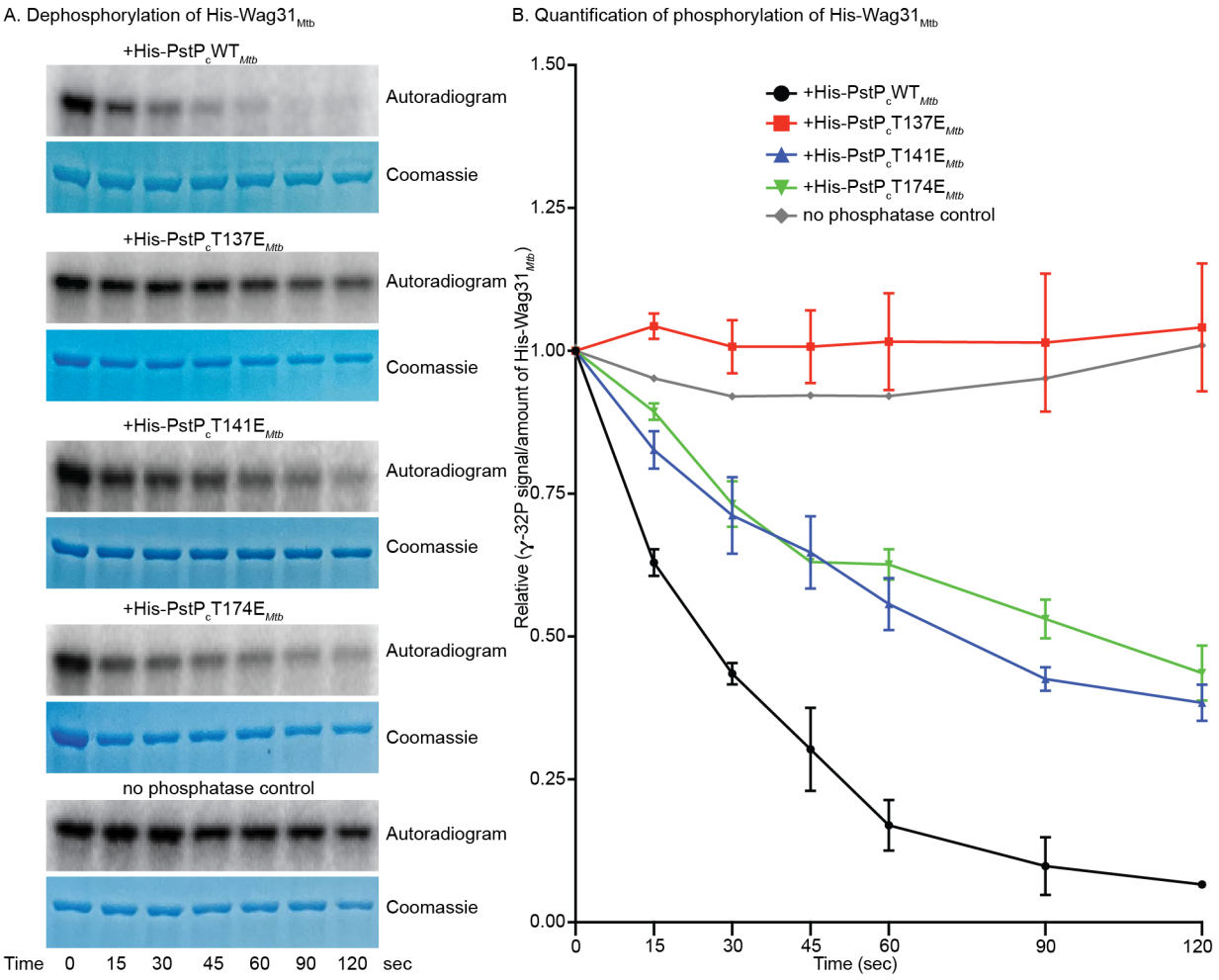

Figure 3.2 $PstP_{Mtb}$ dephosphorylates $Wag31_{Mtb}$

A. Autoradiograms and their respective Coomassie stained SDS-gels of *in vitro* phosphatase assays performed with ATP-[γ-^{32}P]-phosphorylated His-$Wag31_{Mtb}$ and His-$PstP_cWT_{Mtb}$ (top panel), His-$PstP_cWT_{Mtb}$ (second panel), His-$PstP_cT141E_{Mtb}$ (third panel), His-$PstP_cT174E_{Mtb}$ (fourth panel) and no phosphatase control reaction (bottom panel). One set of representative images for each reaction is shown here from two individual assays performed with individually purified batches of phosphatases.

B. Quantification of relative intensities of [γ-^{32}P] on His-$Wag31_{Mtb}$ on autoradiogram over amount of His-$Wag31_{Mtb}$ on the SDS-gel. P values were calculated using two-tailed unpaired t-test.

P-values of T137E at 0 sec *vs.* 15 sec = 0. 0.1947 and 0 sec *vs.* 120sec= 0.7493, WT *vs.* T137E at 120 sec= 0.0130, WT *vs.* T141E at 120 sec =0.0106 and WT *vs.* T174E at 120 sec = 0.170. The error bars represent standard error of means.

Our previous biochemical data that demonstrated $PstP_{Mtb}$ dephosphorylates $CwlM_{Mtb}$

(Shamma *et al.*, 2021) is reproducible in our in vitro assays with ATP [γ-^{32}P] where we see a 97% decrease in phosphorylation on His-SUMO-Cwlm$_{Mtb}$~P over a time period of 40 minutes after addition of His-PstP$_c$WT$_{Mtb}$ (Figure 3.4A top panel and B).

In all the assays, we see no phosphorylation signals on the WT and phosphomimetic PstPs on the autoradiograms (data not shown) since PstP can quickly dephosphorylate itself (Sajid *et al.*, 2011) and the purified forms are thus unphosphorylated.

3.5.2 Phosphorylation on PstPT137$_{Mtb}$ negatively regulates its activity

PstP$_{Mtb}$ is phosphorylated on its threonine (T) residues 137, 141, 174, and 290 and when phosphorylated, shows increased activity against small molecule substrates *in vitro* (Sajid *et al.*, 2011) (Figure 3.3). We hypothesized that phosphorylation of the threonine residues of PstP individually might help regulate PstP's activity through switching its catalytic activity against different substrates or by affecting PstP's substrate specificity.

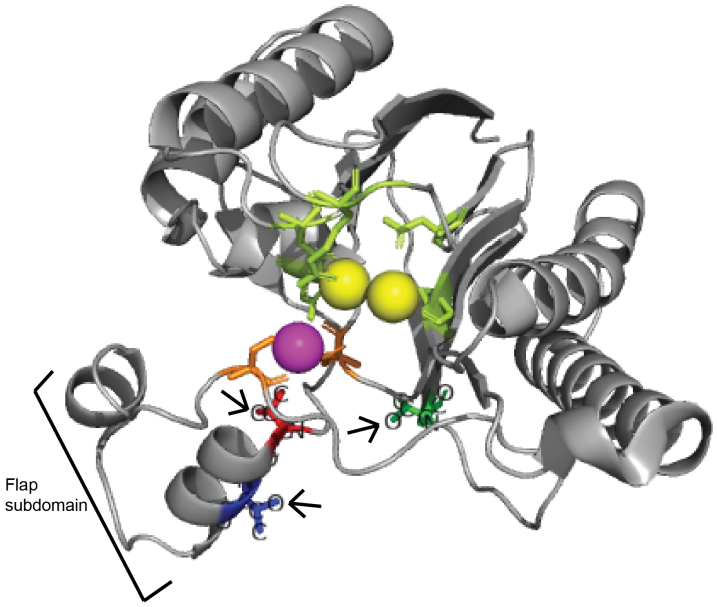

Figure 3.3 Crystal structure of the cytoplasmic domain of PstP$_{Mtb}$WT.

Schematic of the crystal structure of PstP from *M. tuberculosis* (PstP$_{Mtb}$WT) (Pullen *et al.*, 2004) (PDB code 1TXO) showing the conserved threonine (T) which are phosphorylated by the kinases PknA and PknB (Sajid et al. 2011). Highlighted on the structure are: red, PstP$_{Mtb}$T137 (PstPT134 in PstP$_{Msmeg}$); blue, PstP$_{Mtb}$T141 (PstPT138 in PstP$_{Msmeg}$) green, PstP$_{Mtb}$T174 (PstPT171 in PstP$_{Msmeg}$); yellow, Mn^{2+} present at the conserved two-metal center seen in PP2Cα, which are part of the active site core; pink, the unique third Mn^{2+} ion bound in the catalytic core of PstP$_{Mtb}$ but not in the human PP2Cα and sits in a groove created by the flap subdomain next to the active site, orange, Ser60 and Asp118 that act as ligands for the third Mn ion; lime green, residues of the catalytic sites surrounding the two-metal center. Arrows point to position of the OH-groups on T137, T141 and T174 that can be phosphorylated.

To see if the phosphorylations on PstP$_{Mtb}$ individually affect PstP's activity, we made phosphomimetic (T to E) (Cottin *et al.*, 1999) mutants of PstP$_{Mtb}$ at each of the three conserved phosphorylation sites of PstP$_{Mtb}$ in the catalytic domain and purified them (His-PstP$_c$T137E$_{Mtb}$, His-PstP$_c$T141E$_{Mtb}$ and his-PstP$_c$T174E$_{Mtb}$).

We previously showed that *in vitro* PstPWT$_{Mtb}$ dephosphorylates CwlM$_{Mtb}$ and PstPT174E$_{Mtb}$ showed no significant difference in activity against CwlM compared to

PstPWT$_{Mtb}$ (Shamma *et al.*, 2021). Here we wanted to see if these conserved phosphosites regulated PstP's activity against all three PG regulators.

We performed separate *in vitro* phosphatase assays with the substrates His-FhaA $_{Mtb}$, His-Wag31$_{Mtb,}$ His-SUMO-CwlM$_{Mtb}$ where His-FhaA $_{Mtb}$ and His-SUMO-CwlM$_{Mtb}$ were phosphorylated with His-MBP-PknB$_{Mtb}$ and His-Wag31$_{Mtb}$ was phosphorylated with His-MBP-PknA$_{Mtb}$. With the addition of His-PstP$_c$T137E$_{Mtb}$, we see no significant decrease of phosphorylation signal over time on His-FhaA $_{Mtb}$~P (Figure 3.1A, second panel and B), His-Wag31$_{Mtb}$~P (Figure 3.2A, second panel and B) and His-SUMO-CwlM$_{Mtb}$ (Figure 3.4A, second panel and B). These data clearly show that PstP$_c$T137E$_{Mtb}$ suppresses PstP's catalytic activity almost fully against different substrates. This is direct biochemical evidence that supports our hypothesis that an individual phosphosite may direct regulation of PstP's activity against substrates.

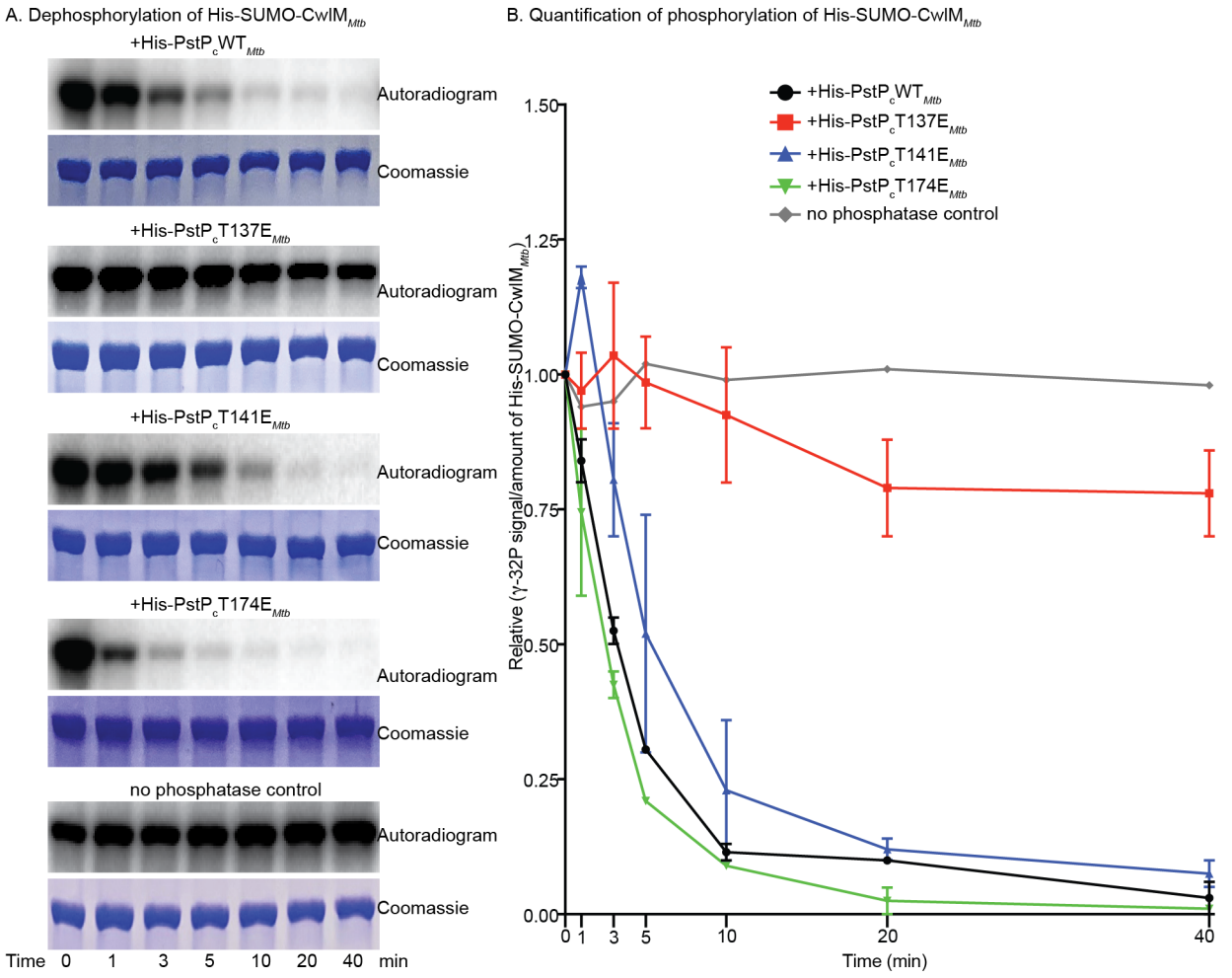

Figure 3.4 PstP$_{Mtb}$ dephosphorylates CwlM$_{Mtb}$.

A. Autoradiograms and their respective Coomassie stained SDS-gels of *in vitro* phosphatase assays performed with ATP-[γ-^{32}P]-phosphorylated His-SUMO-CwlM$_{Mtb}$ and His-PstP$_c$WT$_{Mtb}$ (top panel), His-PstP$_c$WT$_{Mtb}$ (second panel), His-PstP$_c$T141E$_{Mtb}$ (third panel), His-PstP$_c$T174E$_{Mtb}$ (fourth panel) and no phosphatase control reaction (bottom panel). One set of representative images for each reaction is shown here from two individual assays performed with individually purified batches of phosphatases.

B. Quantification of relative intensities of [γ-^{32}P] on His-SUMO-CwlM$_{Mtb}$ on autoradiogram over amount of His-SUMO-CwlM$_{Mtb}$ on the SDS-gel. P values were calculated using two-tailed unpaired t-test. P-values of T137E at 0 min *vs.* 40 min= 0.1107, WT *vs*. T137E at 40 min= 0.0127, WT *vs*. T141E at 40 min=0.3683 and WT *vs*. T174E at 40 min= 0.5918. The error bars represent standard error of means.

3.5.3 Phosphorylations on PstPT141$_{Mtb}$ and PstPT174$_{Mtb}$ regulate PstP$_{Mtb}$'s substrate specificity

To understand if phosphorylations on PstPT141$_{Mtb}$ and PstPT174$_{Mtb}$ affect PstP$_{Mtb}$'s activity, we tested changes in phosphorylation signals on phosphorylated His-FhaA $_{Mtb}$, His-Wag31$_{Mtb}$ and His-SUMO-CwlM$_{Mtb}$ in presence of His-PstP$_c$T141E$_{Mtb}$ and His-PstP$_c$T174E$_{Mtb}$ in separate *in vitro* phosphatase assays.

We see decrease in phosphorylation on His-FhaA $_{Mtb}$~P over time in presence of His-PstP$_c$T141E$_{Mtb}$ (Figure 3.1A, third panel and B) and His-PstP$_c$T174E$_{Mtb}$ (Figure 3.1A, fourth panel and B) in a manner similar to that in presence of His-PstP$_c$WT$_{Mtb}$ (Figure 3.1A, top panel and B) with no significant difference in activities (Figure 3.1B). When added to His-SUMO-CwlM$_{Mtb}$~P, His-PstP$_c$T141E$_{Mtb}$ (Figure 3.4A, third panel and B), like His-His-PstP$_c$T174E$_{Mtb}$ as reported previously (Shamma *et al.*, 2021) and also in this study (Figure 3.4A, fourth panel and B), has similar activity as PstP$_c$WT$_{Mtb}$ in dephosphorylating His-SUMO-CwlM$_{Mtb}$~P.

Interestingly, the phosphorylation signal on His-Wag31$_{Mtb}$ decreased significantly slowly in presence of His-PstP$_c$T141E$_{Mtb}$ (Figure 3.2A, third panel and B), and His-PstP$_c$T174E$_{Mtb}$ (Figure 3.2A, fourth panel and B), compared to His-PstP$_c$WT$_{Mtb}$ (Figure 3.2A, top panel and B).

These data clearly show that both PstP$_c$T141E$_{Mtb}$ and PstP$_c$T174E$_{Mtb}$ do not affect PstP's activity against certain substrates but do affect its activity against some other. These biochemical data support our hypothesis that phosphorylation on PstP may modulate its activity by affecting its substrate specificity.

3.5.4 Phospho-site T137 of PstP $_{Msmeg}$ affects peptidoglycan regulation in starvation

Phosphorylation regulates CwlM's interaction with the first PG biosynthetic enzyme MurA to stimulate PG precursor synthesis (Boutte *et al.*, 2016). Phosphorylation of CwlM also affects its binding to FhaA and the lipid-II precursor flippase MurJ (Turapov *et al.*, 2018). CwlM is quickly dephosphorylated in transition to stasis (Boutte *et al.*, 2016) likely by PstP (Shamma *et al.*, 2021). The PG regulator Wag31 is strongly phosphorylated in the log. phase and less or non-phosphorylated in the stationary phase (Jani *et al.*, 2010). These facts hint to the possibility that dephosphorylation of these regulators may be important for downregulation of PG metabolism in stasis.

Previously we showed that phospho-regulation of PstP regulates PG metabolism in stasis (Shamma *et al.*, 2021). In this study, we show that, *in vitro* PstPWT$_{Mtb}$ dephosphorylates three PG regulators FhaA$_{Mtb}$, Wag31$_{Mtb}$ and CwlM$_{Mtb}$ but when phosphorylated on T137 its activity against these PG regulatory substrates is significantly inhibited (Figure 3.1A and B, 3.2A and B and 3.4A and B). We wanted to see if this corresponding phosphosite on PstP (PstPT134$_{Msmeg}$) might affect PG metabolism *in vivo* in *Msmeg*.

We made *Msmeg* strains with phosphomimetic *pstP*T134$_{Msmeg}$ alleles. We reported previously that the biological replicates of T134E mutant strains showed bimodal distributions of doubling times (Shamma *et al.*, 2021) probably due to potential suppressor mutations. We performed growth curves with newly constructed *pstP*T134$_{Msmeg}$ allelic strains and observed a similar pattern of bimodal doubling times in different biological replicates (Figure 3.5).

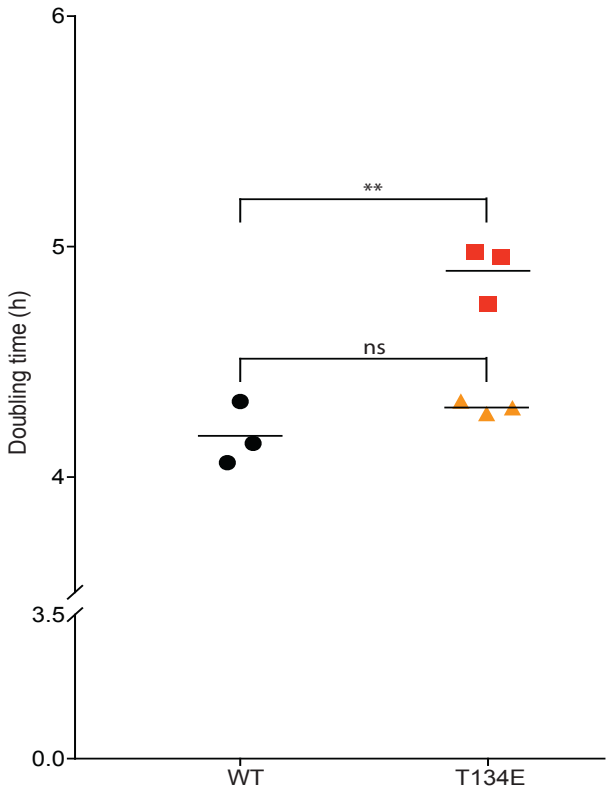

Figure 3.5 Doubling times of *pstP*$_{Msmeg}$ T134 phospho-mimetic strains

Doubling times of *Msmeg* strains carrying the phospho-mimetic *pstP*T134E and the WT alleles. Each symbol represents the average doubling time of one biological replicate of different genotypes. The *pstP*T134E allelic replicates showing similar doubling times in the bimodal distribution of doubling times are represented with red squares or orange triangles. The average doubling time of each strain was calculated from growth curves performed at least twice on different dates. The bars represent mean with standard deviation. **, P value= 0.0026, ns, P value= 0.1976.

We used the three biological phosphomimetic replicates that showed consistent slower growth phenotypes compared to the *pstP*WT$_{Msmeg}$ allelic strains (Figure 3.5, red squares) in our next experiment. In these phosphomimetic strains and WT strains, we used a fluorescent D-amino acid HADA (Kuru *et al.*, 2012) as a metric of active PG metabolism in the exponentially growing cells and cells starved in PBS with Tween80 for a total of 30 minutes .

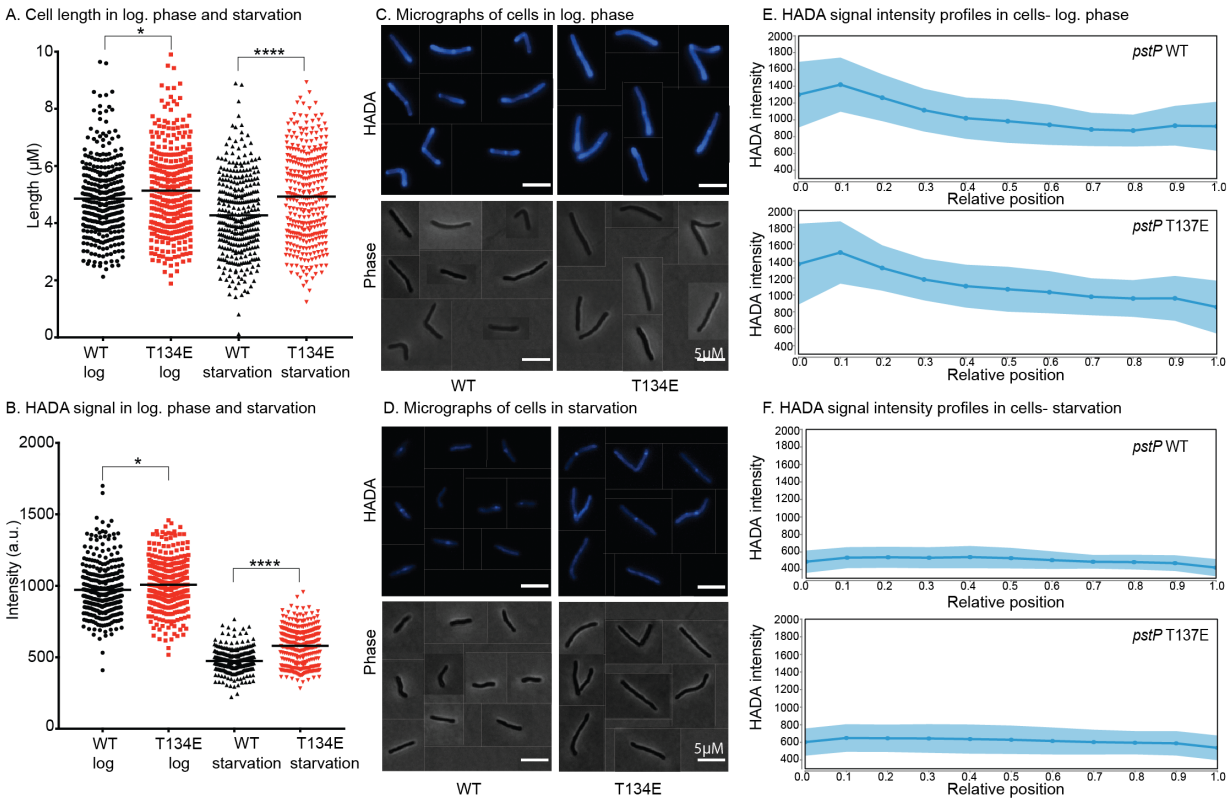

Figure 3.6 Phosphosite on T134 on PstP$_{Msmeg}$ is important in regulating PG metabolism

A. Quantification of cell lengths of isogenic *pstP* allele strains (WT and T134E) grown in 7H9 in log. phase and starved in PBS with Tween80. At least 100 cells from each of three biological replicates were quantified. P values were calculated by unpaired t-test. *, P value = 0.0122, ****, P value= 0.000000031.

B. Quantification of mean intensities of HADA of *pstP* allele strains (WT and T134E) grown in 7H9 in log. phase and starved in PBS with Tween90. Cells were stained after 15 minutes of starvation and washed and fixed after another 15 minutes (starved for a total of 30 minutes). At least 100 cells from each of three biological replicates were quantified. P values were calculated by unpaired t-test. *, P value = 0.0109, ****, P value= <0.000000000000001.

C and D. Representative HADA and phase images of cells from *pstP* allele strains (WT and T134E) grown in 7H9 in log. phase (C) and after 30 minutes of starvation in PBS with Tween80 (D).

E and F. Intensity profiles of HADA signals in cells of *pstP* allele strains (WT and T134E) in log. phase (E) and after starving for 30 minutes in PBS supplemented with Tween80 (F). The shaded regions denote standard deviations and the solid lines

represent the mean intensity values. Signal intensities from at least 110 cells from each of three biological replicates of every *pstP* allelic variant genotype were quantified and used to analyze the signal profiles in MicrobeJ. 0 to 1 on the X-axes represent cells from the old (brightest) to the new pole respectively.

We see a slight increase in length (Figure 3.6A and C, 3.7A and B) and HADA intensity (Figure 3.6B and C, 3.7A and B) in the *pstP*T134$_{Msmeg}$ strains in the log. phase compared to the WT strains. After they were starved in PBS with Tween80, these differences increase (Figure 3.6A, B and D, Figure 3.7C and D). In the log. phase, the increase in mean intensity of the HADA signal in the *pstP*T134$_{Msmeg}$ allelic strains is likely due to the higher HADA intensity at the old pole compared to the WT allelic strains as evident from the signal intensity profiles of cells (Figure 3.6E, Figure 3.7A and B). The starved *pstP*WT$_{Msmeg}$ strains show decreased HADA signal compared to that in the log. phase (Figure 3.6B, E and F top panels, Figure 3.7A and C) which indicates downregulation of PG metabolism in transition to stasis, whereas the starved *pstP*T134E$_{Msmeg}$ allele strains show significantly higher HADA signal (Figure 3.6B, E and F bottom panels, Figure 3.7B and D) indicating a defect in downregulating PG metabolism. We see some septal HADA signal mainly and significantly downregulated HADA signal at the poles (Figure 3.6D and F top panel, Figure 3.7C) in the starved *pstP*WT$_{Msmeg}$ cells. The *pstP*T134E$_{Msmeg}$ allele cells, in comparison, show somewhat delocalized HADA staining (Figure 3.6D and F bottom panel, Figure 3.7D) suggesting that the presence of a constant negative charge on phosphosite T134 on PstP$_{Msmeg}$ is affecting the downregulation of PG synthesis likely by suppressing PstP's activity against different PG regulatory substrates.

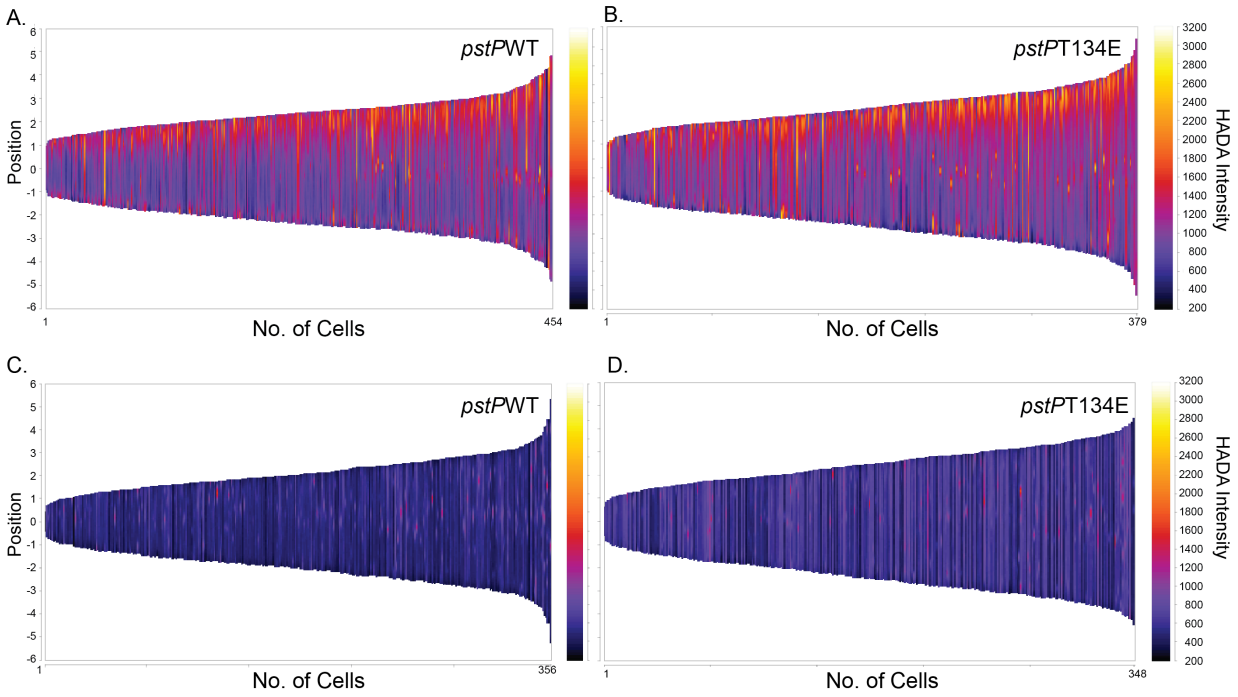

Figure 3.7 Demographic profiles of HADA signal intensity in *pstP*$_{Msmeg}$ strains in growth and starvation

A and **B.** Demographs showing intensities of the fluorescent dye HADA signal in individual cells from *pstP*WT allele strains (A) and *pstP*T134E allele strains (B) in log. phase.

C and **D.** Demographs showing intensities of the fluorescent dye HADA signal in individual cells from *pstP*WT allele strains (C) and *pstP*T134E allele strains (D) starved in PBS with Tween80 for a total time period of 30 minutes.

Biological triplicates of each *pstP* allelic variant were analyzed. Signal intensities from at least 340 cells from each *pstP* allelic variant (at least 100 cells from each biological triplicate of each genotype) in log. phase and starvation were plotted in the demographs.

Our data showing that the *pstP*134E$_{Msmeg}$ strains have higher HADA intensity (Figure 3.6B,C and E bottom panel, Figure 3.7B) in the log. phase support the notion (Jani *et al.*, 2010; Turapov *et al.*, 2018) that PG regulation involves a subtle balance in phosphorylated and dephosphorylated forms of its regulatory substrates and PstP's

phospho-regulation contributes to this regulation likely by maintaining the phosphorylation states of PG regulatory substrates.

The misregulation of PG metabolism (Figure 3.6B, C, D, E and F bottom panels, Figure 3.7B and D) may account for the slower growth of the *pstP*134E$_{Msmeg}$ strains that we see in our data (Fig 2.5). The increased length (Figure 3.6A) and the HADA intensity (Figure 3.6B) in the log. phase despite their slower growth indicate that the PG metabolism is likely disordered .

3.6 Conclusion

We suggest a model where FhaA is phospho-regulated, because it is phosphorylated by PknB and dephosphorylated by PstP, although the role of phosphorylation of FhaA phosphorylation has not been elucidated. This work may be useful to find out more on the role of reversible phosphorylation of FhaA in the cell in future. This also supports the model that PknB is the master regulator of phosphorylation and PstP is its negative regulatory switch (Iswahyudi *et al.*, 2019; Dulberger *et al.*, 2020; Shamma *et al.*, 2021).

Also, our *in vivo* data (Figure 3.6) indicate that in addition to downregulation of PG synthesis in stasis, PG synthesis needs to be continuously regulated in log phase as well. PstP's phospho-regulation plays an important role in all of this. Individual phosphosites play a role in regulating its activity and specificity and thus contributes PstP mediated dephosphorylation of substrates. To find how exactly the phosphosite T134 on PstP$_{Msmeg}$ may be important in PG metabolism, we intend to examine the key PG regulator CwlM's phosphorylation *in vivo* in *pstP*T134E *Msmeg* strains next.

Our finding that PstP dephosphorylates Wag31 (Figure 3.2A and B) suggests a possible model of phopsho-regulation of polar PG metabolism where phospho- and non-phospho-forms of Wag31 are needed to balance PG synthesis. Wag31 is known to oligomerize to form higher ordered structures (Nguyen *et al.*, 2007; Choukate and Chaudhuri, 2020) and it has been suggested that phosphorylation may favor interaction of Wag31 molecules (Jani *et al.*, 2010). While conducting *in vitro* phosphatase assays with $Wag31_{Mtb}$~P, we found that with ten times less $PstPWT_{Mtb}$ than the amount of $Wag31_{Mtb}$ used in the reaction, phosphorylation signal diminishes immediately but after that appears stabilized over time (data not shown). We assume that the oligomerization of Wag31 in the assay reaction may somehow affect PstP's access to all of the substrate present in the reaction mixture, but we do not know if or how oligomerization may be a factor that causes $PstPT141E_{Mtb}$ and $T174E_{Mtb}$ to act somewhat reluctantly on Wag31 (Figure 3.2). It is more plausible that the orientation of the phosphorylation sites T141, which maps on the flap subdomain and T174 on $PstP_{Mtb}$ (Figure 3.3) may contribute to toggling specificity of PstP against different substrates when a phosphate group is added on them.

Chapter 4

Identifying mutations in *pstP*$_{Msmeg}$ variants that suppress a growth-restrictive phenotype

Farah Shamma[1], Karen Samaga-de-Tembiwa[1] and Cara Boutte[1]

[1]Department of Biology, University of Texas Arlington, Arlington, Texas

4.1 Preface

This chapter builds on the bimodal distribution of doubling times of different *pstP*$_{Msmeg}$ strains that we see in Chapter 2, Figure 2.1B (Shamma *et al.*, 2021). The consistent presence of two populations in different *pstP*$_{Msmeg}$ phospho-variants with doubling times slower and similar to the *pstP*WT$_{Msmeg}$ strains led us to hypothesize that some suppressor mutations might be arising in some of the biological replicates masking the slower growth phenotype. In this project, we raised some faster growing strains from different *pstP*$_{Msmeg}$ phospho-allele slow-grower strains, confirmed absence of reversions in the respective phospho-ablative (T134A and T138A) and phospho-mimetic (T134E and T138E) *pstP*$_{Msmeg}$ alleles, sequenced the genomes of these clones to find mutations elsewhere in the genome other than in the phospho-ablative and phospho-mimetic *pstP*$_{Msmeg}$ alleles. I passaged all the strains to raise potential suppressor-mutation containing strains from the slow-growing parents and performed growth curves to

phenotype them. Once the faster-growing phenotypes were identified, Karen Samaga-de-Tembiwa isolated the genomic DNA and sent them for sequencing.

4.2 Abstract

PstP is a key negative regulator of the Serine/Threonine protein kinases (STPK) in Mycobacteria; this reversible phosphorylation is important in regulating the cell wall. PstP is itself phosphorylated by the STPKs and phospho-regulation of PstP affects cell wall metabolism. But the role of each phospho-site of PstP in regulating its substrates or interactions with other proteins *in vivo* is yet unclear. Suppressor mutations can often be used to find new genetic interactions. In this study, I aimed to see if faster-growing strains could be raised from slow-growing parents of different $pstP_{Msmeg}$ phospho-variants, and to see if I could find mutations in some genes important for cell-wall regulation or metabolism, which suppressed the growth-limiting effect of the $pstP_{Msmeg}$ phospho-mutations. These genes might give useful information on PstP's interaction network. I found that some $pstP_{Msmeg}$ phospho-ablative and phospho-mimetic strains contained mutations in some genes that restored the normal doubling times in the parental slow-growth pheonotypes. Among the genes that underwent mutations to restore the normal growth pheonotype, we think that the arabinogalactan synthesis enzyme encoded by *aftA* is an important one and might be a part of PstP's regulatory network *in vivo.*

4.3 Introduction

The reversible Serine/Threonine (S/T) phosphorylation of various proteins and enzymes is a crucial cell wall regulatory mechanism in Mycobacteria (Kang *et al.*, 2005; Gee *et*

al., 2012; Baer *et al.*, 2014; Boutte *et al.*, 2016). PstP being the only cognate S/T phosphatase of the 11 Serine/Threonine protein kinases (STPKs) in *Mycobacterium tuberculosis* (*Mtb*) (Cole *et al.*, 1998; Bach *et al.*, 2009) serves as the major negative regulator of phosphorylation (Iswahyudi *et al.*, 2019) to revert the effects of phosphorylation (Molle *et al.*, 2006; Shamma *et al.*, 2021) on cell wall metabolism. $PstP_{Mtb}$ is itself phosphorylated (Sajid *et al.*, 2011) and I have shown in Chapter 3 (Figure 3.1, 3.2 and 3.4) of this dissertation that $PstP_{Mtb}$'s activity is phospho-regulated *in vitro*. PstP's phospho-regulation is also imperative *in vivo*- the phosphosite T171 on PstP *Mycobacterium smegmatis (Msmeg)* is important in regulating cell growth, length, antibiotic tolerance, the peptidoglycan and the mycolic acid metabolism (Shamma *et al.*, 2021) and the phospho-site T134 on $PstP_{Msmeg}$ is important in regulating PG metabolism in both log. phase and starvation (Chapter 3 Figure 3.6).

The mycobacterial cell wall core consists of different covalently cross-linked layers- peptidoglycan (PG)-arabinogalactan (AG)-Mycolic acid (MA) (Daffé and Draper, 1997) and involves a plethora of enzymes and proteins that coordinate and regulate the synthesis of different layers (Dulberger *et al.*, 2020), a lot of which are controlled by STPK phosphorylation (Prisic and Husson, 2014). PstP is suggested to serve as the negative phospho-regulatory switch in the cell (Iswahyudi *et al.*, 2019), but how each phosphosite may regulate PstP spatio-temporally to control PstP's catalytic activity or specificity against and interaction with different cell-wall substrates in the complex scenario of cell wall regulation *in vivo* is still unknown.

The three conserved phospho-sites on PstP$_{Msmeg}$ are T134, T138 and T171 (Sajid *et al.*, 2011). That each phospho-site might be individually important is evident from the bimodal growth pheonotypes of phospho-ablative (T→A) and phospho-mimetic (T→E) *pstP*$_{Msmeg}$ strains (Shamma *et al.*, 2021). In addition to a slower-growth phenotype, a group of the *pstP*$_{Msmeg}$ T134A, T134E, T138A and T138E strains also consistently showed doubling times similar to the *pstP*$_{Msmeg}$ WT strains (Shamma *et al.*, 2021), so I suspected that some mutations might be occurring in the genomes of these strains which were able to suppress the growth-restrictive effect of *pstP*$_{Msmeg}$ phospho-mutations in these strains. We hypothesized that these suppressor mutations could be occurring in the substrates of PstP or in the genetic pathways that are redundant with PstP, its substrates or their regulators, which could shed light on important genetic connections of PstP in the reversible phospho-regulatory network. In this study, I aimed to map the potential suppressor mutations in the *pstP*$_{Msmeg}$ T134 and T138 phospho-mutants to identify PstP's genetic interactions and intersecting biological pathways.

In this study, I raised some fast-growers from the slow-growing parental *pstP*$_{Msmeg}$ phospho-variants and used them to map potential suppressor-mutations in the genome. I found different mutations in the genome that we think suppressed the growth-limiting effect of *pstP*$_{Msmeg}$ phospho-mutations. Among these, the likeliest to be true suppressors are the genes encoding: AftA (galactan 5-O-arabinofuranosyltransferase), MoxR (ATPase family protein associated with various cellular activities (AAA)) and a putative NiFe hydrogenase, beta subunit in *Msmeg.*

4.4 Methods and materials

4.4.1 Bacterial strains and culture conditions

All *Mycobacterium smegmatis* mc^{2}155 ATCC 700084 cultures were grown in 7H9 (Becton, Dickinson, Franklin Lakes, NJ) medium containing 5 g/liter bovine serum albumin (BSA), 0.003 g/liter catalase, 2 g/liter dextrose, 0.85 g/liter NaCl, 0.2% glycerol, and 0.05% Tween 80 and incubated at 37°C until log. phase. 1xPBS with 0.05% Tween 80 was used for starvation assays. Cultures were plated on LB lennox agar (Fisher BP1427-2). Antibiotic concentrations for *M. smegmatis* were 25µg/ml kanamycin and 20 µg/ml zeocin..

4.4.2 Strain construction

The phospho-ablative and phospho-mimetic *pstP*$_{Msmeg}$ allelic strains (*Msmeg* mc^{2}155 Δ*pstP*::lox L5::pCT94-p766tetON6-*pstP*$_{Msmeg}$T134A, T134E, T138A and T138E) and *Msmeg* mc^{2}155 Δ*pstP*::lox L5::pCT94-p766tetON6-*pstP*$_{Msmeg}$WT strains were generated by swapping *pstP*$_{Msmeg}$ T134A, T134E, T138A, T138E and WT alleles respectively under the promoter p766tetON6 in the integrative vector pCT94 at the L5 site of the *M. smeg* mc^{2}155 Δ*pstP*::lox strain as described previously (Pashley and Parish, 2003; Shamma *et al.*, 2021).

4.4.3 Raising strains with potential suppressor-mutations

At least three biological replicates of the slow growing phenotypes of *pstP*$_{Msmeg}$ allele variants (T134A, T134E, T138A, T138E) and the WT were plated on LB agar plates supplemented with Kanamycin 25µg/ml. At least three smallest colonies were picked

from each biological replicate of each genotype and each colony was inoculated in 7H9 media to raise suppressors individually.

Each culture was allowed to grow up to their stationary phases to allow increase of potential mutant cells containing the suppressors. The cultures were passaged upon reaching their stationary phases in to fresh 7H9 media daily for at least 12 days. In order to see if any faster growing variants occurred in the cultures, each culture was plated on LB agar plates and differences in colony sizes on each plate were observed. Some of the bigger colonies were picked for each genotype from the plates and grown in 7H9 medium to perform growth curves to see changes in doubling times compared to the parental strains.

4.4.4 Growth Curve Assays

For finding out the growth phenotypes of different parental *pstP*$_{Msmeg}$ allele variants (T134A, T134E, T138A, T138E and WT) at first, at least three biological replicates of different *pstP*$_{Msmeg}$ allele variants (T134A, T134E, T138A, T138E and WT) were grown in 7H9 media up to log. phase as described in (Shamma *et al.*, 2021). For finding out the change in growth phenotypes of the suppressor strains raised from the parental *pstP*$_{Msmeg}$ strains (T134A, T134E, T138A and T138E), all the suppressor strains were grown in 7H9 media up to log. phase to perform growth curves.

The growth curves were performed in non-treated non-tissue culture 96-well plates using a plate reader (BioTek Synergy neo2 multi mode reader) in 200µl 7H9 media starting at OD_{600}=0.1. Doubling times were calculated using the Exponential growth

equation using the least squared ordinary fit method in GraphPad Prism (Version 7.0d). P values were calculated using two-tailed, unpaired t-tests.

4.4.5 Isolation of genomic DNA

To check whether faster-growing phenotypes arisen from their slower growing parents due to reversions of the mutant *pstP*$_{Msmeg}$ alleles (T134A, T134E, T138A and T138E) to the WT allele, the phospho-ablative and phospho-mimetic allelic regions were sequenced first. The faster-growing clones that showed reversion of the phospho-ablative and phospho-mimetic mutations in *pstP*$_{Msmeg}$ were excluded from further experimentation.

The genomic DNA was purified from nine faster-growing potential suppressor mutation-containing biological replicate strains of the *pstP*$_{Msmeg}$ T134A, T138A and T138E genotypes in total in the standard phenol:chloroform:isoamyl alcohol (25:24:1) method (Sambrook and Russel, 2001). Purity of the prepared samples was checked using spectrophotometer (NanoDrop One/One Microvolume UV-Vis, ThermoFisher). Sequencing libraries were generated by MiGS Inc. (PA, USA) using the Illumina (NEB, MA, USA) DNA library preparations. The prepared DNA library was sequenced on the NextSeq 2000 platform according to the manufacturer's instruction for paired end (2x151) reads. bcl2fastq was used for quality control and adapter trimming for the Illumina sequencing. The variant caller breseq (0.35.4) was used to align and compare sequencing data using the following commands:

breseq -r [reference file] [sample name]_.fastq.gz [sample name]_fastq.gz -o [output file name]

4.5 Results

4.5.1 Faster-growing phenotypes arise from slow-growing *pstP*$_{Msmeg}$ strains

Biological replicates with identical *pstP*$_{Msmeg}$ phospho-mutations showing bimodal doubling times is indicative of the significance of the respective phospho-site of PstP$_{Msmeg}$ in normal cell growth regulation. I hypothesized that the phospho-ablative (T134A, T138A) and the phospho-mimetic (T134E and T138E) mutations on PstP$_{Msmeg}$ severely impaired the growth of some of the biological strains giving rise to mutations to overcome the phospho-site mutation-induced growth defect, enabling the strains to revert to faster/normal growth rate. These mutations might as well arise and accumulate in the slow-growth phenotypes of these *pstP*$_{Msmeg}$ phospho-mutant strains over time.

I decided to grow some of the slow-growing biological replicates containing *pstP*$_{Msmeg}$ T134A, T134E, T138A and T138E alleles (referred to as parental strains in this chapter onwards) (Figure 4.1A) over several days individually to see if suppressor mutations occurred in them. Biological replicates of each genotype were plated on LB agar some of the smallest colonies, which grew the slowest, were inoculated individually in 7H9 medium (Figure 4.1B). Cells of each colony thus grew in different culture tubes, which would mean a different environment for each of them This was done see if different individual mutations might occur in different biological replicates of the same slow-growing strains growing in different tubes.

The slow-growing *pstP*$_{Msmeg}$ biological replicates were grown up to the stationary phase everyday before passaging them into new 7H9 medium for at least 12 days (Figure 4.1C and D). If mutations occurred in any of the cells of a strain that suppressed the

slow-growth phenotype, it would replicate faster and eventually outnumber the slow-growing cells in the tube (Figure 4.1D).

Cultures containing both faster and slower growing cells would show bigger and small colonies respectively if plated on LB agar. So after plating these repeatedly passaged cultures from each test tube on LB agar, at least three bigger colonies were picked from each (referred to as clones of potential suppressor-containing strains), grown in 7H9 to perform growth curves in order to phenotype them (Figure 4.1D).

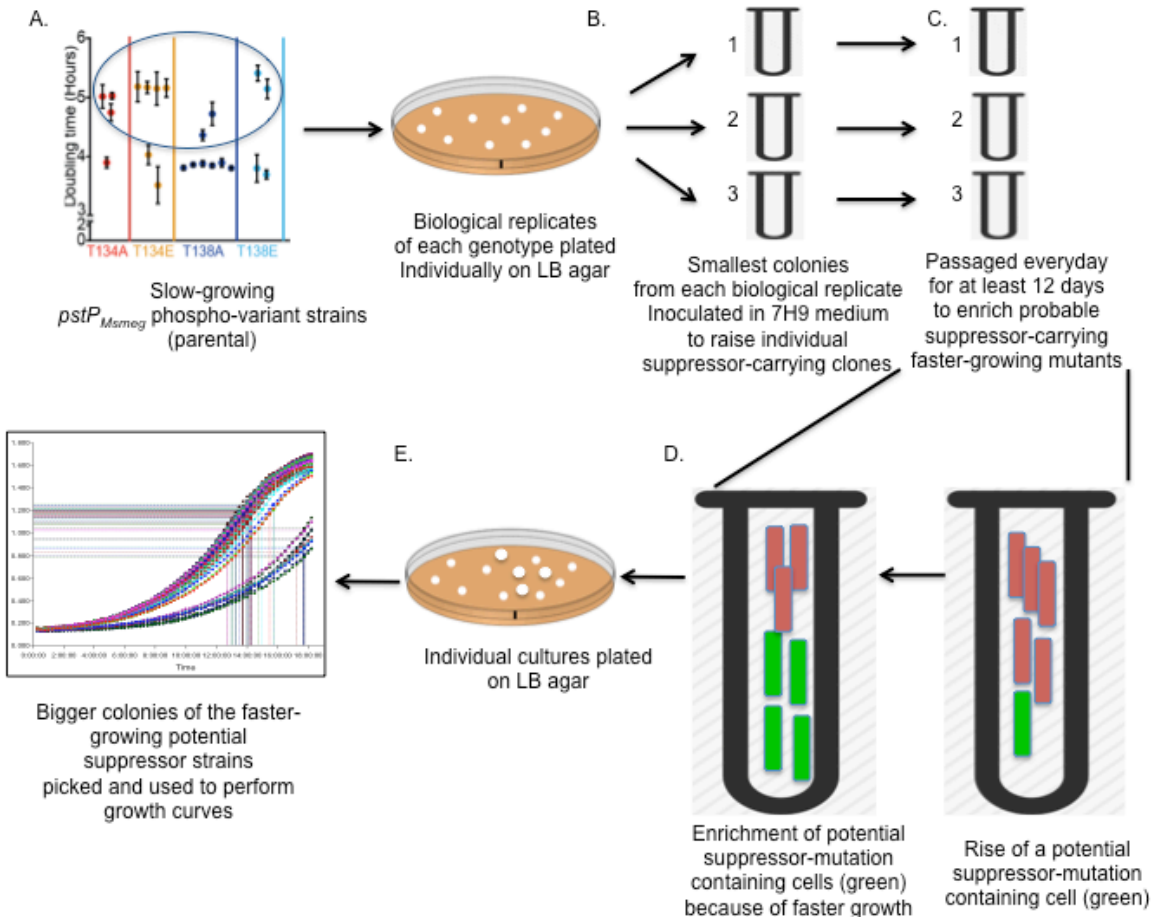

Figure 4.1 Schematic of raising potential suppressor-mutation containing strains from parental strains

A. At least three biological replicates of each genotype that had slow doubling times depicted in the table were plated on LB agar. **B.** At least three smallest colonies were picked and inoculated individually in 7H9 medium to let individual colonies have their own growth-environment to allow occurrence of potential individual mutations. **C.** Each culture was passaged everyday in to new media after growing them up to stationary phase. **D.** Concept of enrichment of potential-suppressor mutants. Red cells represent slow-growth phenotypes. Green cells represent fast-growth phenotype. **E.** Each culture was plated on LB agar to see the presence of bigger (growing faster) and smaller (growing slower) on the same agar plate. Bigger colonies were grown in 7H9 up to log. phase to perform growth curves. All LB agar and 7H9 media were supplemented with Kanamycin 25 µg/ml.

I then calculated and compared the doubling times of the clones to that of their parents.

I saw some strains gained faster doubling times compared to their slow-growing parents

(Figure 4.2). I got at least one strain from each parent which showed restored WT

growth phenotype compared to their parental slow-growing strain (Figure 4.2).

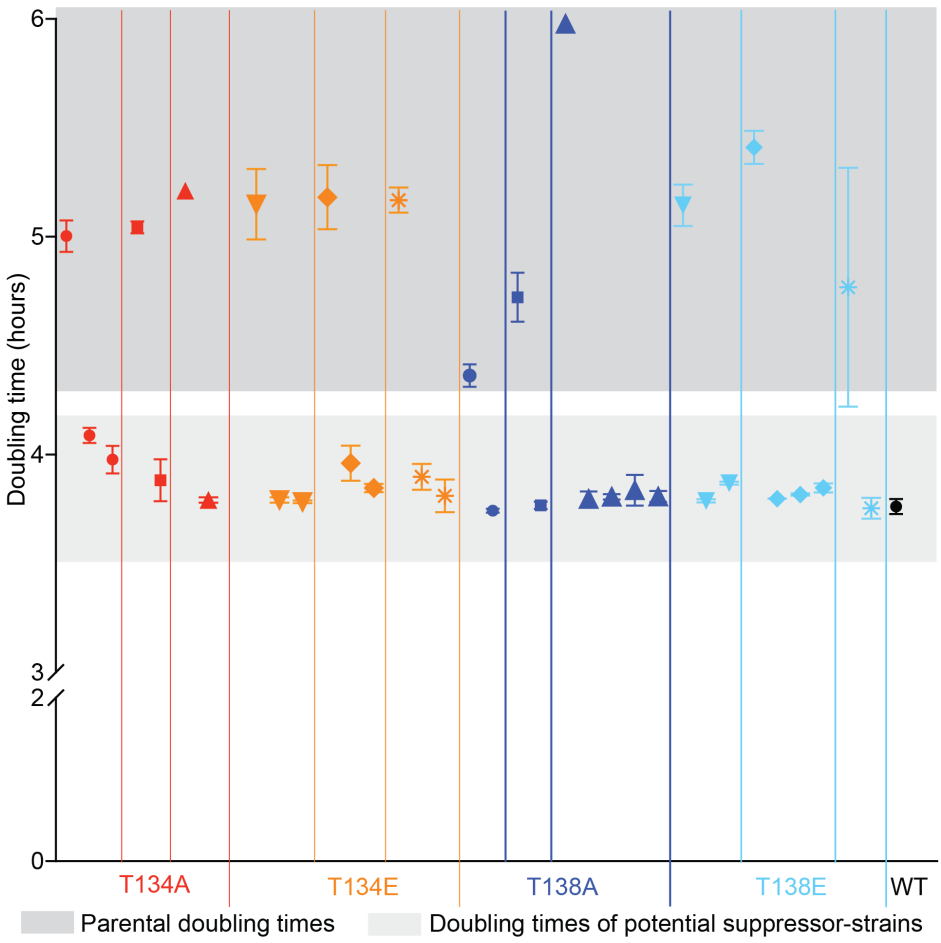

Figure 4.2 Doubling times of strains raised from their slow-growing *pstP*$_{Msmeg}$ phospho-mutant parents

Each symbol represents the mean doubling time of one biological replicate of different genotypes. The mean for each potential suppressor-containing strain raised from their parent was calculated was calculated from the doubling times of their biological clones. The first symbol of each section (of doubling times separated from another by colored vertical lines) is the mean parental doubling time and the next one(s) in the same section represent(s) the mean doubling time of the strain(s) raised from it. All the symbols in the top dark-gray shaded region are mean parental doubling times and in the bottom light-gray shaded region are the strains raised from them. The error bars represent mean with standard error of mean. The doubling times of the *pstP*$_{Msmeg}$ T134A, T134E, T138A and T138E strains and the vertical lines separating each group of parental and their successors are represented in red, orange, blue and cyan respectively.

4.5.2 Mutations in the genomes restore the wild-type growth phenotypes in the slow-growing *pstP*$_{Msmeg}$ phosphomimetic strains

I aimed to map the potential suppressor-mutations in the rapidly growing *pstP*$_{Msmeg}$ mutants (Figure 4.2) using whole genome sequencing. To rule out the possibility of rapid-growth occurring simply due to reversions of the phospho-mutant *pstP*$_{Msmeg}$ alleles to their WT form, only the *pstP*$_{Msmeg}$ allelic regions were sequenced first. The *pstP*$_{Msmeg}$ alleles in all the *pstP*$_{Msmeg}$ T134E fast-growing strains that were chosen to send for sequencing, showed reversion of T134E to the WT allele. So the other *pstP*$_{Msmeg}$ allelic variants excluding these T134E strains were used for whole genome sequencing.

Mutations in the sequences called with high coverage indicate high confidence level of probable mutation in the genome. So only those high confidence mutations were taken into consideration and presented here in this study (Table 4.1). Some of the genes showing mutations with high confidence level, the two hits *aftA* and OOAFAAHP_01498 in Table 4.2 for example, were also found showing mutations in sequences called with marginal evidences (data not shown) but not presented in Table 4.2.

We found different types of mutations occurring in different growth-restored *pstP*$_{Msmeg}$ clones. We mostly see single base substitutions (nonsense or missense) in genes and mutations in coding and intergenic regions (Table 4.1).

Table 4.1: Summary of mutations in the faster-growing *pstP*$_{Msmeg}$ phospho-variant strains

All the rapidly growing biological replicates of *pstP*$_{Msmeg}$ T134A, T134E, T138A and T138E strains sequenced are represented by different colors. The color group for T134A is red, T138A is blue and T138E is cyan. Squares of the respective colors in the table represent presence of a particular mutation in that strain.

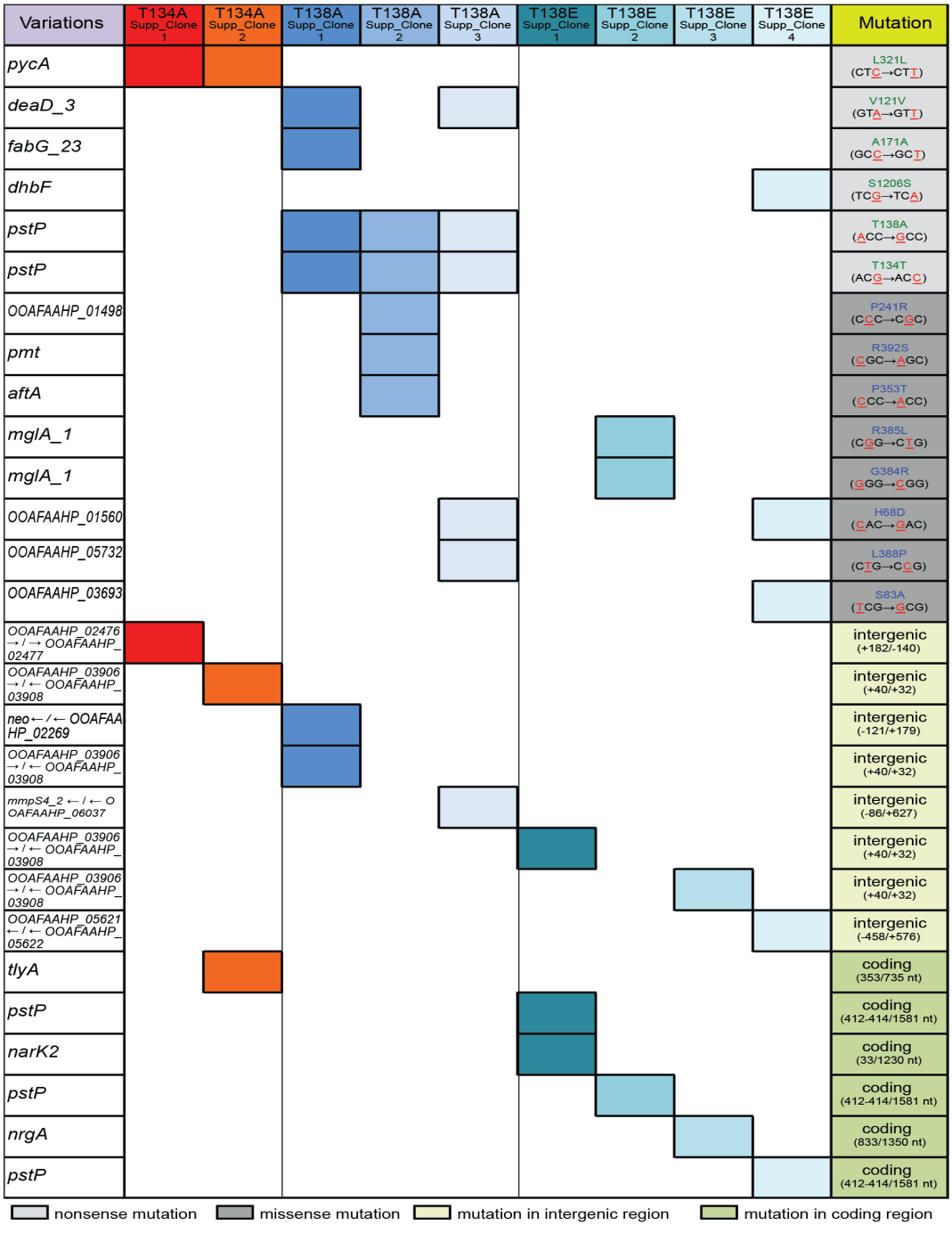

I looked for different mutations in the same genes of individual biological replicates, which would strongly indicate that the gene is important in PstP's interaction network and is prone to mutation events to overcome the growth-inhibitory effect of phospho-mutation on $PstP_{Msmeg}$.

I analyzed some of the genes that had missense mutations and/or occurred multiple times in different strains. The most interesting hits are shown in Table 4.2.

Both the UniProt BLAST (https://www.uniprot.org/blast/) and the NCBI BLASTp (https://blast.ncbi.nlm.nih.gov/Blast.cgi) were used to find *Msmeg* protein sequences that matched with the given peptide sequences for two of the hits- OOAFAAHP_01498 and OOAFAAHP_01560 (Table 4.1). I found the protein sequence of OOAFAAHP_01498 corresponds to MoxR in *Msmeg* and that of OOAFAAHP_01560 corresponds to NiFe hydrogenase, beta subunit in in *Msmeg*.

Table 4.2: Potential suppressors of growth-restrictive *pstP*$_{Msmeg}$ alleles

Gene	Gene ID	Protein	Function	Essentiality
aftA	MSMEG_6386	galactan 5-O-arabinofuranosyltransferase	arabinogalactan biosynthesis	yes
moxR	MSMEG_3867	ATPase family protein associated with various cellular activities (AAA)	ATP binding	--
--	MSMEG_3931	Putative NiFe hydrogenase, beta subunit	Iron-Sulfur cluster binding	--

4.6 Discussion

In this study, I screened for spontaneous mutants that grew rapidly despite only having

the growth–limiting *pstP*$_{Msmeg}$ T134E or T141 alleles in them suppressing the parental growth-restricted phenotypes. I aimed to identify the molecular role of the phosphosites T134 and T141 of PstP$_{Msmeg}$ by mapping potential suppressor mutations in these strains using whole genome sequencing. The identified genes that underwent mutations in the rapidly growing *pstP*$_{Msmeg}$ strains could be important in analyzing genetic connections of PstP which could help understand the function of phospho-sites on PstP better.

The most interesting hits in this study are *aftA* and *moxR* (Table 4.2), which also showed mutations in sequences called with marginal evidence (data not shown).

aftA is the first enzyme in the biosynthesis of the arabinogalactan pathway (Shi *et al.*, 2008). Whether it is phosphorylated is not known though. Since this is an essential cell wall regulatory enzyme undergoing a suppressor mutation to restore wild-type growth phenotype in *pstP*$_{Msmeg}$ phospho-mutant, it could mean that it is a part of PstP's phospho-regulatory network. We speculate that mutation in *aftA* may increase or decrease its cell wall metabolism activity restoring the cell envelope integrity to compensate for the impaired cell growth or it may be taking on a secondary function to restore normal cell growth activity.

MoxR is a putative ATPase family protein associated with various cellular activities (AAA) and has an ATP binding domain and a DUF58 domain. This is a putative transcriptional regulator. STPKs regulate transcription factors involved in the cell wall regulatory pathway (Zheng *et al.*, 2007; Prisic and Husson, 2014). Since PstP is a part of this phospho-regulated network, then it is not unlikely that its phospho-misregulation might affect the transcriptional signals. I speculate that mutation in this transcriptional

regulator may help transcriptionally regulate different cell wall regulatory proteins to compensate for the effect of *pstP*$_{Msmeg}$'s phospho-mutations.

The relationship between *pstP*'s phospho-mutations and *aftA* will be studied in future work.

Chapter 5

Conclusion

5.1 Preface

This chapter summarizes the key findings in chapters 2-4 addressing the research questions asked in chapter 1 of this dissertation. The main contributions of our studies are discussed in the bigger picture context of Mycobacterial cell wall regulation to adapt to the changing environments taking the limitations of our study into consideration. At many places here, using the conclusions from our data and other published findings, we took the liberty of making logical speculations on how PstP might work to regulate the cell wall in an *in vivo* scenario, which may help find important directions in predicting the possible pathways intersecting with PstP's cell wall regulatory network in future works.

5.2 PstP dephosphorylates multiple PG regulators

The first research aim of this dissertation was to find novel substrates of PstP. In my project I identified three peptidoglycan (PG) biosynthesis regulators $CwlM_{Mtb}$ (Chapter 2), $FhaA_{Mtb}$ and $Wag31_{Mtb}$ (Chapter 3) that are dephosphorylated by $PstP_{Mtb}$ *in vitro.* In this dissertation all the *in vitro* assays were performed with *Mtb* proteins so these findings are direct biochemical evidence of PstP's substrates.

These proteins show phosphorylation by their respective STPKs *in vitro* and *in vivo* (Grundner *et al.*, 2005; Kang *et al.*, 2005; Kang *et al.*, 2008; Jani *et al.*, 2010;

Roumestand *et al.*, 2011; Boutte *et al.*, 2016) so our *in vitro* data hint that these regulatory proteins are very likely to be substrates of PstP *in vivo*. The facts that phosphorylated CwlM (Boutte *et al.*, 2016) and Wag31 (Kang *et al.*, 2008; Jani *et al.*, 2010) serve as activators of PG biosynthesis and that FhaA interacts with phosphorylated CwlM (Turapov *et al.*, 2018) *in vivo* suggest that all these proteins upregulate PG synthesis in growth, so PstP may likely dephosphorylate these substrates in stasis to cease PG synthesis.

To expand the knowledge on the repertoire of PstP substrates, we wished to find if PstP dephosphorylated the Mycobacterial cell division protein, FtsZ and the mycolic acid biosynthetic enzyme InhA at some point in our project, which may be done in future works.

5.3 PstP's phospho-sites are important in regulating its activity against substrates thus affecting cell wall metabolism

The second goal of this dissertation was to understand the role of the phospho-sites on PstP in regulating its activity and different cell wall regulatory pathways. We report that the individual phospho-sites of PstP are important in regulating its activity against substrates, the metabolism of different cell wall layers and also cell growth in our *in vitro* (4.3.1) and *in vivo* (4.3.2 - 4.3.4) studies.

5.3.1 The phospho-sites T141 and 174 are important in regulating PstP's substrate specificity and the phospho-site T137 in regulating $PstP_{Mtb}$'s activity

T141 and T174: In chapter 3 of this dissertation, we show *in vitro* that phospho-mimetic $PstP_{Mtb}$T141E and T174E, that are negatively charged at these sites constantly,

dephosphorylate CwlM similarly compared to how PstP$_{Mtb}$WT dephosphorylates CwlM. I see a similar pattern in case of FhaA's dephosphorylation by PstP$_{Mtb}$T141E and T174E. PstP$_{Mtb}$T141E and T174E dephosphorylate Wag31 significantly slower than PstP$_{Mtb}$WT. It is likely that the phospho-regulation of PstP might affect its dephosphorylation of substrates and this specificity might help coordinate multiple substrates' regulatory role in modulating PG synthesis *in vivo*.

T134: In chapter 3 we also show that the phosphomimetic PstP$_{Mtb}$T134E impairs PstP's catalytic activity against CwlM, FhaA and Wag31 *in vitro*, implying PstP's inability to dephosphorylate these PG regulators when there is a negative charge present at this site.

In an *in vivo* setting, it looks like PstP is likely to be phosphorylated on T134 when CwlM, Wag31 and FhaA need to remain phosphorylated to keep on synthesizing PG, but will be phosphorylated on T141 and/or T174 to turn on its dephosphorylating activity against these substrates, but then not all of these substrates will be dephosphorylated at the same rate. So T134 acts as the turn-off switch and T141 and T174 seem to add the nuance in regulation of PstP's activity.

Although the findings are limited to assessment of PstP's activity on certain PG regulatory substrates only, altogether they prove that each phospho-site is important in regulating PstP. Finding substrates of PstP which are involved in regulating other events or pathways, for example cell division or mycolic acid biosynthesis, can help deduce the significance of phospho-regulation of PstP's activity and substrate specificity

in future. Also, the temporal status of phosphorylations on PstP *in vivo* is not known where the kinases that phosphorylate PstP may also play a role. So the *in vitro* data do not mirror the complexity of the STPK-substrate-PstP network *in vivo*.

5.3.2 The phospho-site T134 on PstP in *Mycobacterium smegmatis (Msmeg)* is important in regulating PG metabolism

I see in the $pstP_{Msmeg}$T134E strains, the PG metabolism is higher in starvation conditions compared to the $pstP_{Msmeg}$WT strains, compared to the difference in log. phase. So strains expressing $PstP_{Msmeg}$ with a negative charge always present at T134 (corresponding to T137 in $PstP_{Mtb}$) seem to fail to downregulate PG metabolism. Since the *in vitro* studies show that $PstP_{Mtb}$T137E fail to dephosphorylate CwlM, FhaA and Wag31, which are all PG regulators, it is very likely that *in vivo* the dephosphorylation of these regulators may be impaired by the presence of a constant negative charge on T134 on $PstP_{Msmeg}$ affecting the regulation of PG metabolism mediated in changing conditions by these regulators in turn. To match PG synthesis with growth rate and to downregulate PG synthesis in stasis, balance is to be maintained between phosphorylated and non-phosphorylated states of the PG regulators *in vivo* mediated by Serine/Threonine protein kinases (STPKs) and PstP. The finding suggests that the phospho-site T134 on $PstP_{Msmeg}$ play an important role in mediating this balance where $PstP_{Msmeg}$ cannot be expected to be always phosphorylated on T134 in growth or stasis, which would clearly affect its ability to subtly control PG metabolism most likely by impairing its activity against substrates.

5.3.3 The phospho-site T171 on PstP$_{Msmeg}$ has an impact in regulating PG synthesis in starvation and mycolic acid synthesis in log phase

I report in Chapter 2 that the phosphosite T171 of PstP$_{Msmeg}$ (corresponding to T174 on PstP$_{Mtb}$) has an impact on regulating the cell wall metabolism. I see that PstP$_{Msmeg}$T171 mainly regulates peptidoglycan in the transition to stasis while its role in mycolic acid metabolism may be restricted to log. phase (Figure3DF). The findings describe a regulatory role of PstP in log. phase and stasis in *Msmeg*, where the phospho-site T171 on PstP regulates the PG metabolism in stasis and the mycolic acid metabolism during growth. The non-phosphoform of PstP$_{Msmeg}$T171 seems to be favored over the phosphoform in regulating both PG and mycolic acid metabolism.

This can provide useful information in understanding how the phospho-mediated regulation of PstP could be important in coordinating mycolic acid and PG biosynthesis. In our second research objective, we pondered how PstP may choose to dephosphorylate the mycolic acid enzyme KasA but not the PG regulator CwlM in growth (Chapter 1, Figure 1.5) and whether its phosphorylations may play a role in this. The finding that the phospho-site T171 on PstP$_{Msmeg}$ is significant in regulating mycolic acid biosynthesis but not PG metabolism in growth indicate that this phospho-site may be playing a role in directing PstP's activity against the different substrates of these two cell wall layers in growth.

Peptidoglycan and mycolic acid metabolism are controlled by different systems in growth and the transition to stasis. PG is controlled by phosphorylation at several points along the biosynthesis pathway involving multiple substrates including CwlM, FhaA and Wag31 used in our studies (Kang *et al.*, 2005; Gee *et al.*, 2012; Kieser *et al.*, 2015;

Boutte *et al.*, 2016; Arora *et al.*, 2018; Turapov *et al.*, 2018). PknB likely serves as a master regulator and checkpoint in this pathway by detecting periplasmic lipid II (Kaur *et al.*, 2004) and changing its phosphorylation activity against the regulators CwlM and FhaA (Grundner *et al.*, 2005; Roumestand *et al.*, 2011; Gee *et al.*, 2012; Boutte *et al.*, 2016) and the enzymes MurJ, RodA and PonA1 (Gee *et al.*, 2012; Kieser *et al.*, 2015; Arora *et al.*, 2018) in response. PstP seems to counterbalances the effect of these STPK mediated phosphorylations using its phospho-sites as the regulator for itself. My conclusions from 4.2.1 and this section combined suggest that the phospho-site on PstP is important for PstP to regulate PG metabolism in growth where both T134 and T171 are important in regulating PG synthesis in stasis, and T171 is important in regulating mycolic acid metabolism in growth. Nevertheless, it cannot be ignored that there are likely other mechanisms of cell wall regulation involved in the complex *in vivo* scenario like protein localization or PstP's interaction with other regulatory proteins that may contribute to PstP's regulation as well.

5.3.4 The phospho-site T171 on PstP$_{Msmeg}$ is important in regulating growth

The cell length of *Msmeg* has been observed to decrease from approximately 5µm to under ~2 µm in certain carbon starvation conditions (Wu *et al.*, 2016). It is assumed that this is due to reductive cell division (Smeulders *et al.*, 1999; Baranowski *et al.*, 2019), wherein the relative division/elongation activity increases. I show in Chapter 2 that *pstP*$_{Msmeg}$T171E cells show a slow-growth phenotype and fail to downregulate its size in starvation conditions unlike the *pstP*$_{Msmeg}$WT strains, which showed reductive cell division in the same condition. There can be many reasons why I see this, but the most

plausible hypothesis is that PstP has a possible role in regulating reductive cell division and that the phospho-site T171 may be important for PstP in this activity.

How might PstP's phosphorylation affect reductive cell division? I base our assumptions on published data on the role of the mycobacterial cell division protein FtsZ, whose activity is inhibited by STPK mediated-phosphorylation (Thakur and Chakraborti, 2006). So I propose FtsZ to be a putative substrate of PstP whose dephosphorylation by PstP would mean active cell division.

My data show that the PstP T171 phospho-mimetic strain fails to reductively divide. In transition to starvation, the cell needs to increase its frequency of division relative to elongation, and I might expect that PstP would be even more active against FtsZ. If PstP's putative activity against FtsZ is critical for this reductive cell division, then it appears that phosphorylation on T171 will have an inhibitory effect on PstP's activity against FtsZ. PstP has not yet been shown to dephosphorylate FtsZ or other cell division proteins like FtsQ (Jain *et al.*, 2018), so this very speculative conclusion that we present here may provide a base for finding out in future work whether FtsZ is a substrate of PstP and if it is affected by phospho-regulation of PstP.

Reductive cell division likely also includes regulation of elongation factors. In light of this finding, our other putative substrate of PstP is RodA, which is a PG transglycosylase involved in cell elongation (Meeske *et al.*, 2016; Arora *et al.*, 2018). RodA seems to be activated by phosphorylation in *Mtb* (Arora *et al.*, 2018). So RodA may be dephosphorylated by PstP during reductive division in order to downregulate PG metabolism and cell elongation. The $PstP_{Msmeg}$T171E mutant fails to reductively divide,

this could also partly be through failure to dephosphorylate RodA or other elongation factors that are activated by phosphorylation. In general it seems that PstP, which is unphosphorylated at T171 is important in upregulating elongation and downregulating cell division in the transition to stasis.

5.4 Misregulating PstP affects antibiotic tolerance

This section addresses the third objective of this dissertation, which was to identify the effect of misregulated PstP on drug tolerance. I observed the effect of phospho-misregulated PstP on antibiotic tolerance in Msmeg cells in Chapter 2. I misregulated its phospho-site on T171 on $PstP_{Msmeg}$ and found show that phospho-ablative and phospho-mimetic mutations at T171 of $PstP_{Msmeg}$ affect antibiotic tolerance, suggesting that PstP's phospho-regulation is important in regulating antibiotic tolerance. The antibiotic sensitivity experiments that we performed in *Msmeg* suggest that misregulation of PstP could sensitize mycobacteria to various antibiotics in both growth and stasis.

It seems like PstP influences regulation of mycolic acid synthesis in growth and PG synthesis in starvation via its phosphosites. We see that the mycolic acid metabolism-targeting drug Isoniazid affect the $pstP_{Msmeg}$T171 phospho-mimetic strain in growth and the PG targeting drug Meropenem affect the phosphomimetic strain in starvation. So, misregulation of phosphosites on PstP misregulates the cell wall- the PG in stasis and the mycolic acid in growth, and makes them susceptible to antibiotics.

I propose that PstP may be an Achilles' heel of *Mtb*. It is an essential enzyme, so inhibiting it should kill growing *Mtb* directly. But, it is also a master regulator of antibiotic

tolerance under stress, so inhibiting PstP should misregulate the cell wall and increase permeability to other antibiotics.

5.5 Phospho-sites of PstP give clues to finding important intersecting pathways

In my dissertation, I also report that misregulation of PstP's phospho-sites induce suppressor mutations to compensate for the growth-defect observed in phospho-misregulated *pstP*$_{Msmeg}$ strains.

In chapter 2 I found that misregulating phospho-sites T134 and 138 on *pstP*$_{Msmeg}$ give rise to a slow-growth phenotype in both cases but there are also a population of strains with these same phospho-mutant alleles that show a similar growth profile as the *pstP*$_{Msmeg}$WT strains. In chapter 4, using whole genome sequencing, I identified some mutations in some important genes in the rapid-growing successor strains raised from their slow-growing parents that I think could be responsible for restoring normal growth rate in these strains. That some strains were reverting to the normal growth phenotype suggests that the misregulation of these phospho-sites on PstP$_{Msmeg}$ had severe deterring effect on cell growth to a point where these strains underwent genomic mutations in order to overcome the effect of phospho-misregulation of PstP in the cell. This indicates the importance of these individual phosphosites on PstP$_{Msmeg}$ in overall cell growth regulation.

The functions of the proteins encoded by the mutated-genes I identified give an idea on what pathway might be modulated to compensate for PstP's phospho-misregulated effect. In other words, the pathways that these proteins are a part of can be interconnected with PstP's regulatory circuitry. My finding will thus help to shed light on

PstP's genetic interaction network and can divulge important information about the phospho-regulated PstP mediated cell wall modulation. Future work will entail further characterization of the relationship of the identified proteins- AftA, an arabinogalactan biosynthetic enzyme and MoxR, a putative transcriptional regulator, with PstP.

References

Ardito, F., Giuliani, M., Perrone, D., Troiano, G., and Muzio, L.L. (2017) The crucial role of protein phosphorylation in cell signaling and its use as targeted therapy (Review). *International Journal of Molecular Medicine* **40**: 271–280 https://www.spandidos-publications.com/10.3892/ijmm.2017.3036. Accessed November 19, 2021.

Arora, D., Chawla, Y., Malakar, B., Singh, A., and Nandicoori, V.K. (2018) The transpeptidase PbpA and noncanonical transglycosylase RodA of Mycobacterium tuberculosis play important roles in regulating bacterial cell lengths. *J Biol Chem* **293**: 6497–6516 https://www.ncbi.nlm.nih.gov/pmc/articles/PMC5925798/. Accessed May 23, 2019.

Av-Gay, Y., and Everett, M. (2000) The eukaryotic-like Ser/Thr protein kinases of Mycobacterium tuberculosis. *Trends in Microbiology* **8**: 238–244 https://linkinghub.elsevier.com/retrieve/pii/S0966842X00017340. Accessed November 15, 2021.

Bach, H., Wong, D., and Av-Gay, Y. (2009) Mycobacterium tuberculosis PtkA is a novel protein tyrosine kinase whose substrate is PtpA. *Biochemical Journal* **420**: 155–162 https://portlandpress.com/biochemj/article/420/2/155/44900/Mycobacterium-tuberculosis-PtkA-is-a-novel-protein. Accessed November 15, 2021.

Baer, C.E., Iavarone, A.T., Alber, T., and Sassetti, C.M. (2014) Biochemical and Spatial Coincidence in the Provisional Ser/Thr Protein Kinase Interaction Network of *Mycobacterium tuberculosis*. *J Biol Chem* **289**: 20422–20433 http://www.jbc.org/lookup/doi/10.1074/jbc.M114.559054. Accessed October 23, 2019.

Baranowski, C., Rego, E.H., and Rubin, E.J. (2019) The Dream of a Mycobacterium. *Microbiology Spectrum* **7** http://www.asmscience.org/content/journal/microbiolspec/10.1128/microbiolspec.GPP3-0008-2018. Accessed April 29, 2019.

Barford, D. (1996) Molecular mechanisms of the protein serine/threonine phosphatases. *Trends Biochem Sci* **21**: 407–412.

Batt, S.M., Burke, C.E., Moorey, A.R., and Besra, G.S. (2020) Antibiotics and resistance: the two-sided coin of the mycobacterial cell wall. *The Cell Surface* **6**: 100044 https://linkinghub.elsevier.com/retrieve/pii/S2468233020300116. Accessed October 1, 2020.

Betts, J.C., Lukey, P.T., Robb, L.C., McAdam, R.A., and Duncan, K. (2002) Evaluation of a nutrient starvation model of Mycobacterium tuberculosis persistence by gene and protein expression profiling. *Molecular Microbiology* **43**: 717–731

https://onlinelibrary.wiley.com/doi/abs/10.1046/j.1365-2958.2002.02779.x. Accessed February 8, 2019.

Bhamidi, S., Shi, L., Chatterjee, D., Belisle, J.T., Crick, D.C., and McNeil, M.R. (2012) A bioanalytical method to determine the cell wall composition of Mycobacterium tuberculosis grown in vivo. *Analytical Biochemistry* **421**: 240–249 https://linkinghub.elsevier.com/retrieve/pii/S0003269711007123. Accessed February 5, 2020.

Bibb, J.A., and Nestler, E.J. (2005) Serine and Threonine Phosphorylation. In *Basic Neurochemistry : Molecular, Cellular and Medical Aspects*. Elsevier Science & Technology, pp. 391–393.

Boitel, B., Ortiz-Lombardía, M., Durán, R., Pompeo, F., Cole, S.T., Cerveñansky, C., and Alzari, P.M. (2003) PknB kinase activity is regulated by phosphorylation in two Thr residues and dephosphorylation by PstP, the cognate phospho-Ser/Thr phosphatase, in Mycobacterium tuberculosis: Mycobacterial serine/threonine kinase and phosphatase. *Molecular Microbiology* **49**: 1493–1508 http://doi.wiley.com/10.1046/j.1365-2958.2003.03657.x. Accessed February 6, 2019.

Bollen, M., Peti, W., Ragusa, M.J., and Beullens, M. (2010) The extended PP1 toolkit: designed to create specificity. *Trends in Biochemical Sciences* **35**: 450–458 https://linkinghub.elsevier.com/retrieve/pii/S0968000410000460. Accessed April 27, 2020.

Botella, H., Yang, G., Ouerfelli, O., Ehrt, S., Nathan, C.F., and Vaubourgeix, J. (2017) Distinct Spatiotemporal Dynamics of Peptidoglycan Synthesis between Mycobacterium smegmatis and Mycobacterium tuberculosis. *mBio* **8** https://www.ncbi.nlm.nih.gov/pmc/articles/PMC5596344/. Accessed May 23, 2019.

Boutte, C.C., Baer, C.E., Papavinasasundaram, K., Liu, W., Chase, M.R., Meniche, X., *et al.* (2016) A cytoplasmic peptidoglycan amidase homologue controls mycobacterial cell wall synthesis. *eLife* **5** https://elifesciences.org/articles/14590. Accessed February 6, 2019.

Bradshaw, N., Levdikov, V.M., Zimanyi, C.M., Gaudet, R., Wilkinson, A.J., and Losick, R. (2017) A widespread family of serine/threonine protein phosphatases shares a common regulatory switch with proteasomal proteases. *eLife* **6**: e26111 https://elifesciences.org/articles/26111. Accessed September 19, 2019.

Bradshaw, N., and Losick, R. (2015) Asymmetric division triggers cell-specific gene expression through coupled capture and stabilization of a phosphatase. *eLife* **4**: e08145 https://elifesciences.org/articles/08145. Accessed September 19, 2019.

Brogden, R.N., Carmine, A.A., Heel, R.C., Speight, T.M., and Avery, G.S. (1982) Trimethoprim: A Review of its Antibacterial Activity, Pharmacokinetics and Therapeutic Use in Urinary Tract Infections. *Drugs* **23**: 405–430 http://link.springer.com/10.2165/00003495-198223060-00001. Accessed December 10, 2021.

Carel, C., Nukdee, K., Cantaloube, S., Bonne, M., Diagne, C.T., Laval, F., *et al.* (2014) Mycobacterium tuberculosis Proteins Involved in Mycolic Acid Synthesis and Transport

Localize Dynamically to the Old Growing Pole and Septum. *PLOS ONE* **9**: e97148 https://journals.plos.org/plosone/article?id=10.1371/journal.pone.0097148. Accessed March 13, 2019.

Chai, Q., Zhang, Y., and Liu, C.H. (2018) Mycobacterium tuberculosis: An Adaptable Pathogen Associated With Multiple Human Diseases. *Front Cell Infect Microbiol* **8**: 158 http://journal.frontiersin.org/article/10.3389/fcimb.2018.00158/full. Accessed November 20, 2021.

Chopra, P., Singh, B., Singh, R., Vohra, R., Koul, A., Meena, L.S., *et al.* (2003) Phosphoprotein phosphatase of Mycobacterium tuberculosis dephosphorylates serine-threonine kinases PknA and PknB. *Biochem Biophys Res Commun* **311**: 112–120.

Choukate, K., and Chaudhuri, B. (2020) Structural basis of self-assembly in the lipid-binding domain of mycobacterial polar growth factor Wag31. *IUCrJ* **7**: 767–776 https://www.ncbi.nlm.nih.gov/pmc/articles/PMC7340271/. Accessed July 24, 2020.

Cohen, P. (1989) The structure and regulation of protein phosphatases. *Annu Rev Biochem* **58**: 453–508.

Cole, S.T., Brosch, R., Parkhill, J., Garnier, T., Churcher, C., Harris, D., *et al.* (1998) Deciphering the biology of Mycobacterium tuberculosis from the complete genome sequence. **396**: 27.

Cordillot, M., Dubée, V., Triboulet, S., Dubost, L., Marie, A., Hugonnet, J.-E., *et al.* (2013) *In Vitro* Cross-Linking of Mycobacterium tuberculosis Peptidoglycan by l,d-Transpeptidases and Inactivation of These Enzymes by Carbapenems. *Antimicrob Agents Chemother* **57**: 5940–5945 https://journals.asm.org/doi/10.1128/AAC.01663-13. Accessed December 10, 2021.

Cottin, V., Linden, A.V., and Riches, D.W.H. (1999) Phosphorylation of Tumor Necrosis Factor Receptor CD120a (p55) by p42mapk/erk2 Induces Changes in Its Subcellular Localization. 14.

Cunningham, A.F., and Spreadbury, C.L. (1998) Mycobacterial Stationary Phase Induced by Low Oxygen Tension: Cell Wall Thickening and Localization of the 16-Kilodalton ـ-Crystallin Homolog. *J BACTERIOL* **180**: 8.

Daffé, M., and Draper, P. (1997) The Envelope Layers of Mycobacteria with Reference to their Pathogenicity. In *Advances in Microbial Physiology*. Elsevier, pp. 131–203 https://linkinghub.elsevier.com/retrieve/pii/S0065291108600168. Accessed November 14, 2021.

Deb, C., Lee, C.-M., Dubey, V.S., Daniel, J., Abomoelak, B., Sirakova, T.D., *et al.* (2009) A Novel In Vitro Multiple-Stress Dormancy Model for Mycobacterium tuberculosis Generates a Lipid-Loaded, Drug-Tolerant, Dormant Pathogen. *PLoS ONE* **4**: e6077 https://dx.plos.org/10.1371/journal.pone.0006077. Accessed November 19, 2021.

DeJesus, M.A., Gerrick, E.R., Xu, W., Park, S.W., Long, J.E., Boutte, C.C., *et al.* (2017) Comprehensive Essentiality Analysis of the *Mycobacterium tuberculosis* Genome via Saturating

Transposon Mutagenesis. *mBio* **8**: e02133-16, /mbio/8/1/e02133-16.atom https://mbio.asm.org/content/8/1/e02133-16. Accessed August 1, 2020.

Doerks, T., Noort, V. van, Minguez, P., and Bork, P. (2012) Annotation of the M. tuberculosis Hypothetical Orfeome: Adding Functional Information to More than Half of the Uncharacterized Proteins. *PLoS ONE* **7**: e34302 https://dx.plos.org/10.1371/journal.pone.0034302. Accessed November 14, 2021.

Ducret, A., Quardokus, E.M., and Brun, Y.V. (2016) MicrobeJ, a tool for high throughput bacterial cell detection and quantitative analysis. *Nature Microbiology* **1**: 16077 https://www.nature.com/articles/nmicrobiol201677. Accessed May 3, 2019.

Dulberger, C.L., Rubin, E.J., and Boutte, C.C. (2020) The mycobacterial cell envelope — a moving target. *Nat Rev Microbiol* **18**: 47–59 http://www.nature.com/articles/s41579-019-0273-7. Accessed May 20, 2021.

Durán, R., Villarino, A., Bellinzoni, M., Wehenkel, A., Fernandez, P., Boitel, B., *et al.* (2005) Conserved autophosphorylation pattern in activation loops and juxtamembrane regions of Mycobacterium tuberculosis Ser/Thr protein kinases. *Biochemical and Biophysical Research Communications* **333**: 858–867 https://linkinghub.elsevier.com/retrieve/pii/S0006291X05011848. Accessed September 19, 2019.

Echenique, J., Kadioglu, A., Romao, S., Andrew, P.W., and Trombe, M.-C. (2004) Protein Serine/Threonine Kinase StkP Positively Controls Virulence and Competence in *Streptococcus pneumoniae*. *Infect Immun* **72**: 2434–2437 https://journals.asm.org/doi/10.1128/IAI.72.4.2434-2437.2004. Accessed November 15, 2021.

Feng, Z., and Barletta, R.G. (2003) Roles of *Mycobacterium smegmatis* D -Alanine: D -Alanine Ligase and D -Alanine Racemase in the Mechanisms of Action of and Resistance to the Peptidoglycan Inhibitor D -Cycloserine. *Antimicrob Agents Chemother* **47**: 283–291 https://journals.asm.org/doi/10.1128/AAC.47.1.283-291.2003. Accessed December 10, 2021.

Fernandez, P., Saint-Joanis, B., Barilone, N., Jackson, M., Gicquel, B., Cole, S.T., and Alzari, P.M. (2006) The Ser/Thr Protein Kinase PknB Is Essential for Sustaining Mycobacterial Growth. *Journal of Bacteriology* **188**: 7778–7784 http://jb.asm.org/cgi/doi/10.1128/JB.00963-06. Accessed February 6, 2019.

Flärdh, K. (2003) Essential role of DivIVA in polar growth and morphogenesis in Streptomyces coelicolor A3(2): DivIVA and tip growth in Streptomyces. *Molecular Microbiology* **49**: 1523–1536 http://doi.wiley.com/10.1046/j.1365-2958.2003.03660.x. Accessed February 6, 2019.

Fogel, N. (2015) Tuberculosis: A disease without boundaries. *Tuberculosis* **95**: 527–531 https://linkinghub.elsevier.com/retrieve/pii/S1472979214206950. Accessed November 18, 2021.

Galyov, E.E., Håkansson, S., Forsberg, Å., and Wolf-Watz, H. (1993) A secreted protein kinase of Yersinia pseudotuberculosis is an indispensable virulence determinant. *Nature* **361**: 730–732 http://www.nature.com/articles/361730a0. Accessed November 19, 2021.

García-Heredia, A., Pohane, A.A., Melzer, E.S., Carr, C.R., Fiolek, T.J., Rundell, S.R., *et al.* (2018) Peptidoglycan precursor synthesis along the sidewall of pole-growing mycobacteria. *eLife* **7** https://www.ncbi.nlm.nih.gov/pmc/articles/PMC6191288/. Accessed May 23, 2019.

Gee, C.L., Papavinasasundaram, K.G., Blair, S.R., Baer, C.E., Falick, A.M., King, D.S., *et al.* (2012) A Phosphorylated Pseudokinase Complex Controls Cell Wall Synthesis in Mycobacteria. *Sci Signal* **5**: ra7–ra7 https://stke.sciencemag.org/content/5/208/ra7. Accessed June 25, 2019.

Gengenbacher, M., Rao, S.P.S., Pethe, K., and Dick, T. (2010) Nutrient-starved, non-replicating Mycobacterium tuberculosis requires respiration, ATP synthase and isocitrate lyase for maintenance of ATP homeostasis and viability. *Microbiology* **156**: 81–87 https://www.microbiologyresearch.org/content/journal/micro/10.1099/mic.0.033084-0. Accessed August 3, 2020.

Getahun, H., Matteelli, A., Chaisson, R.E., and Raviglione, M. (2015) Latent *Mycobacterium tuberculosis* Infection. *N Engl J Med* **372**: 2127–2135 http://www.nejm.org/doi/10.1056/NEJMra1405427. Accessed November 18, 2021.

Gomez, J.E., and McKinney, J.D. (2004) M. tuberculosis persistence, latency, and drug tolerance. *Tuberculosis* **84**: 29–44 https://linkinghub.elsevier.com/retrieve/pii/S1472979203000866. Accessed September 19, 2019.

Greenstein, A.E., MacGurn, J.A., Baer, C.E., Falick, A.M., Cox, J.S., and Alber, T. (2007) M. tuberculosis Ser/Thr Protein Kinase D Phosphorylates an Anti-Anti–Sigma Factor Homolog. *PLoS Pathog* **3**: e49 https://dx.plos.org/10.1371/journal.ppat.0030049. Accessed May 26, 2021.

Grundner, C., Gay, L.M., and Alber, T. (2005) *Mycobacterium tuberculosis* serine/threonine kinases PknB, PknD, PknE, and PknF phosphorylate multiple FHA domains. *Protein Sci* **14**: 1918–1921 http://doi.wiley.com/10.1110/ps.051413405. Accessed September 19, 2019.

Gupta, M., Sajid, A., Arora, G., Tandon, V., and Singh, Y. (2009) Forkhead-associated Domain-containing Protein Rv0019c and Polyketide-associated Protein PapA5, from Substrates of Serine/Threonine Protein Kinase PknB to Interacting Proteins of Mycobacterium tuberculosis. *Journal of Biological Chemistry* **284**: 34723–34734 https://linkinghub.elsevier.com/retrieve/pii/S0021925820375967. Accessed May 26, 2021.

Hancock, R.E.W., and Bell, A. (1988) Antibiotic uptake into gram-negative bacteria. *EurJ ClinMicrobiolInfect Dis* **7**: 713–720.

Harth, G., Lee, B.Y., Wang, J., Clemens, D.L., and Horwitz, M.A. (1996) Novel insights into the genetics, biochemistry, and immunocytochemistry of the 30-kilodalton major extracellular protein of Mycobacterium tuberculosis. *Infect Immun* **64**: 3038–3047 https://journals.asm.org/doi/10.1128/iai.64.8.3038-3047.1996. Accessed December 10, 2021.

Hartmans, S., Bont, J.A.M. de, and Stackebrandt, E. (2006) The Genus Mycobacterium--Nonmedical. In *The Prokaryotes*. Dworkin, M., Falkow, S., Rosenberg, E., Schleifer, K.-H., and Stackebrandt, E. (eds). Springer New York, New York, NY. pp. 889–918 http://link.springer.com/10.1007/0-387-30743-5_33. Accessed November 2, 2020.

Hett, E.C., and Rubin, E.J. (2008) Bacterial Growth and Cell Division: a Mycobacterial Perspective. *Microbiology and Molecular Biology Reviews* **72**: 126–156 http://mmbr.asm.org/cgi/doi/10.1128/MMBR.00028-07. Accessed September 19, 2019.

Hoffmann, C., Leis, A., Niederweis, M., Plitzko, J.M., and Engelhardt, H. (2008) Disclosure of the mycobacterial outer membrane: Cryo-electron tomography and vitreous sections reveal the lipid bilayer structure. *Proceedings of the National Academy of Sciences* **105**: 3963–3967 http://www.pnas.org/cgi/doi/10.1073/pnas.0709530105. Accessed November 14, 2021.

Irmler, A., and Forchhammer, K. (2001) A PP2C-type phosphatase dephosphorylates the PII signaling protein in the cyanobacterium Synechocystis PCC 6803. *Proceedings of the National Academy of Sciences* **98**: 12978–12983 http://www.pnas.org/cgi/doi/10.1073/pnas.231254998. Accessed September 19, 2019.

Iswahyudi, Mukamolova, G.V., Straatman-Iwanowska, A.A., Allcock, N., Ajuh, P., Turapov, O., and O'Hare, H.M. (2019) Mycobacterial phosphatase PstP regulates global serine threonine phosphorylation and cell division. *Sci Rep* **9**: 8337 http://www.nature.com/articles/s41598-019-44841-9. Accessed June 14, 2019.

Jain, P., Malakar, B., Khan, M.Z., Lochab, S., Singh, A., and Nandicoori, V.K. (2018) Delineating FtsQ-mediated regulation of cell division in *Mycobacterium tuberculosis*. *Journal of Biological Chemistry* **293**: 12331–12349 http://www.jbc.org/lookup/doi/10.1074/jbc.RA118.003628. Accessed February 6, 2019.

Jani, C., Eoh, H., Lee, J., Hamasha, K., Sahana, M., Han, J.-S., *et al.* (2010) Regulation of Polar Peptidoglycan Biosynthesis by Wag31 Phosphorylation in Mycobacteria. *BMC Microbiol* **10**: 327 http://bmcmicrobiol.biomedcentral.com/articles/10.1186/1471-2180-10-327. Accessed May 10, 2019.

Jarlier, V., and Nikaido, H. (1990) Permeability barrier to hydrophilic solutes in Mycobacterium chelonei. *J Bacteriol* **172**: 1418–1423 https://journals.asm.org/doi/10.1128/jb.172.3.1418-1423.1990. Accessed November 14, 2021.

Jarlier, V., and Nikaido, H. (1994) Mycobacterial cell wall: Structure and role in natural resistance to antibiotics. *FEMS Microbiology Letters* 11–18.

Johnson, L.N., and Barford, D. (1993) The Effects of Phosphorylation on the Structure and Function of Proteins. *Annual Review* .

Juris, S.J., Rudolph, A.E., Huddler, D., Orth, K., and Dixon, J.E. (2000) A distinctive role for the Yersinia protein kinase: Actin binding, kinase activation, and cytoskeleton disruption. *Proceedings of the National Academy of Sciences* **97**: 9431–9436 http://www.pnas.org/cgi/doi/10.1073/pnas.170281997. Accessed November 15, 2021.

Kamariza, M., Shieh, P., and Bertozzi, C.R. (2018) Chapter Thirteen - Imaging Mycobacterial Trehalose Glycolipids. In *Methods in Enzymology*. Imperiali, B. (ed.). Academic Press, pp. 355–369 http://www.sciencedirect.com/science/article/pii/S0076687917303099. Accessed February 6, 2019.

Kang, C.-M., Abbott, D.W., Park, S.T., Dascher, C.C., Cantley, L.C., and Husson, R.N. (2005) The Mycobacterium tuberculosis serine/threonine kinases PknA and PknB: substrate identification and regulation of cell shape. *Genes Dev* **19**: 1692–1704 https://www.ncbi.nlm.nih.gov/pmc/articles/PMC1176007/. Accessed July 15, 2019.

Kang, C.-M., Nyayapathy, S., Lee, J.-Y., Suh, J.-W., and Husson, R.N. (2008) Wag31, a homologue of the cell division protein DivIVA, regulates growth, morphology and polar cell wall synthesis in mycobacteria. *Microbiology* **154**: 725–735 http://mic.microbiologyresearch.org/content/journal/micro/10.1099/mic.0.2007/014076-0. Accessed February 6, 2019.

Kaur, D., Brennan, P.J., and Crick, D.C. (2004) Decaprenyl Diphosphate Synthesis in Mycobacterium tuberculosis. *Journal of Bacteriology* **186**: 7564–7570 https://jb.asm.org/content/186/22/7564. Accessed March 18, 2019.

Kaur, P., Rausch, M., Malakar, B., Watson, U., Damle, N.P., Chawla, Y., *et al.* (2019) LipidII interaction with specific residues of Mycobacterium tuberculosis PknB extracytoplasmic domain governs its optimal activation. *Nature Communications* **10** http://www.nature.com/articles/s41467-019-09223-9. Accessed March 16, 2019.

Keshavjee, S., and Farmer, P.E. (2012) Tuberculosis, Drug Resistance, and the History of Modern Medicine. *N Engl J Med* **367**: 931–936 http://www.nejm.org/doi/10.1056/NEJMra1205429. Accessed November 20, 2021.

Khan, S., Nagarajan, S.N., Parikh, A., Samantaray, S., Singh, A., Kumar, D., *et al.* (2010) Phosphorylation of Enoyl-Acyl Carrier Protein Reductase InhA Impacts Mycobacterial Growth and Survival. *Journal of Biological Chemistry* **285**: 37860–37871 http://www.jbc.org/lookup/doi/10.1074/jbc.M110.143131. Accessed February 6, 2019.

Kieser, K.J., Baranowski, C., Chao, M.C., Long, J.E., Sassetti, C.M., Waldor, M.K., *et al.* (2015) Peptidoglycan synthesis in Mycobacterium tuberculosis is organized into networks with varying drug susceptibility. *PNAS* **112**: 13087–13092 https://www.pnas.org/content/112/42/13087. Accessed March 12, 2019.

Kieser, K.J., and Rubin, E.J. (2014) How sisters grow apart: mycobacterial growth and division. *Nature Reviews Microbiology* **12**: 550–562 http://www.nature.com/articles/nrmicro3299. Accessed February 6, 2019.

Kuru, E., Hughes, H.V., Brown, P.J., Hall, E., Tekkam, S., Cava, F., *et al.* (2012) In Situ Probing of Newly Synthesized Peptidoglycan in Live Bacteria with Fluorescent D -Amino Acids. *Angewandte Chemie International Edition* **51**: 12519–12523 http://doi.wiley.com/10.1002/anie.201206749. Accessed February 6, 2019.

Kusebauch, U., Ortega, C., Ollodart, A., Rogers, R.S., Sherman, D.R., Moritz, R.L., and Grundner, C. (2014) Mycobacterium tuberculosis supports protein tyrosine phosphorylation. *Proceedings of the National Academy of Sciences* **111**: 9265–9270 http://www.pnas.org/cgi/doi/10.1073/pnas.1323894111. Accessed November 15, 2021.

Le, N.-H., Locard-Paulet, M., Stella, A., Tomas, N., Molle, V., Burlet-Schiltz, O., *et al.* (2020) The protein kinase PknB negatively regulates biosynthesis and trafficking of mycolic acids in mycobacteria. *J Lipid Res* jlr.RA120000747 http://www.jlr.org/lookup/doi/10.1194/jlr.RA120000747. Accessed June 4, 2020.

Li, K.-K., Qu, D.-H., Zhang, H.-N., Chen, F.-Y., Xu, L., Wang, M.-Y., *et al.* (2020) Global discovery the PstP interactions using Mtb proteome microarray and revealing novel connections with EthR. *Journal of Proteomics* **215**: 103650 https://linkinghub.elsevier.com/retrieve/pii/S187439192030018X. Accessed May 26, 2021.

Lin, K., Hwang, P.K., and Fletterick, R.J. (1997) Distinct phosphorylation signals converge at the catalytic center in glycogen phosphorylases. *Structure* **5**: 1511–1523 https://linkinghub.elsevier.com/retrieve/pii/S0969212697003006. Accessed April 27, 2020.

Liu, J., Barry, C.E., Besra, G.S., and Nikaido, H. (1996) Mycolic Acid Structure Determines the Fluidity of the Mycobacterial Cell Wall. *Journal of Biological Chemistry* **271**: 29545–29551 http://www.jbc.org/lookup/doi/10.1074/jbc.271.47.29545. Accessed March 13, 2019.

Liu, Y., Tan, S., Huang, L., Abramovitch, R.B., Rohde, K.H., Zimmerman, M.D., *et al.* (2016) Immune activation of the host cell induces drug tolerance in *Mycobacterium tuberculosis* both in vitro and in vivo. *J Exp Med* **213**: 809–825 http://www.jem.org/lookup/doi/10.1084/jem.20151248. Accessed May 9, 2019.

Lu, G., and Wang, Y. (2008) FUNCTIONAL DIVERSITY OF MAMMALIAN TYPE 2C PROTEIN PHOSPHATASE ISOFORMS: NEW TALES FROM AN OLD FAMILY: Function of PP2C isoforms. *Clinical and Experimental Pharmacology and Physiology* **35**: 107–112 https://onlinelibrary.wiley.com/doi/10.1111/j.1440-1681.2007.04843.x. Accessed November 19, 2021.

Mailaender, C., Reiling, N., Engelhardt, H., Bossmann, S., Ehlers, S., and Niederweis, M. (2004) The MspA porin promotes growth and increases antibiotic susceptibility of both Mycobacterium bovis BCG and Mycobacterium tuberculosis. *Microbiology* **150**: 853–864 https://www.microbiologyresearch.org/content/journal/micro/10.1099/mic.0.26902-0. Accessed December 11, 2021.

Marquardt, J.L., Siegele, D.A., Kolter, R., and Walsh, C.T. (1992) Cloning and sequencing of Escherichia coli murZ and purification of its product, a UDP-N-acetylglucosamine enolpyruvyl transferase. *J Bacteriol* **174**: 5748–5752 https://journals.asm.org/doi/10.1128/jb.174.17.5748-5752.1992. Accessed November 15, 2021.

Marrakchi, H., Lanéelle, M.-A., and Daffé, M. (2014) Mycolic Acids: Structures, Biosynthesis, and Beyond. *Chemistry & Biology* **21**: 67–85 http://www.sciencedirect.com/science/article/pii/S1074552113004201. Accessed February 6, 2019.

Meeske, A.J., Riley, E.P., Robins, W.P., Uehara, T., Mekalanos, J.J., Kahne, D., *et al.* (2016) SEDS proteins are a widespread family of bacterial cell wall polymerases. *Nature* **537**: 634–638 http://www.nature.com/articles/nature19331. Accessed July 22, 2019.

Meniche, X., Otten, R., Siegrist, M.S., Baer, C.E., Murphy, K.C., Bertozzi, C.R., and Sassetti, C.M. (2014) Subpolar addition of new cell wall is directed by DivIVA in mycobacteria. *Proceedings of the National Academy of Sciences* **111**: E3243–E3251 http://www.pnas.org/cgi/doi/10.1073/pnas.1402158111. Accessed August 12, 2021.

Minnikin, D.E. (1991) Chemical principles in the organization of lipid components in the mycobacterial cell envelope. *Research in Microbiology* **142**: 423–427 https://linkinghub.elsevier.com/retrieve/pii/092325089190114P. Accessed November 18, 2021.

Mir, M., Asong, J., Li, X., Cardot, J., Boons, G.-J., and Husson, R.N. (2011) The Extracytoplasmic Domain of the Mycobacterium tuberculosis Ser/Thr Kinase PknB Binds Specific Muropeptides and Is Required for PknB Localization. *PLoS Pathog* **7**: e1002182 http://dx.plos.org/10.1371/journal.ppat.1002182. Accessed September 19, 2019.

Molle, V., Brown, A.K., Besra, G.S., Cozzone, A.J., and Kremer, L. (2006) The Condensing Activities of the Mycobacterium tuberculosis Type II Fatty Acid Synthase Are Differentially Regulated by Phosphorylation. *Journal of Biological Chemistry* **281**: 30094–30103 https://linkinghub.elsevier.com/retrieve/pii/S0021925819339158. Accessed May 26, 2021.

Molle, V., and Kremer, L. (2010) Division and cell envelope regulation by Ser/Thr phosphorylation: *Mycobacterium* shows the way. *Molecular Microbiology* **75**: 1064–1077 http://doi.wiley.com/10.1111/j.1365-2958.2009.07041.x. Accessed February 6, 2019.

Mougous, J.D., Gifford, C.A., Ramsdell, T.L., and Mekalanos, J.J. (2007) Threonine phosphorylation post-translationally regulates protein secretion in Pseudomonas aeruginosa. *Nat Cell Biol* **9**: 797–803 http://www.nature.com/articles/ncb1605. Accessed November 19, 2021.

Muñoz-Elías, E.J., and McKinney, J.D. (2006) Carbon metabolism of intracellular bacteria. *Cell Microbiol* **8**: 10–22 https://onlinelibrary.wiley.com/doi/10.1111/j.1462-5822.2005.00648.x. Accessed November 20, 2021.

Neuhaus, F.C., and Hammes, W.P. (1981) Inhibition of cell wall biosynthesis by analogues of alanine. *Pharmacology & Therapeutics* **14**: 265–319 https://linkinghub.elsevier.com/retrieve/pii/0163725881900309. Accessed December 10, 2021.

Nguyen, L. (2016) Antibiotic resistance mechanisms in M. tuberculosis: an update. *Arch Toxicol* **90**: 1585–1604 http://link.springer.com/10.1007/s00204-016-1727-6. Accessed September 19, 2019.

Nguyen, L., Scherr, N., Gatfield, J., Walburger, A., Pieters, J., and Thompson, C.J. (2007) Antigen 84, an Effector of Pleiomorphism in Mycobacterium smegmatis. *Journal of Bacteriology* **189**: 7896–7910 http://jb.asm.org/cgi/doi/10.1128/JB.00726-07. Accessed December 29, 2018.

Ortega, C., Liao, R., Anderson, L.N., Rustad, T., Ollodart, A.R., Wright, A.T., *et al.* (2014) Mycobacterium tuberculosis Ser/Thr Protein Kinase B Mediates an Oxygen-Dependent Replication Switch. *PLoS Biology* **12**: e1001746 http://dx.plos.org/10.1371/journal.pbio.1001746. Accessed February 6, 2019.

Pallen, M., Chaudhuri, R., and Khan, A. (2002) Bacterial FHA domains: neglected players in the phospho-threonine signalling game? *Trends in Microbiology* **10**: 556–563 https://linkinghub.elsevier.com/retrieve/pii/S0966842X02024769. Accessed November 11, 2021.

Pashley, C.A., and Parish, T. (2003) Efficient switching of mycobacteriophage L5-based integrating plasmids in *Mycobacterium tuberculosis*. *FEMS Microbiology Letters* **229**: 211–215 https://academic.oup.com/femsle/article-lookup/doi/10.1016/S0378-1097(03)00823-1. Accessed February 6, 2019.

Prisic, S., Dankwa, S., Schwartz, D., Chou, M.F., Locasale, J.W., Kang, C.-M., *et al.* (2010) Extensive phosphorylation with overlapping specificity by Mycobacterium tuberculosis serine/ threonine protein kinases. *Proceedings of the National Academy of Sciences* **107**: 7521–7526.

Prisic, S., and Husson, R.N. (2014) Mycobacterium tuberculosis Serine/Threonine Protein Kinases. *Microbiology Spectrum* **2** http://www.asmscience.org/content/journal/microbiolspec/10.1128/microbiolspec.MGM2-0006-2013. Accessed February 6, 2019.

Pullen, K.E., Ng, H.-L., Sung, P.-Y., Good, M.C., Smith, S.M., and Alber, T. (2004) An Alternate Conformation and a Third Metal in PstP/Ppp, the M. tuberculosis PP2C-Family Ser/Thr Protein Phosphatase. *Structure* **12**: 1947–1954 https://linkinghub.elsevier.com/retrieve/pii/S096921260400334X. Accessed May 26, 2021.

Roumestand, C., Leiba, J., Galophe, N., Margeat, E., Padilla, A., Bessin, Y., *et al.* (2011) Structural Insight into the Mycobacterium tuberculosis Rv0020c Protein and Its Interaction with the PknB Kinase. *Structure* **19**: 1525–1534 http://www.sciencedirect.com/science/article/pii/S096921261100253X. Accessed March 27, 2019.

Roy, J., and Cyert, M.S. (2009) Cracking the Phosphatase Code: Docking Interactions Determine Substrate Specificity. *Science Signaling* **2**: re9–re9 https://stke.sciencemag.org/lookup/doi/10.1126/scisignal.2100re9. Accessed April 27, 2020.

Sajid, A., Arora, G., Gupta, M., Upadhyay, S., Nandicoori, V.K., and Singh, Y. (2011) Phosphorylation of Mycobacterium tuberculosis Ser/Thr Phosphatase by PknA and PknB. *PLoS ONE* **6**: e17871 https://dx.plos.org/10.1371/journal.pone.0017871. Accessed December 9, 2021.

Sakamoto, K. (2012) The Pathology of *Mycobacterium tuberculosis* Infection. *Vet Pathol* **49**: 423–439 http://journals.sagepub.com/doi/10.1177/0300985811429313. Accessed November 19, 2021.

Sambrook, J., and Russel, D. (2001) *Molecular Cloning A Laboratory Manual*. 3rd ed., Cold Spring Harbour Laboratory Press, Cold Spring Harbour, New York.

Sarathy, J., Dartois, V., Dick, T., and Gengenbacher, M. (2013) Reduced Drug Uptake in Phenotypically Resistant Nutrient-Starved Nonreplicating Mycobacterium tuberculosis. *Antimicrobial Agents and Chemotherapy* **57**: 1648–1653 http://aac.asm.org/lookup/doi/10.1128/AAC.02202-12. Accessed February 6, 2019.

Sarathy, J.P., Via, L.E., Weiner, D., Blanc, L., Boshoff, H., Eugenin, E.A., *et al.* (2017) Extreme Drug Tolerance of *Mycobacterium tuberculosis* in Caseum. *Antimicrobial Agents and Chemotherapy* **62** http://aac.asm.org/lookup/doi/10.1128/AAC.02266-17. Accessed February 6, 2019.

Sassetti, C.M., and Rubin, E.J. (2003) Genetic requirements for mycobacterial survival during infection. *Proceedings of the National Academy of Sciences* **100**: 12989–12994 http://www.pnas.org/cgi/doi/10.1073/pnas.2134250100. Accessed August 1, 2020.

Schlicker, C., Fokina, O., Kloft, N., Grüne, T., Becker, S., Sheldrick, G.M., and Forchhammer, K. (2008) Structural Analysis of the PP2C Phosphatase tPphA from Thermosynechococcus elongatus: A Flexible Flap Subdomain Controls Access to the Catalytic Site. *Journal of Molecular Biology* **376**: 570–581 https://linkinghub.elsevier.com/retrieve/pii/S0022283607015987. Accessed December 10, 2021.

Schnappinger, D., O'Brien, K.M., and Ehrt, S. (2015) Construction of Conditional Knockdown Mutants in Mycobacteria. In *Mycobacteria Protocols*. Parish, T., and Roberts, D.M. (eds). Springer New York, New York, NY. pp. 151–175 http://link.springer.com/10.1007/978-1-4939-2450-9_9. Accessed December 10, 2021.

Seiler, P., Ulrichs, T., Bandermann, S., Pradl, L., Jörg, S., Krenn, V., *et al.* (2003) Cell-Wall Alterations as an Attribute of *Mycobacterium tuberculosis* in Latent Infection. *The Journal of Infectious Diseases* **188**: 1326–1331 https://academic.oup.com/jid/article-lookup/doi/10.1086/378563. Accessed February 6, 2019.

Shamma, F., Quintanilla, S., Bandekar, A., Sassetti, C., and Boutte, C. (2021) Phosphorylation on PstP Regulates Cell Wall Metabolism and Antibiotic Tolerance in Mycobacterium smegmatis. *Journal of Bacteriology* **203**: e00563-20.

Sharma, A.K., Arora, D., Singh, L.K., Gangwal, A., Sajid, A., Molle, V., *et al.* (2016) Serine/Threonine Protein Phosphatase PstP of *Mycobacterium tuberculosis* Is Necessary for Accurate Cell Division and Survival of Pathogen. *Journal of Biological Chemistry* **291**: 24215–24230 http://www.jbc.org/lookup/doi/10.1074/jbc.M116.754531. Accessed February 6, 2019.

Sharma, K., Gupta, M., Krupa, A., Srinivasan, N., and Singh, Y. (2006) EmbR, a regulatory protein with ATPase activity, is a substrate of multiple serine/threonine kinases and phosphatase in *Mycobacterium tuberculosis*. *FEBS Journal* **273**: 2711–2721 http://doi.wiley.com/10.1111/j.1742-4658.2006.05289.x. Accessed May 26, 2021.

Shi, L., Zhou, R., Liu, Z., Lowary, T.L., Seeberger, P.H., Stocker, B.L., *et al.* (2008) Transfer of the First Arabinofuranose Residue to Galactan Is Essential for *Mycobacterium smegmatis* Viability. *J Bacteriol* **190**: 5248–5255 https://journals.asm.org/doi/10.1128/JB.00028-08. Accessed November 18, 2021.

Shi, Y. (2009) Serine/Threonine Phosphatases: Mechanism through Structure. *Cell* **139**: 468–484 https://linkinghub.elsevier.com/retrieve/pii/S0092867409012549. Accessed November 19, 2021.

Slama, N., Leiba, J., Eynard, N., Daffé, M., Kremer, L., Quémard, A., and Molle, V. (2011) Negative regulation by Ser/Thr phosphorylation of HadAB and HadBC dehydratases from Mycobacterium tuberculosis type II fatty acid synthase system. *Biochemical and Biophysical Research Communications* **412**: 401–406 https://linkinghub.elsevier.com/retrieve/pii/S0006291X11012770. Accessed March 31, 2019.

Smeulders, M.J., Keer, J., Speight, R.A., and Williams, H.D. (1999) Adaptation of Mycobacterium smegmatis to Stationary Phase. *J Bacteriol* **181**: 270–283 https://JB.asm.org/content/181/1/270. Accessed June 8, 2020.

Stephan, J., Mailaender, C., Etienne, G., Daffé, M., and Niederweis, M. (2004) Multidrug Resistance of a Porin Deletion Mutant of *Mycobacterium smegmatis*. *Antimicrob Agents Chemother* **48**: 4163–4170 https://journals.asm.org/doi/10.1128/AAC.48.11.4163-4170.2004. Accessed December 10, 2021.

Su, J., and Forchhammer, K. (2013) Determinants for substrate specificity of the bacterial PP2C protein phosphatase tPphA from Thermosynechococcus elongatus. *The FEBS Journal* **280**: 694–707 https://febs.onlinelibrary.wiley.com/doi/abs/10.1111/j.1742-4658.2011.08466.x. Accessed July 10, 2019.

Thakur, M., and Chakraborti, P.K. (2006) GTPase Activity of Mycobacterial FtsZ Is Impaired Due to Its Transphosphorylation by the Eukaryotic-type Ser/Thr Kinase, PknA. *J Biol Chem* **281**: 40107–40113 http://www.jbc.org/lookup/doi/10.1074/jbc.M607216200. Accessed May 8, 2019.

Turapov, O., Forti, F., Kadhim, B., Ghisotti, D., Sassine, J., Straatman-Iwanowska, A., *et al.* (2018) Two Faces of CwlM, an Essential PknB Substrate, in Mycobacterium tuberculosis. *Cell Rep* **25**: 57-67.e5 https://www.ncbi.nlm.nih.gov/pmc/articles/PMC6180346/. Accessed July 22, 2020.

Typas, A., Banzhaf, M., Gross, C.A., and Vollmer, W. (2012) From the regulation of peptidoglycan synthesis to bacterial growth and morphology. *Nature Reviews Microbiology* **10**: 123–136 http://www.nature.com/articles/nrmicro2677. Accessed February 6, 2019.

Veyron-Churlet, R., Molle, V., Taylor, R.C., Brown, A.K., Besra, G.S., Zanella-Cléon, I., *et al.* (2009) The *Mycobacterium tuberculosis* β-Ketoacyl-Acyl Carrier Protein Synthase III Activity Is Inhibited by Phosphorylation on a Single Threonine Residue. *Journal of Biological Chemistry* **284**: 6414–6424 http://www.jbc.org/lookup/doi/10.1074/jbc.M806537200. Accessed March 31, 2019.

Veyron-Churlet, R., Zanella-Cléon, I., Cohen-Gonsaud, M., Molle, V., and Kremer, L. (2010) Phosphorylation of the *Mycobacterium tuberculosis* β-Ketoacyl-Acyl Carrier Protein Reductase MabA Regulates Mycolic Acid Biosynthesis. *Journal of Biological Chemistry* **285**: 12714–12725 http://www.jbc.org/lookup/doi/10.1074/jbc.M110.105189. Accessed February 6, 2019.

Vijay, K., Brody, M.S., Fredlund, E., and Price, C.W. (2000) A PP2C phosphatase containing a PAS domain is required to convey signals of energy stress to the sB transcription factor of Bacillus subtilis. *Molecular Microbiology* 9.

Vijay, S., Nagaraja, M., Sebastian, J., and Ajitkumar, P. (2014) Asymmetric cell division in Mycobacterium tuberculosis and its unique features. *Arch Microbiol* **196**: 157–168 http://link.springer.com/10.1007/s00203-014-0953-7. Accessed November 10, 2019.

Vilchèze, C., and Kremer, L. (2017) Acid-Fast Positive and Acid-Fast Negative Mycobacterium tuberculosis: The Koch Paradox. *Microbiology Spectrum* **5** http://www.asmscience.org/content/journal/microbiolspec/10.1128/microbiolspec.TBTB2-0003-2015. Accessed January 13, 2020.

Vilchèze, C., Molle, V., Carrère-Kremer, S., Leiba, J., Mourey, L., Shenai, S., *et al.* (2014) Phosphorylation of KasB Regulates Virulence and Acid-Fastness in Mycobacterium tuberculosis. *PLoS Pathogens* **10**: e1004115 http://dx.plos.org/10.1371/journal.ppat.1004115. Accessed February 6, 2019.

Viswanathan, G., Joshi, S.V., Sridhar, A., Dutta, S., and Raghunand, T.R. (2015) Identifying novel mycobacterial stress associated genes using a random mutagenesis screen in Mycobacterium smegmatis. *Gene* **574**: 20–27 https://linkinghub.elsevier.com/retrieve/pii/S037811191500904X. Accessed November 11, 2021.

Viswanathan, G., Yadav, S., and Raghunand, T.R. (2017) Identification of Mycobacterial Genes Involved in Antibiotic Sensitivity: Implications for the Treatment of Tuberculosis with β-Lactam-Containing Regimens. *Antimicrobial Agents and Chemotherapy* **61** http://aac.asm.org/lookup/doi/10.1128/AAC.00425-17. Accessed February 6, 2019.

Wallis, R.S., Patil, S., Cheon, S.-H., Edmonds, K., Phillips, M., Perkins, M.D., *et al.* (1999) Drug Tolerance in *Mycobacterium tuberculosis*. *Antimicrobial Agents and Chemotherapy* **43**: 2600–2606 http://aac.asm.org/lookup/doi/10.1128/AAC.43.11.2600. Accessed February 6, 2019.

Wang, J., Li, C., Yang, H., Mushegian, A., and Jin, S. (1998) A Novel Serine/Threonine Protein Kinase Homologue of *Pseudomonas aeruginosa* Is Specifically Inducible within the Host Infection Site and Is Required for Full Virulence in Neutropenic Mice. *J Bacteriol* **180**: 6764–6768 https://journals.asm.org/doi/10.1128/JB.180.24.6764-6768.1998. Accessed November 15, 2021.

Wayne, L.G., and Hayes, L.G. (1996) An In Vitro Model for Sequential Study of Shiftdown of Mycobacterium tuberculosis through Two Stages of Nonreplicating Persistence. *INFECT IMMUN* **64**: 8.

World Health Organization (2019) *Global Tuberculosis Report 2019*. World Health Organization, Geneva.

World Health Organization (2021) *Global tuberculosis report 2021*. World Health Organization, Geneva. https://apps.who.int/iris/handle/10665/346387. Accessed November 14, 2021.

Wu, M.-L., Chan, C.L., and Dick, T. (2016) Rel Is Required for Morphogenesis of Resting Cells in Mycobacterium smegmatis. *Frontiers in Microbiology* **7** http://journal.frontiersin.org/Article/10.3389/fmicb.2016.01390/abstract. Accessed April 12, 2019.

Xie, Z., Siddiqi, N., and Rubin, E.J. (2005) Differential Antibiotic Susceptibilities of Starved Mycobacterium tuberculosis Isolates. *Antimicrobial Agents and Chemotherapy* **49**: 4778–4780 http://aac.asm.org/cgi/doi/10.1128/AAC.49.11.4778-4780.2005. Accessed February 6, 2019.

Xu, Z., Meshcheryakov, V.A., Poce, G., and Chng, S.-S. (2017) MmpL3 is the flippase for mycolic acids in mycobacteria. *PNAS* **114**: 7993–7998 https://www.pnas.org/content/114/30/7993. Accessed March 13, 2019.

Zheng, X., Papavinasasundaram, K.G., and Av-Gay, Y. (2007) Novel substrates of Mycobacterium tuberculosis PknH Ser/Thr kinase. *Biochemical and Biophysical Research Communications* **355**: 162–168 https://linkinghub.elsevier.com/retrieve/pii/S0006291X07001805. Accessed November 20, 2021.